

Indice

Editorial	2
Carbon Nanomaterials-based modified electrodes for Electrocatalysis	3
Carbon aerogels used in carbon dioxide capture	9
Using activated carbon based technologies for the removal of emerging contaminants from water/wastewater – UQTA (LNEC) Projects	13
Critical discussion on activated carbons from bio-wastes – environmental risk assessment	18
Micropore size distribution of activated carbons: a key factor for a deeper understanding of the adsorption mechanism of pharmaceuticals	22
When carbon meets light: synergistic effect between carbon nanomaterials and metal oxide semiconductors for photocatalytic applications	28
Development of carbon materials as metal catalyst supports and metal-free catalysts for catalytic reduction of ions and advanced oxidation processes	36
Functional Carbon-Based Nanomaterials for Energy Storage: Towards Smart Textile Supercapacitors	42
Reseña. Biogas valorisation through catalytic decomposition to produce synthesis gas and carbon nanofibres	49

Editor Jefe:

F. José Maldonado Hódar
Universidad de Granada

Editores:

Miguel Montes
INCAR. Oviedo

Patricia Álvarez
INCAR. Oviedo

Olga Guerrero
Universidad de Málaga

Jorge Bedia
Universidad Autónoma Madrid

M. Ángeles Lillo-Ródenas
Universidad de Alicante

Manuel Sánchez-Polo
Universidad de Granada

Isabel Suelves
ICB-CSIC, Zaragoza

Editoras invitadas:

Ana Sofía Mestre
Margarida Galhetas
Marta Amaral Andrade

Editorial

The fruitful relation between the Spanish and Portuguese scientific communities working in the field of carbon materials is a well-established reality. As part of a younger generation of researchers in the field of carbon materials, we were very honoured to receive the invitation of Professor F. Maldonado to be Invited Editors of this 40th issue of the Boletín del Grupo Español del Carbón, which we accepted with great pleasure. In the following of the previous issue that reported the work developed by Portuguese groups devoted to carbon research, we here aimed to give an insight on the contributions of young Portuguese researchers, highlighting the versatility of carbon materials.

The wide range of perspectives herein presented along with the quality of the works developed by Portuguese young researchers in the field of carbon materials are certainly the result of the teaching activities of senior Portuguese professors that created reference research groups in Porto, Lisboa and Évora. In this context, young Portuguese researchers have been contributing to the growth of carbon research with high quality works that has been published in top journals focused on carbon materials science.

This issue gathers contributions mainly from Post-doc researchers and PhD students which develop their work in laboratories of Portuguese Universities (Porto – FEUP and FCUP, Lisboa - FCUL, Nova de Lisboa – FCT-UNL and Évora - UÉvora) and also in the National Civil Engineering Laboratory (LNEC). Interestingly both fundamental and applied approaches are reported.

The versatility of carbon materials to assure a more sustainable society is clearly presented in the contributions that focus on fields related with renewable energies and environmental protection. Regarding the energy applications one contribution reports the use of carbon nanomaterials-based electrodes for oxygen reduction reaction (ORR) electrocatalysts while the other reviews the importance of these nanomaterials as electrodes for the design of high performance supercapacitors. The remaining contributions address the issue of environmental protection, in both gaseous and aqueous phase. In what concerns greenhouse gases control, a study reporting CO₂ capture by lab-made carbon aerogels, as well as by commercial samples, is presented. Two of the manuscripts focus on the evaluation of textural and surface properties of carbon nanomaterials for catalytic degradation of organic pollutants in aqueous medium. The importance of the micropore size distribution to understand the adsorption mechanism of pharmaceutical compounds onto activated carbons is also illustrated. Another work discusses the need of an environmental risk assessment when the use of biomass-derived carbon materials in environmental remediation applications is envisaged. Finally, there is also a manuscript reporting the use of commercial activated carbons at pilot scale water/wastewater treatment plants in both conventional and hybrid configurations for controlling emerging contaminants such as pharmaceuticals, pesticides and cyanotoxins.

We could not finish this editorial without acknowledging all the authors that contributed to this issue by their interest and willingness to share their research with the Portuguese and Spanish carbon communities. The strengthening of the relationships of young researchers are certainly the guarantee that the collaboration between the groups of Portugal and Spain will continue to be a reality in the future.

Ana Sofia Mestre
Margarida Galhetas
Marta Amaral Andrade

Carbon Nanomaterials-based modified electrodes for Electrocatalysis

Electrodos modificados con base en Nanomateriales de Carbono para Electrocatálisis

D. M. Fernandes*, M. Nunes, M. P. Araújo

REQUIMTE/LAQV, Departamento de Química e Bioquímica, Faculdade de Ciências, Universidade do Porto, 4169-007 Porto, Portugal.

*Corresponding author: diana.fernandes@fc.up.pt

Abstract

Since their discovery, carbon nanomaterials have been attracting considerable experimental and theoretical interest because of their unique structures and properties which make them suitable and very attractive for a great number of applications in several research fields. Additionally, the possibility of chemical modification/functionalization broadens their utility and gives rise to favourable electrocatalytic properties with regard to several electrochemical processes.

This paper aims to provide an overview of the work developed by our research group regarding the use of carbon-based nanomaterials as electrocatalysts. Firstly, the sensing performance of carbon-based nanocomposites containing magnetic nanoparticles (Fe_3O_4 and MnFe_2O_4) or polyoxometalates (POMs) in oxidative electrocatalysis for detection/sensing of several biomolecules are reviewed. Then, the application of carbon-based electrocatalysts for oxygen reduction reaction is also presented.

Resumen

Desde su descubrimiento, los nanomateriales de carbono han atraído un considerable interés experimental y teórico debido a sus estructuras y propiedades únicas, que los hace adecuados y muy atractivos para un gran número de aplicaciones en varios campos de investigación. Además, la posibilidad de modificación química/funcionalización amplía su utilidad y da lugar a propiedades electrocatalíticas aún más favorables respecto a varios procesos electroquímicos.

Este documento tiene como objetivo proporcionar una visión general del trabajo desarrollado por nuestro grupo de investigación sobre el uso de nanomateriales basados en el carbono como electrocatalizadores. En primer lugar, se muestra el rendimiento de detección de nanocompuestos basados en el carbono que contienen nanopartículas magnéticas (Fe_3O_4 y MnFe_2O_4) o polioxometalatos (POMs) en electrocatalisis oxidativa para la detección/oxidación de varias biomoléculas. A continuación, se presenta también la aplicación de los electrocatalizadores a base de carbono en la reacción de reducción de oxígeno.

1. Introduction

Due to the structural diversity of the various carbon allotropic forms and the ease of tuning their chemical, electronic and crystalline properties, carbon materials are attractive for a wide range of electrochemical applications, such as sensing, electrocatalysis, fuel cells, batteries and supercapacitors [1-3].

Since the conception of carbon paste electrode in the late 1950s [4], which remains one of the most

popular electrode material for electroanalysis, and the development of electrodes based on *classical* carbon materials (glassy carbon, pyrolytic graphite and highly pyrolytic graphite (HOPG) and carbon black), the field of carbon electrochemistry has experienced a robust development over the last decades with the emergence of multidimensional carbon nanomaterials, including fullerenes, carbon nanotubes (CNTs), graphene and its derivatives, carbon nanofibers (CNFs) and diamond/carbon nanoparticles [3].

In comparison with other material electrodes, carbon-based electrodes present many important advantages, namely low cost production, high surface areas, a wide working potential window in both aqueous and non-aqueous media, high electrocatalytic activities for different redox-active chemical and biological systems and chemical inertness. Furthermore, the richness of their surface chemistry enables the functionalization of these carbon platforms *via* strong covalent or noncovalent methods with a variety of surface modifiers, which broadens the utility of carbon electrodes and improves their electrochemical performance [3,5].

Nanostructured materials, in particular, carbon-based nanomaterials such as carbon nanotubes and graphene, have also attracted considerable interest in the field of modified electrodes, with hundreds of papers and many patents published every year covering this topic [6-8], owing to their unique physical, chemical and electrochemical properties. They present, besides the advantages referred above, low residual current and readily renewable surfaces, providing an important and feasible platform for electroanalysis [9]. Also, their properties, such as fast electron transportation, high thermal conductivity, excellent mechanical strength and high surface area, suggest their ability to detect analyte molecules and to promote a fast electron transfer between the electrode and the analyte, which make them promising electrocatalysts [9]. In fact, several reports showed the good electrocatalytic activity of pristine graphene/CNT and graphene/CNT-based hybrid nanocomposites on the electrochemical sensing of several biomolecules (*e.g.* dopamine (DA), ascorbic acid (AA), uric acid (UA), glucose, hydrogen peroxide and DNA) [10-13]. Actually, higher sensitivities, lower limits of detection, wide linear responses, and faster electron transfer kinetics are generally achieved with CNT- or graphene-based sensors, comparing with traditional carbon electrodes.

Carbon-based nanomaterials have also been presented as effective electrocatalysts that fulfill the requirements for several electrochemical reactions of massive importance in energy conversion systems, such as oxygen reduction reaction (ORR), oxygen

evolution reaction (OER), hydrogen oxidation reaction (HOR) and hydrogen evolution reaction (HER) [14]. Concerning ORR electrocatalysis, significant progress has been achieved using carbon nanomaterials as support for Pt nanoparticles, as well as for non-precious metal catalysts, which promote an enhancement of the electrochemical stability, activity and durability of the supported catalysts [2,5]. Moreover, several works have also been reported showing the ORR electrocatalytic activity of carbon-based materials as standalone catalysts, such as activated carbons [15] and heteroatom doped graphene [16].

This paper intends to provide an overview of the recent work developed by our group on carbon-based electrocatalysis. The first part will be focused on the sensing performance of carbon-based nanocomposites containing polyoxometalates or magnetic nanoparticles for the detection of several biomolecules, namely AA, DA, UA, acetaminophen (AC), caffeine (CF) and theophylline (TP). In the second part, our latest results on carbon-based electrocatalysts for ORR will also be presented.

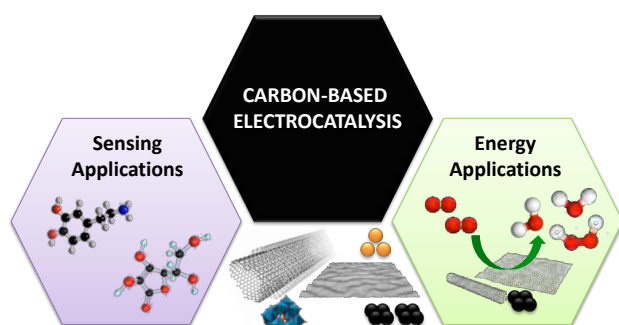


Figure 1. Electrochemical applications of carbon-based electrocatalysts addressed in this work.

Figura 1. Aplicaciones electroquímicas de electrocatalizadores a base de carbono tratados en este trabajo.

2. Carbon-based electrocatalysts for sensing applications

Today, electrochemical and electrocatalytic sensing represents one of the key topics in current science and technology. Taking advantage of the electroactivity of some drugs and biomolecules, the application of electrochemical sensors for biological analysis has been growing rapidly, mainly due to the simplicity, accuracy, precision, low cost and rapidity of the electrochemical techniques. In order to develop electrochemical sensors with higher selectivity and sensitivity, the chemical modification of electrode surfaces has been a major focus of research. The modified electrodes present lower overpotential values and improved mass transfer kinetics, decreasing the effect of interferences and avoiding surface fouling [17].

In this context, recently we reported the preparation of different hybrid materials and their application as electrode modifiers for subsequent use in oxidative electrocatalysis. One set of these materials were based on N-doped carbon nanotubes (N-CNT) and magnetic nanoparticles namely, magnetite (Fe_3O_4) and manganese(II) ferrite (MnFe_2O_4) [10,12]. In both cases, the pristine N-CNT nanomaterial with a multiwall bamboo-like structure was prepared by catalytic chemical vapor decomposition and then functionalized with the magnetic nanoparticles formed *in situ* by coprecipitation in the presence of

N-CNT. The Fe_3O_4 @N-CNT modified electrodes were then used for the voltammetric determination (by cyclic and square wave voltammetry) of AA, DA and UA while the MnFe_2O_4 @N-CNT ones for AA, CF and AC. Cyclic voltammetric results showed that for most of the biomolecules, the modification of GCE with N-CNT leads to a decrease in the oxidation potentials, more significant to DA, AA and UA, and to an increase in peak currents. These effects outcome from the combination of the high electrical conductivity of N-CNT and the possible interactions between the biomolecules and the CNTs surface, through π - π interactions and/or hydrogen bonds between their hydroxyl or amine groups and nitrogen atoms from N-CNT [10]. However, much more noteworthy results were obtained for GCE modification with the nanocomposites Fe_3O_4 @N-CNT and MnFe_2O_4 @N-CNT: larger decrease in over-potentials and increase in peak currents which are decisive aspects for the application of modified electrodes in electrocatalysis. Square wave voltammograms also presented significant changes in peak potentials and currents upon electrode modification as can be observed, as an example, in Fig. 2.

For N-CNT/GCE the most distinctive changes were observed for UA in which the i_p is almost 13 times higher when compared to bare GCE; for DA the i_p increase is of the same magnitude, but for AA the i_p increase is about 2 times. At the Fe_3O_4 @N-CNT/GCE, the same distinctive changes are also observed for UA where the i_p is ≈ 30 times higher when compared to bare GCE; for AA and DA peak currents increase approximately 3 and 7 times, respectively [10]. Similar results were obtained for the MnFe_2O_4 @N-CNT/GCE where the more significant results were observed for AA with a decrease in overpotential of ≈ 0.200 V and an increase in peak current of $\approx 520\%$. Then, SWV was used to study the electrochemical behaviour of the modified electrodes towards a mixture of 3 different biomolecules [12]. The major outcome of these modifications was the possibility of the simultaneously determination of the biomolecules since all peaks could be resolved (Fig. 2d, red). At the bare electrode only one broad peak was observed what makes impossible their determination.

The second set of materials reported by us was based on single-walled carbon nanotubes (SWCNT), graphene flakes (GF) and/or N-doped few layer graphene (N-FLG), and POMs ($\text{PMo}_{12}\text{O}_{40}$, $\text{PMo}_{11}\text{O}_{39}$, $\text{PMo}_{11}\text{VO}_{40}$ and $\text{PMo}_{10}\text{V}_2\text{O}_{40}$) [11,18]. POMs are a well-known class of discrete early transition metal-oxide clusters with a variety of sizes, shapes, composition and physical and chemical properties. One of their most important properties is their ability to undergo reversible multi-valence reductions/oxidations, leading to the formation of mixed-valence species, which brings about favourable electrocatalytic properties with regard to several electrochemical processes. The preparation of POM@SWCNT and POM@GF modified electrodes revealed to be easy to perform giving rise to stable and reproducible electrodes. Their voltammetric features were studied and showed that all POM peaks were much better resolved and had higher current intensities compared with the analogous POM-modified electrodes (Fig. 3), which suggested faster electron-transfer kinetics, which was associated with the exceptional electronic properties of SWCNT and GF.

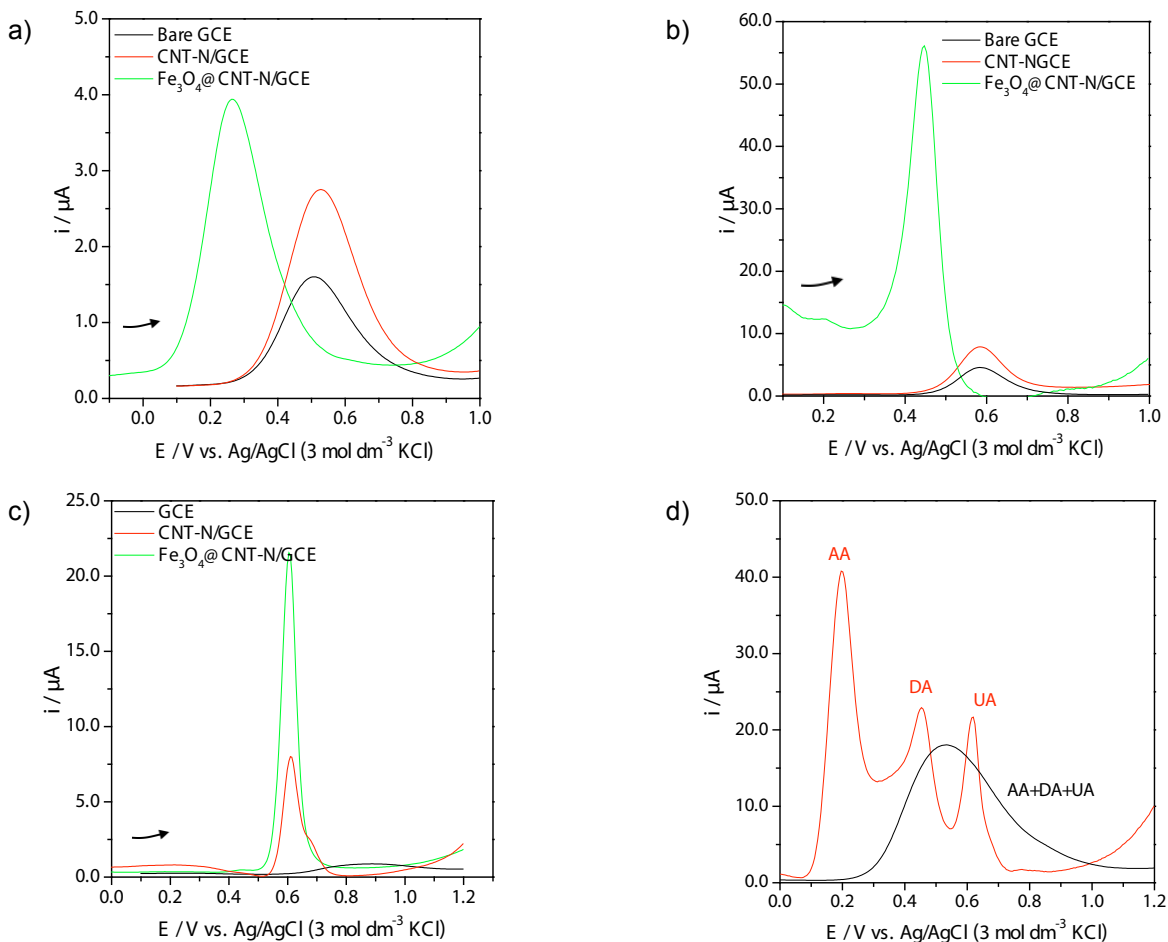


Figure 2. SWV responses of: 0.5 mM AA (a), 0.5 mM DA (b) and 0.5 mM UA (c) at bare GCE, N-CNT/GCE and Fe₃O₄@N-CNT/GCE; and 5 mM AA, 0.05 mM DA and 0.05 mM UA (d) at Fe₃O₄@N-CNT/GCE (red) and GCE (black); in pH 2.5 H₂SO₄/Na₂SO₄ buffer solution. Reprinted from J Colloid Int Sci, 432, Diana M. Fernandes *et. al*, page 211, Copyright (2014), with permission from Elsevier.

Figura 2. SWV respuestas de: AA 0,5 mM (a), DA 0,5 mM (b) y UA 0,5 mM (c) al GCE desnudo, N-CNT/GCE y Fe₃O₄@N-CNT/GCE; y AA 5 mM, DA 0,05 mM y 0,05 mM UA (d) Fe₃O₄@N-CNT/GCE (rojo) y GCE (negro); en pH 2.5 H₂SO₄/Na₂SO₄ solución tampón. Reimpreso de J Colloid Int Sci, 432, Diana M. Fernandes *et. al*, pág 211, Copyright (2014), con permiso de la Elsevier.

Then, their electrocatalytic properties were evaluated and with the exception of PMo₁₁, all presented electrocatalytic behaviour towards AA oxidation. Nevertheless, the best results were obtained for PMo₁₁V@GF and PMo₁₀V₂@GF with catalytic efficiencies (CAT) of 666% and 274%, respectively ($CAT = 100\% \times [i_{p(POM, substrate)} - i_{p(POM)}] / i_{p(POM)}$, where $i_{p(POM)}$ and $i_{p(POM, substrate)}$ are the catalytic currents of the POM in the absence and presence of substrate). Additionally,

the PMo₁₁V@GF modified electrode was also applied towards the DA oxidation. This was able to detect and measure the amount of DA in the presence of AA with a detection limit (DL) of 0.88 μmol dm⁻³ (LR = 2 – 300 μmol dm⁻³).

The same PMo₁₁V was also immobilized onto N-FLG. The electrocatalytic and sensing properties of PMo₁₁V@N-FLG modified electrodes were evaluated towards AC and TP and showed that peak current increased linearly with AC concentration in the

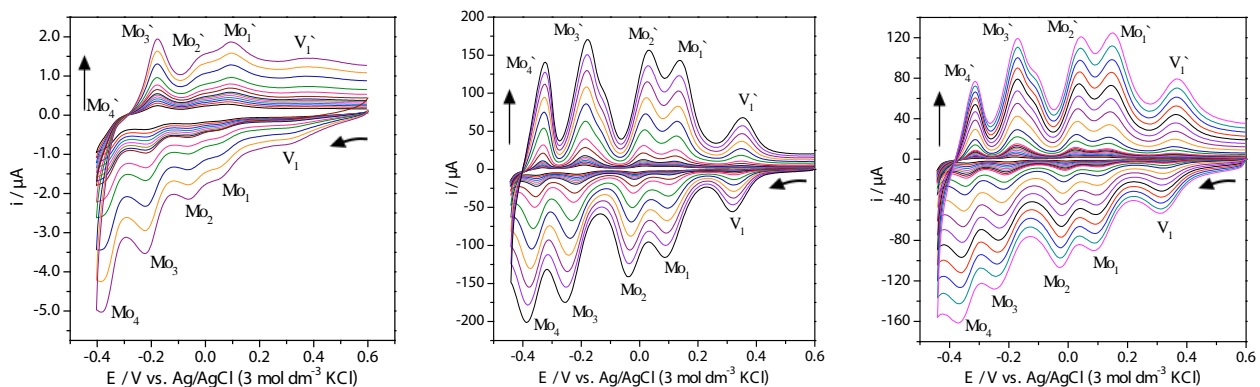


Figure 3. CVs at different scan rates of PMo₁₁V (a), PMo₁₁V@SWCNT (b) and PMo₁₁V@GF (c), in pH 2.5 H₂SO₄/Na₂SO₄ buffer solution. Reprinted with permission from Fernandes, D.M., *et. al* ChemElectroChem (2015) 2, 269. Copyright©2015 Wiley-VCH Verlag GmbH & Co. kGaA, Weinheim.

Figura 3. CVs a diferentes velocidades de barrido de PMo₁₁V (a), PMo₁₁V@SWCNT (b) y PMo₁₁V@GF (c), en pH 2.5 H₂SO₄/Na₂SO₄ solución tampón. Reimpreso con permiso de Fernandes, D.M., *et. al* ChemElectroChem (2015) 2, 269. Copyright©2015 Wiley-VCH Verlag GmbH & Co. kGaA, Weinheim.

presence of TP, showing two linear ranges: 1.2 – 120 and 120 – 480 $\mu\text{mol dm}^{-3}$, with different AC sensitivity values, 0.022 and 0.035 $\mu\text{A}/\text{mmol dm}^{-3}$, respectively (DL = 0.75 $\mu\text{mol dm}^{-3}$) [11].

The importance of carbon materials in these hybrids is in great part associated with the fact that they allow a much higher amount of electroactive species to be deposited at the electrode surface due to their nanostructures which constitutes an outstanding advantage when developing superior modified electrodes [18].

3. Carbon-based electrocatalysts for energy applications

In order to face the current global energy crisis, fuel cells and metal-air batteries have attracted a lot of attention as sustainable alternative technologies for energy conversion and storage [19]. The operation of these technologies is based in several electrochemical processes, among which the oxygen reduction reaction plays a crucial role in controlling the overall devices performance. Platinum nanoparticles supported on carbon materials (Pt/C) are the most effective known ORR catalysts, leading to low ORR overpotential and large current densities, with selectivity toward a direct 4-electron pathway [20]. Nevertheless, the required high Pt loading (40-80 %) associated with its high cost, scarcity, declining activity and possible Pt-deactivation by methanol crossover have limited the large-scale application of Pt-based electrocatalysts [20,21]. Therefore, research efforts have been devoted to developing alternative ORR electrocatalysts, with a competitive activity with the Pt/C catalysts but more stable and cost-effective [22]. In this context, carbon-based materials, with their versatile properties, appeared as ideal to be applied in ORR as metal-free electrocatalysts itself or as catalyst supports in functional composites.

Several works have reported the application of graphite [23], CNTs [24], GF [25], ordered mesoporous carbons [21] and carbon nanoparticles [20] as metal-free ORR catalysts. In this context, recently we reported the application of two activated carbons (ACs) as ORR electrocatalysts [15].

The ACs were prepared from a sucrose-derived hydrochar [26], which was a valuable green approach considering the availability, low cost and environmental friendliness of the starting material. Both ACs, denoted as SH800 and SC800, exhibited ORR electrocatalytic activity in alkaline and acidic media. In alkaline medium (Fig. 4a), the two ACs showed similar onset potentials ($E_{\text{onset}} \approx -0.20$ V vs. Ag/AgCl), which were only 60 mV more negative than the observed for the state-of-the-art Pt/C electrocatalyst [15]. Moreover, the higher limiting current densities recorded for SH800 [15] showed the advantage of the high surface areas and large pores of this material, as favourable conditions for a high ORR electrocatalytic performance, once increase the number of active sites exposed to the electrolyte [27]. The selectivity of the electrocatalysts showed to be dependent of the applied potential, moving closer to the 4-electron process (direct O_2 reduction) as the potential became more negative. Furthermore, the ACs revealed excellent tolerance to methanol, with the SH800 also exhibiting greater long-term electrochemical stability than the Pt/C electrocatalyst, which are important

advantages considering a possible application in direct methanol fuel cells.

The ACs-based electrocatalysts also showed ORR electrocatalytic activity in acidic medium, which was a key result considering the common inactivity or low ORR activity of carbon materials in acidic medium and an application in proton exchange fuel cells; however, the ORR performance was lower than in alkaline medium, probably due to active sites deactivation [28].

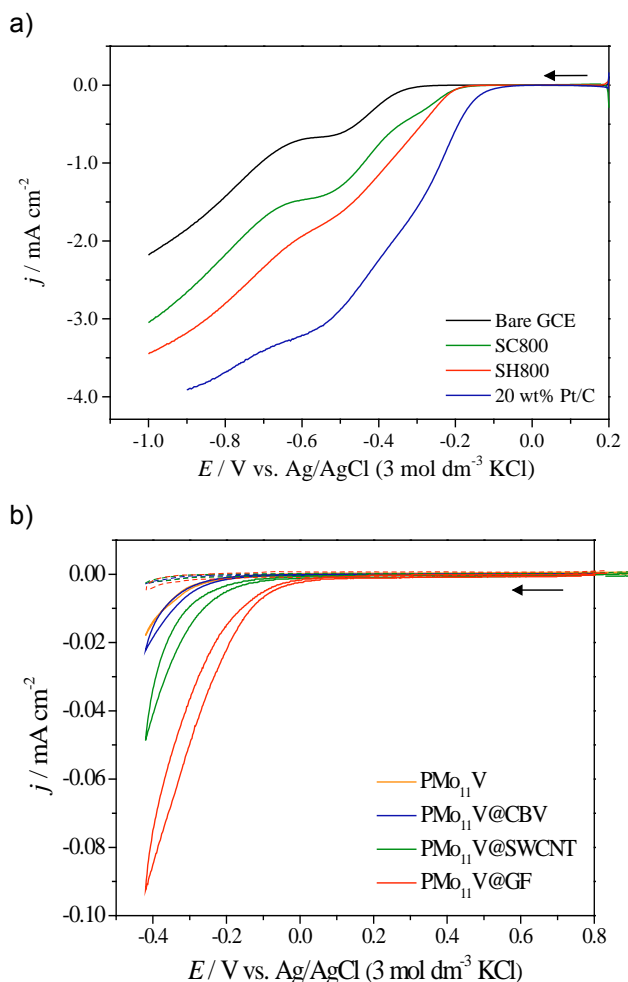


Figure 4. ORR results of (a) ACs in O_2 -saturated solution in alkaline medium and (b) PMo_{11}V and $\text{PMo}_{11}\text{V@carbon}$ -based composites in N_2 - and O_2 -saturated solutions in acidic medium. Reproduced by permission of the Royal Society of Chemistry.

Figura 4. Resultados de ORR de (a) ACs en una solución saturada de oxígeno en medio alcalino y (b) PMo_{11}V y $\text{PMo}_{11}\text{V@carbon}$ compuestos en una solución saturada de nitrógeno y oxígeno. Reproducido con permiso de la Royal Society of Chemistry.

The use of carbon materials as catalyst support also has several advantages: higher electroactive surface area, enhanced conductivities and brings the catalyst particles close to the reactants, improving the catalytic activity and durability [1]. Carbon black is the most commonly used support catalyst due to its low cost, but its susceptibility to oxidation sometimes results in active surface area loss and alteration of the pore surface characteristics. Carbon nanotubes and graphene supports, although more expensive, normally result in high catalyst utilization, owing to their high crystallinity and surface area [1]. Currently, we are studying the application of several composites as ORR electrocatalysts, prepared through the incorporation of a vanadium-substituted phosphomolybdate (PMo_{11}V) into carbon black Vulcan (CBV), SWCNT and GF [29]. At this regard, the ability of POM to mediate

electron, proton and oxygen transfer reactions was an additional value [11]. All composites, designated by $\text{PMo}_{11}\text{V@CBV}$, $\text{PMo}_{11}\text{V@SWCNT}$ and $\text{PMo}_{11}\text{V@GF}$, showed ORR electrocatalytic ability, with a strong dependency between the ORR performance and the carbon-based material employed as support (Fig. 4b).

In comparison with the pristine PMo_{11}V , the composites showed the peak associated with the reduction of oxygen at more positive potentials and with higher current densities, which indicated the advantage of the incorporation of POM into the carbon-based supports; these results were corroborated by the higher electroactive surface coverages obtained for composites-modified electrodes [29]. The $\text{PMo}_{11}\text{V@SWCNT}$ and $\text{PMo}_{11}\text{V@GF}$ composites exhibited the best ORR performances, as consequence of the high conductivity of these SWCNT and GF supports that improved the charge transfer between the modified layer and the GCE electrode and promoted a beneficial synergistic effect with PMo_{11}V .

4. Concluding remarks

In this paper the electrocatalytic applications of several carbon-based electrocatalysts developed by our group in two major areas of high current impact, electrochemical sensing and renewable energy, were overviewed. Firstly, the *carbon-based electrocatalysts for sensing applications* was reviewed: initially, was covered the oxidative electrocatalysis by hybrids based on carbon and magnetic nanoparticles and then those based on carbon and POMs. The last topic, *carbon-based ORR electrocatalysts for energy applications*, addressed the application of our contribution regarding this type of electrocatalysts for one of the reactions that play a key role in several promising energy systems, the oxygen reduction reaction.

Even though the electrocatalytic application of carbon-based electrocatalysts is growing in great part because of the huge advantage of offering higher amount of electroactive species at the electrode surface and less soluble electrocatalysts, there is definitely huge room for improvement and discovery in carbon-based materials research.

5. Acknowledgments

This work was co-financed by Fundação para a Ciência e a Tecnologia (FCT) and FEDER under Programme PT2020 (Project UID/QUI/50006/2013). DF (SFRH/BPD/74877/2010), MN (SFRH/BD/79171/2011), and MA (SFRH/BD/89156/2012) also thank FCT for their grants. Thanks are also due to COST Action CM-1203 PoCheMoN.

6. References

- [1] Trogadas P, Fuller TF, Strasser P. Carbon as catalyst and support for electrochemical energy conversion. *Carbon* 2014; 75:5-42.
- [2] Higgins D, Zamani P, Yu AP, Chen ZW. The application of graphene and its composites in oxygen reduction electrocatalysis: a perspective and review of recent progress. *Energy Environ Sci* 2016; 9(2):357-390.
- [3] Yang NJ, Swain GM, Jiang X. Nanocarbon Electrochemistry and Electroanalysis: Current Status and Future Perspectives. *Electroanal* 2016; 28(1):27-34.
- [4] Adams RN. Carbon paste electrodes. *Anal Chem* 1958; 30(9):1576-1576.
- [5] Mao XW, Rutledge GC, Hatton TA. Nanocarbon-based electrochemical systems for sensing, electrocatalysis, and energy storage. *Nano Today* 2014; 9(4):405-432.
- [6] Wang Y, Shao YY, Matson DW, Li JH, Lin YH. Nitrogen-Doped Graphene and Its Application in Electrochemical Biosensing. *ACS Nano* 2010; 4(4):1790-1798.
- [7] Wildgoose GG, Banks CE, Leventis HC, Compton RG. Chemically modified carbon nanotubes for use in electroanalysis. *Microchim Acta* 2006; 152(3-4):187-214.
- [8] Yang WR, Ratnac KR, Ringer SP, Thordarson P, Gooding JJ, Braet F. Carbon Nanomaterials in Biosensors: Should You Use Nanotubes or Graphene?. *Angew Chem Int Edit* 2010; 49(12):2114-2138.
- [9] Wu SX, He QY, Tan CL, Wang YD, Zhang H. Graphene-Based Electrochemical Sensors. *Small* 2013; 9(8):1160-1172.
- [10] Fernandes DM, Costa M, Pereira C, Bachiller-Baeza B, Rodriguez-Ramos I, Guerrero-Ruiz A, Freire C. Novel electrochemical sensor based on N-doped carbon nanotubes and Fe_3O_4 nanoparticles: Simultaneous voltammetric determination of ascorbic acid, dopamine and uric acid. *J Colloid Interface Sci* 2014; 432:207-213.
- [11] Fernandes DM, Freire C. Carbon Nanomaterial-Phosphomolybdate Composites for Oxidative Electrocatalysis. *ChemElectroChem* 2015; 2(2):269-279.
- [12] Fernandes DM, Silva N, Pereira C, Moura C, Magalhaes J, Bachiller-Baeza B, Rodriguez-Ramos I, Guerrero-Ruiz A, Delerue-Matos C, Freire C. MnFe_2O_4 @CNT-N as novel electrochemical nanosensor for determination of caffeine, acetaminophen and ascorbic acid. *Sens Actuator B Chem* 2015; 218:128-136.
- [13] Sherigara BS, Kutner W, D'Souza F. Electrocatalytic properties and sensor applications of fullerenes and carbon nanotubes. *Electroanal* 2003; 15(9):753-772.
- [14] Liang YY, Li YG, Wang HL, Dai HJ. Strongly Coupled Inorganic/Nanocarbon Hybrid Materials for Advanced Electrocatalysis. *J Am Chem Soc* 2013; 135(6):2013-2036.
- [15] Nunes M, Rocha IM, Fernandes DM, Mestre AS, Moura CN, Carvalho AP, Pereira MFR, Freire C. Sucrose-derived activated carbons: electron transfer properties and application as oxygen reduction electrocatalysts. *RSC Adv* 2015; 5(124):102919-102931.
- [16] Pan FP, Jin J, Fu XG, Liu Q, Zhang JY. Advanced Oxygen Reduction Electrocatalyst Based on Nitrogen-Doped Graphene Derived from Edible Sugar and Urea. *ACS Appl Mater Interfaces* 2013; 5(21):11108-11114.
- [17] Murray RW. Chemically modified electrodes. In: *AJ Bard Ed., Electroanalytical Chemistry*. 1984 p191-368.
- [18] Fernandes DM, Nunes M, Carvalho, RJ, Bacsa R, Mboemkalle I.-M, Serp P, Oliveira P, Freire C. Biomolecules Electrochemical Sensing Properties of $\text{PMo}_{11}\text{V@N-Doped Few Layer Graphene Nanocomposite}$. *Inorganics* 2015; 3:178-193.
- [19] Liu RJ, Xian ZW, Zhang SS, Chen CH, Yang ZH, Li H, Zheng WQ, Zhang GJ, Cao HB. Electrochemical-reduction-assisted assembly of ternary Ag nanoparticles/polyoxometalate/graphene nanohybrids and their activity in the electrocatalysis of oxygen reduction. *RSC Adv* 2015; 5(91):74447-74456.
- [20] Panomsuwan G, Saito N, Ishizaki T. Nitrogen-doped carbon nanoparticles derived from acrylonitrile plasma for electrochemical oxygen reduction. *Phys Chem Chem Phys* 2015; 17(9):6227-6232.
- [21] Tao GJ, Zhang LX, Chen LS, Cui XZ, Hua ZL, Wang M, Wang JC, Chen Y, Shi JL. N-doped hierarchically macro/mesoporous carbon with excellent electrocatalytic activity and durability for oxygen reduction reaction. *Carbon* 2015; 86:108-117.
- [22] Guo CZ, Liao WL, Li ZB, Chen CG. Exploration of the catalytically active site structures of animal biomass-modified on cheap carbon nanospheres for oxygen reduction reaction with high activity, stability and methanol-tolerant performance in alkaline medium. *Carbon* 2015; 85:279-288.

[23] Shen A, Zou Y, Wang Q, Dryfe RAW, Huang X, Dou S, Dai L, Wang S. Oxygen reduction reaction in a droplet on graphite: direct evidence that the edge is more active than the basal plane. *Angew Chem Int Edit* 2014; 53(40):10804-8.

[24] Vikkisk M, Kruusenberg I, Ratsõ S, Joost U, Shulga E, Kink I, Rauwel P, Tammeveski K. Enhanced electrocatalytic activity of nitrogen-doped multi-walled carbon nanotubes towards the oxygen reduction reaction in alkaline media. *RSC Adv* 2015; 5(73):59495-59505.

[25] Wu JJ, Ma LL, Yadav RM, Yang YC, Zhang X, Vajtai R, Lou J, Ajayan PM. Nitrogen-Doped Graphene with Pyridinic Dominance as a Highly Active and Stable Electrocatalyst for Oxygen Reduction. *ACS Appl Mater Interfaces* 2015; 7(27):14763-14769.

[26] Mestre AS, Tyszko E, Andrade MA, Galhetas M, Freire C, Carvalho AP. Sustainable activated carbons prepared from a sucrose-derived hydrochar: remarkable adsorbents for pharmaceutical compounds. *RSC Adv* 2015; 5(25):19696-19707.

[27] Song MY, Park HY, Yang DS, Bhattacharjya D, Yu JS. Seaweed-Derived Heteroatom-Doped Highly Porous Carbon as an Electrocatalyst for the Oxygen Reduction Reaction. *ChemSusChem* 2014; 7(6):1755-1763.

[28] Chen P, Wang LK, Wang G, Gao MR, Ge J, Yuan WJ, Shen YH, Xie AJ, Yu SH. Nitrogen-doped nanoporous carbon nanosheets derived from plant biomass: an efficient catalyst for oxygen reduction reaction. *Energy Environ. Sci.* 2014; 7(12):4095-4103.

[29] Nunes M, Fernandes DM, Rocha IM, Pereira MFR, Mbomekalle I.-M, Oliveira P, Freire C. Phosphomolybdate@ carbon-based nanocomposites as electrocatalysts for oxygen reduction reaction. *RSC Adv* Submitted. 2016.

Carbon aerogels used in carbon dioxide capture

Aerogeles de carbono utilizados en la captura de dióxido de carbono

L.M. Marques*, P.J.M. Carrott, M.M.L. Ribeiro Carrott

Centro de Química de Évora, Instituto de Investigação e Formação Avançada e Departamento de Química, Escola de Ciências e Tecnologia, Universidade de Évora – Rua Romão Ramalho, 59, 7000-671 Évora, Portugal.

*Corresponding author: luisasmarques@gmail.com

Abstract

In this work the maximum carbon dioxide adsorption capacity of carbon aerogels, obtained by a sol-gel process using 2,4-dihydroxybenzoic acid/formaldehyde (DHBAF) and resorcinol/formaldehyde (RF) as precursors, was studied. The effect of increasing the temperature of carbonization and physical activation of the samples DHBAF was also studied. The results showed that the maximum adsorption capacity is favoured at lower temperatures, adsorption and desorption are rapid and the performance is maintained over several cycles of CO₂ adsorption/desorption. A comparison with samples of commercial carbons was also made and it was concluded that carbon aerogels exhibit a behaviour comparable or superior to that obtained for the commercial carbons studied.

Resumen

En este trabajo se ha estudiado la capacidad máxima de adsorción de dióxido de carbono de aerogeles de carbono, obtenidos mediante un proceso sol-gel utilizando ácido 2,4-dihidroxibenzoico / formaldehído (DHBAF) y resorcinol / formaldehído (RF) como precursores. También fue estudiado el efecto del aumento de la temperatura de carbonización y la activación física de las muestras DHBAF. Los resultados mostraron que la capacidad máxima de adsorción se ve favorecida a temperaturas más bajas, la adsorción y desorción son rápidas y el rendimiento se mantiene durante varios ciclos de adsorción/desorción de CO₂. También se hizo una comparación con las muestras de carbones comerciales donde se concluyó que los aerogeles de carbono exhiben un comportamiento comparable o superior a la obtenido para los carbones comerciales estudiados.

1. Introduction

Climate change is regarded as one of the biggest environmental threats worldwide as a result of global warming [1]. According to the scientific community the CO₂ emitted by burning fossil fuels is the main cause of the drastic global warming [2, 3] and ways of reducing its emission are currently investigated and developed, based on strategies of capture, transport and storage of CO₂ [4, 5].

The technology of CO₂ capture and storage, “carbon capture and storage” (CCS), drawn up by the G8 (eight major industrial countries) in the year 2008, allows the CO₂ emitted by various industrial sources to be captured, transported and stored in adapted geological formations. Currently CO₂ capture technology consists of three methods (pre-combustion, post-combustion and oxy-combustion) with several technical options [6] indicated in Figure 1.

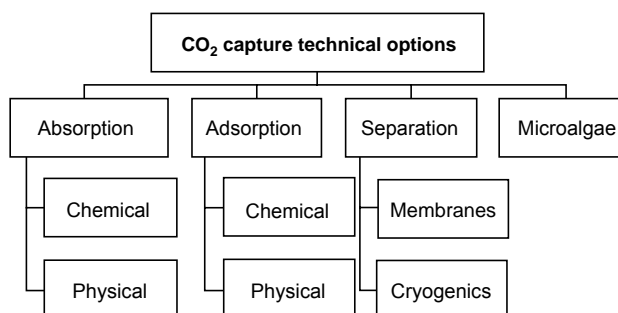


Figure 1: CO₂ capture technical options.

Figura 1: Opciones técnicas para la captura de CO₂.

In the present work adsorption was studied. As key features, the solid adsorbent should present a high selectivity, high rate of adsorption or desorption, regenerative capacity and energy efficiency. The various adsorbents usually studied include zeolites [7], activated carbons [8, 9] and mesoporous silicas [10]. Currently MOFs (Metal Organic Frameworks) [11] and carbon aerogels [12] show potential as adsorbents in the medium and long term. A carbon aerogel is a form of microporous carbon obtained by carbonization or activation of a polymer precursor which is prepared by a sol-gel route followed by supercritical drying. This procedure results in products with monolithic form and high mesopore surface area, which makes them interesting materials for use in fuel cells, supercapacitors, lithium batteries, gas separation, hydrocarbon vapour recovery, electric conductors and carbon capture [13-15].

In this article we will focus just on the performance of some unmodified low density carbon aerogels. Results for carbon aerogels modified by CVD or amine deposition have previously been published [15, 16].

2. Experimental

2.1. Preparation of organic and carbon aerogels

Polymer aerogels were prepared from 2,4-dihydroxybenzoic acid (DHBA) or resorcinol (R) and formaldehyde (F) under basic conditions using the procedure described by Carrott *et al* [17]. All the aerogels were synthesized using the stoichiometric molar ratio (0.5) and a solids content of 4%, equivalent to dilution ratios of 80 (RF) or 100 (DHBAF).

Carbon aerogels were obtained using a vertical tube furnace by heating individual monoliths in a 90 cm³ min⁻¹ N₂ flow to 1073 and 1223 K (only the samples of type DHBAF) at a rate of 5 K min⁻¹ and maintaining the monoliths at this temperature for 180 minutes. The temperature was then allowed to fall below 323 K before removing the carbon aerogel from the furnace.

The activation of the sample DHBAF was carried out at 1073 K in a horizontal tubular furnace by heating under N₂ from room temperature to 1073 K at a rate of

5 K min⁻¹, maintaining at this temperature for 180 min before switching to CO₂ for 5 h and then allowing it to cool down to room temperature under N₂ flow. The N₂ and CO₂ flow rates were both 90 cm³ min⁻¹.

2.2. Characterization by nitrogen adsorption

The characterization of the porosity of the aerogels produced was performed by nitrogen adsorption at 77 K using a Quantachrome Quadrasorb automated N₂ adsorption analyser and analysis of the adsorption isotherms by application of the BET, DR and α_s methods. The mesopore size distributions were calculated by the NLDFT method.

2.3. CO₂ adsorption/desorption

The CO₂ adsorption and desorption performance of the samples was evaluated using a Perkin-Elmer STA6000. CO₂ capture tests at 298, 308, 328, 348 and 373 K were carried out, with repeat run cycles at 298 K to evaluate the suitability of the samples for cyclic operation. In each case, the sample mass was allowed to stabilize at the selected temperature and then the carrier flow was changed from He (100 cm³min⁻¹) to CO₂ (100 cm³min⁻¹) in order to measure the adsorption capacity. Once the mass had stabilized, the carrier gas was changed back to He in order to measure the desorption of CO₂. In the case of stability testing, this procedure was repeated during 6 cycles of adsorption/desorption at 298 K.

3. Results and discussion

3.1. Characterization of organic aerogels

The N₂ at 77 K isotherms determined on the organic aerogels were similar to previously published results [18]. The N₂ isotherms were analysed by the BET and α_s methods and the results are given in Table 1. It can be seen that the values of A_s and A_{BET} are very similar. Additionally, the values of C are low which indicates the absence of microporosity.

Also included in the table are the total mesopore volumes and mesopore sizes obtained from the NLDFT analysis. The NLDFT mesopore size distributions indicated that the samples have mesopore widths greater than 40 nm.

3.2. Characterization of carbon aerogels

The N₂ at 77 K isotherms determined on the carbon

aerogels were similar to previously published results [19]. In the case of the carbon aerogels, it is observed that the values (shown in Table 1) of A_s are lower than the values of A_{BET} since they correspond to the external surface area only. In all cases, the C values are much larger than those determined on the samples of organic aerogels, which indicates the presence of ultramicropores.

It should be noted that both an increase in the temperature of carbonization as well as physical activation allowed an increase of ultramicroporosity in the aerogel structure, since the C values are larger when compared with the sample DHBAF-1073. By application of the α_s method, it can be seen that the values of V_{mic} are between 0.19-0.24 cm³g⁻¹. By applying the DR method, it is observed that the d_{mic} values are approximately 1 nm for the DHBAF samples and close to 2 nm for the RF sample. As pointed out previously [19] the DR method overestimates the micropore width of carbon aerogels due to their large specific external surface area. However, the C values indicate that the DHBAF aerogels have narrower ultramicropores than RF. Modification of the DHBAF sample induces only a small change in the average width of the micropores. By application of NLDFT, it is observed that the modification of the DHBAF aerogel results in only a small decrease in mesopore volume but a significant reduction in mesopore diameter of the carbon aerogels in comparison with the DHBAF-1073 sample. The RF sample is the sample with the highest mesopore volume.

3.3. CO₂ adsorption/desorption

3.3.1. Stability tests

In order to assess the stability of the adsorbents, multiple adsorption/desorption cycles were performed at 298 K. The CO₂ adsorption capacity after six cycles confirmed the stability. The same type of study was carried out with some commercial carbons and the results can also be observed in Table 2. Based on the results obtained it is possible to observe that the behaviour observed in the case of commercial carbons is similar to that obtained with carbon aerogels prepared in the laboratory.

It is also possible to infer that the differences in adsorption capacity of the samples presented are due to the difference in the width of the micropores, as

Table 1: Textural parameters determined in organic and carbon aerogels.

Tabla 1: Parámetros texturales determinados en aerogeles orgánicos y de carbono.

Aerogel	BET		a _s		DR	NLDFT	
	A _{BET} / m ² g ⁻¹	C	A _s / m ² g ⁻¹	V _{mic} / cm ³ g ⁻¹	d _{mic} / nm	d _{p(mes.)} / nm	V _{T(mes.)} / cm ³ g ⁻¹
Organic							
DHBAF	557	158	532	n.a	n.a	> 40	1.33
RF	619	85	612	n.a	n.a	>40	4.36
Carbon							
DHBAF-1073	798	1587	323	0.20	0.98	> 40	1.50
DHBAF-1223	811	3249	264	0.22	1.01	17.30	1.39
DHBAF-(AC)	942	34509	349	0.24	1.08	27.39	1.49
RF-1073	1083	626	656	0.19	1.92	> 40	4.03

A_{BET} = Apparent specific surface area obtained by the BET method; C = BET C parameter; A_s = Specific external surface area obtained by a_s the method; V_{mic} = Total micropore volume obtained by a_s the method; d_{mic} = DR micropore width; d_{p(mes.)} = Mesopore mean width obtained from the maximum of the NLDFT pore size distribution; V_{T(mes.)} = Mesopore volume calculated by the NLDFT method; n.a = not applicable.

Table 2. Comparison of the CO₂ maximum adsorption capacity achieved for carbon aerogels and commercial carbons at 298 K.

Tabla 2. Comparación de la capacidad de adsorción máxima de CO₂ alcanzada para aerogeles de carbono y carbones comerciales a 298 K.

Sample	1 cycle	2 cycle	3 cycle	4 cycle	5 cycle	6 cycle
	n (CO ₂) / mmolg ⁻¹					
DHBAF-1073	2.13	2.13	2.13	2.13	2.13	2.13
DHBAF-1223	2.15	2.11	2.11	2.11	2.11	2.11
DHBAF-(AC)	2.06	2.07	2.07	2.07	2.06	2.06
RF-1073	1.87	1.88	1.88	1.90	1.90	1.91
Carbosieve	2.15	2.11	2.13	2.13	2.15	2.14
Maxsorb	1.87	1.88	1.88	1.90	1.90	1.91
Takeda 4A	1.15	1.23	1.23	1.22	1.21	1.20

reported by other authors [20-22]. Higher and lower CO₂ adsorption capacity are presented by the DHBAF and RF samples, respectively.

3.3.2. Influence of temperature

Figure 2 shows representative TGA curves for 2 cycles of adsorption and desorption of CO₂ at different temperatures. Values of the maximum adsorption capacity for all samples are given in Table 3. The comparison of CO₂ adsorption capacity at different temperatures, shown in Table 3, indicates that the results obtained in this work for carbon aerogels are comparable or superior to those obtained with other carbon adsorbents.

The same results also show that the increase in temperature of analysis contributed to a sharp decrease of the maximum capacities of adsorption, indicating a physical adsorption process between the adsorbent and CO₂ molecules. Additionally, it can be seen that in the case of the carbon aerogels the highest and lowest adsorption capacities are obtained for the samples DHBAF (1073 or 1223, depending on the temperature) and RF, respectively. The results corroborate the view of several authors [20, 22, 23] who have pointed out that the maximum adsorption capacity of CO₂ at atmospheric pressure on carbon materials depends on the presence of narrow micropores.

The values in Table 3 of adsorption capacity at different temperatures allow us to estimate values of adsorption capacity at other temperatures. Of particular interest is the adsorption capacity at 273 K, as many authors quote results for this temperature. As found in previous work [16], plots of ln(n(CO₂)) as a function of 1/T are linear. Representative examples are given in Figure 3 for the two samples with the highest

adsorption capacity at 298 K, namely, the carbon aerogel DHBAF-1073 and the carbon molecular sieve Carbosieve. At 298 K Carbosieve has a slightly higher adsorption capacity. However, it is one of the samples with the lowest temperature dependence, with a slope of 1695 K on Figure 3. On the other hand, DHBAF-1073 is the sample with the greatest temperature dependence, the slope on Figure 3 being 1977 K. As a result, the predicted adsorption capacity of DHBAF-1073 becomes greater than that of Carbosieve at temperatures below about 293 K. In fact, it is the only sample which has a predicted adsorption capacity greater than 4 mmol g⁻¹ at 273 K.

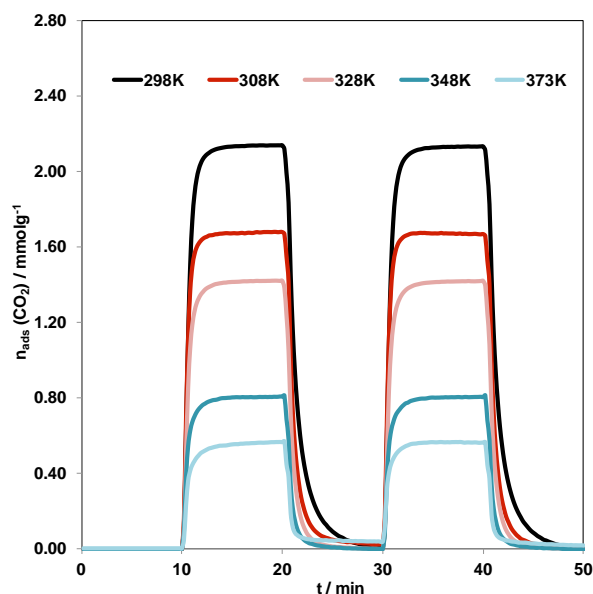

Figure 2. Adsorption/desorption cycles corresponding to the sample DHBAF-1073.

Figura 2. Adsorción/desorción de ciclos correspondiente a la muestra DHBAF-1073.

Table 3. Average maximum capacity for adsorption of CO₂ at different temperatures, at atmospheric pressure obtained on samples of carbon aerogels and commercial carbons.

Tabla 3. Promedio de la capacidad máxima de adsorción de CO₂ a diferentes temperaturas, a presión atmosférica, obtenidos en muestras de aerogeles de carbono y carbones comerciales.

Sample	298 K	308 K	328 K	348 K	373 K
	n (CO ₂) / mmolg ⁻¹				
DHBAF-1073	2.13	1.68	1.42	0.81	0.56
DHBAF-1223	2.12	1.89	1.42	1.06	0.68
DHBAF-(AC)	2.07	1.60	1.08	0.87	0.59
RF-1073	1.89	1.59	1.23	0.86	0.57
Carbosieve	2.15	1.96	1.41	1.02	0.70
Maxsorb	1.87	1.58	1.07	0.80	0.49
Takeda 4A	1.15	1.49	1.13	0.83	0.55

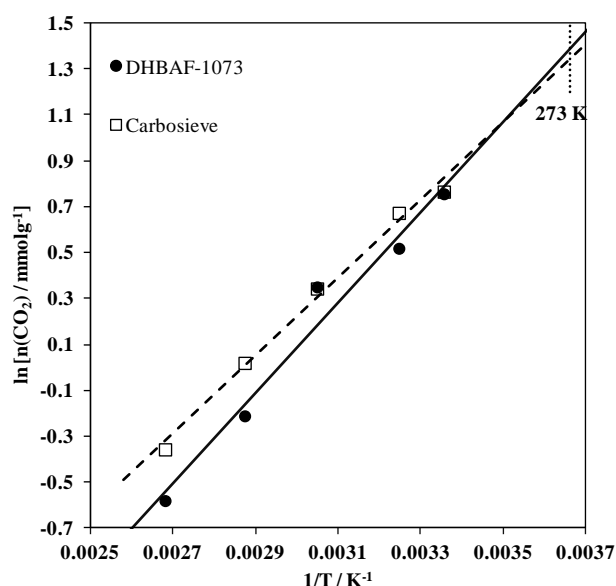


Figure 3. CO₂ maximum capture capacities determined at different temperatures.

Figura 3. Capacidades máximas de captura CO₂ determinadas a diferentes temperaturas.

4. Conclusions

In the current work, a set of different porous carbon samples, including carbon aerogels and commercial carbons was studied. The carbon aerogels featured high stability and reproducible performance in the CO₂ adsorption/desorption tests. Furthermore, the maximum CO₂ adsorption capacities of the carbon aerogels were found to be comparable or superior to those of the commercial carbons studied. Additionally, the results also showed that the adsorption and desorption are very fast, a feature suitable for future applications of these carbon aerogels in CO₂ capture.

5. Acknowledgements

The work was funded by the Fundação para a Ciência e a Tecnologia (Ph.D. Grant No. SFRH/BD/70543/2010, Project PTDC/EQU-EQU/64842/2006 (Grant No. FCOMP-01-0124-FEDER-007307) and Strategic Project PEst-OE/QUI/UI0619 with National (OE) and European community (FEDER, program COMPETE of QREN) funds.

6. References

- [1] Olajire AA. CO₂ capture and separation technologies for end-of-pipe applications – A review. *Energy*. 2010;35:2610-28.
- [2] Arenillas A, Smith KM, Drage TC, Snape CE. CO₂ capture using some fly ash-derived carbon materials. *Fuel*. 2005;84:2204-10.
- [3] Plaza MG, Pevida C, Arenillas A, Rubiera F, Pis JJ. CO₂ capture by adsorption with nitrogen enriched carbons. *Fuel*. 2007;86:2204-12.
- [4] Orr JFM. CO₂ capture and storage: are we ready? *Energy & Environmental Science*. 2009;2:449.
- [5] Gibbins J, Chalmers H. Carbon capture and storage. *Energy Policy*. 2008;36:4317-22.
- [6] Pires JCM, Martins FG, Alvim-Ferraz MCM, Simões M. Recent developments on carbon capture and storage: An overview. *Chemical Engineering Research and Design*. 2011;89:1446-60.
- [7] Cheung O, Bacsik Z, Liu Q, Mace A, Hedin N. Adsorption kinetics for CO₂ on highly selective zeolites NaKA and nano-NaKA. *Applied Energy*. 2013;112:1326-36.

[8] Builes S, Roussel T, Ghimbeu CM, Parmentier J, Gadiou R, Vix-Guterl C. Microporous carbon adsorbents with high CO₂ capacities for industrial applications. *Physical chemistry chemical physics : PCCP*. 2011;13:16063-70.

[9] Sevilla M, Fuertes AB. CO₂ adsorption by activated templated carbons. *Journal of colloid and interface science*. 2012;366:147-54.

[10] Chandrasekar G, Son W-J, Ahn W-S. Synthesis of mesoporous materials SBA-15 and CMK-3 from fly ash and their application for CO₂ adsorption. *Journal of Porous Materials*. 2008;16:545-51.

[11] Zhao Z, Li Z, Lin YS. Adsorption and Diffusion of Carbon Dioxide on Metal-Organic Framework (MOF-5). *Industrial & Engineering Chemistry Research*. 2009;48:10015-20.

[12] Martín CF, Plaza MG, García S, Pis JJ, Rubiera F, Pevida C. Microporous phenol-formaldehyde resin-based adsorbents for pre-combustion CO₂ capture. *Fuel*. 2011;90:2064-72.

[13] Fricke J, Tillotson T. Aerogels: production, characterization, and applications. *Thin Solid Films*. 1997;297:212-23.

[14] Akimov YK. Fields of Application of Aerogels (Review). *Instruments and Experimental Techniques*. 2003;46:287-99.

[15] Marques LM, Carrott PJM, Carrott MMLR. Amine-modified Carbon Aerogels for CO₂ Capture. *Adsorption Science & Technology*. 2013;31:223-32.

[16] Marques LM, Conceição FL, Ribeiro Carrott MML, Carrott PJM. Diffusion of gases in metal containing carbon aerogels. *Fuel Proc Technol*. 2011;92:229-233.

[17] Carrott PJM, Marques LM, Ribeiro Carrott MML. Core-shell polymer aerogels prepared by co-polymerisation of 2,4-dihydroxybenzoic acid, resorcinol and formaldehyde. *Microporous and Mesoporous Materials*. 2012;158:170-4.

[18] Carrott PJM, Marques LM, Carrott MMLR. Characterisation of the porosity of polymer and carbon aerogels containing Fe, Ni or Cu prepared from 2,4-dihydroxybenzoic acid by n-nonane pre-adsorption and density functional theory. *Microporous and Mesoporous Materials*. 2010;131:75-81.

[19] Carrott PJM, Conceição FL, Carrott MMLR. Use of n-nonane pre-adsorption for the determination of micropore volume of activated carbon aerogels. *Carbon*. 2007;45:1310-3.

[20] Olivares-Marin M, Garcia S, Pevida C, Wong MS, Maroto-Valer M. The influence of the precursor and synthesis method on the CO₂ capture capacity of carpet waste-based sorbents. *Journal of environmental management*. 2011;92:2810-7.

[21] Rashidi NA, Yusup S, Hameed BH. Kinetic studies on carbon dioxide capture using lignocellulosic based activated carbon. *Energy*. 2013;61:440-6.

[22] Zhang Z, Zhou J, Xing W, Xue Q, Yan Z, Zhuo S. Critical role of small micropores in high CO₂ uptake. *Physical chemistry chemical physics : PCCP*. 2013;15:2523-9.

[23] Yoo H-M, Lee S-Y, Park S-J. Ordered nanoporous carbon for increasing CO₂ capture. *Journal of Solid State Chemistry*. 2013;197:361-5.

Using activated carbon based technologies for the removal of emerging contaminants from water/wastewater – UQTA (LNEC) Projects

El uso de tecnologías basadas en carbón activo para la eliminación de contaminantes emergentes de aguas /aguas residuales – Proyectos UQTA (LNEC)

M. Campinas¹, E. Mesquita¹, R.M.C. Viegas¹, M.J. Rosa¹

¹ Water Quality and Treatment Laboratory (UQTA), Urban Water Unit, Hydraulics and Environment Department, LNEC – National Civil Engineering Laboratory, Av. do Brasil 101, 1700-066 Lisboa, Portugal

*Corresponding author: mcampinas@lnec.pt

Abstract

An overview is presented on the projects that are being carried out by Water Quality and Treatment Laboratory team of LNEC which use activated carbon based technologies for treating water or wastewater. Emphasis is given to the chemical enhancement of conventional wastewater treatment using “green” powdered activated carbon options, hybrid adsorption/membrane processes or biologically active carbon (BAC) filtration which are considered promising options for upgrading the water/wastewater treatment plants for controlling emerging contaminants such as pharmaceuticals, pesticides and cyanotoxins.

Resumen

Este artículo presenta una visión general de los proyectos que se están llevando a cabo por nuestro equipo en el Laboratorio de Calidad y Tratamiento

del Agua de LNEC que utilizan tecnologías basadas en carbón activado para el tratamiento de agua o aguas residuales. Se da énfasis a la mejora química del tratamiento convencional de aguas residuales utilizando soluciones “green” con carbón activos en polvo y a los procesos híbridos adsorción/membrana o filtración con carbón biológicamente activo (BAC), que se consideran opciones prometedoras para la mejora de las plantas de tratamiento de agua/aguas residuales en el control de contaminantes emergentes, tales como productos farmacéuticos, pesticidas y cianotoxinas.

1. The problem – emerging contaminants

Anthropogenic pressures and global climate change are putting increasing stress on Europe’s freshwater resources, being responsible for sharp variations of raw water availability and quality, and for the degradation of water sources by emerging contaminants (ECs). Besides defying drinking water management, water scarcity and asymmetric space-time distribution is also driving many countries to seek non-conventional water sources. WWTPs play therefore a crucial role both in the safeguard of the drinking water sources and the production of an alternative water source, the treated wastewater which, depending on its use(s), may require an increased level of water treatment. Two of the greatest challenges for WWTPs in a near future are the monitoring and reduction of trace pollutants and the adaptation/development of existing/new wastewater treatment technologies in order to minimize costs and optimize resource consumption [1-2].

Emerging contaminants include: personal care products and pharmaceuticals, increasingly used by the population and not fully retained by the wastewater treatment plants; pesticides from agriculture and cyanotoxins produced by toxic cyanobacterial (blue-green algal) blooms in surface waterbodies. In the last years, regulators and the general public have been expressing an increased concern regarding the presence of emerging contaminants in drinking water and treated wastewaters, since some of the compounds are implied in risk cancer increase, bacterial resistance to antibiotics and reproductive abnormalities in aquatic organisms, based on which a more restrictive legislation is expected in a near future.

For microcystin-LR (MC-LR), a potent hepatotoxin which is one of the most frequently detected cyanotoxin in toxic bloom events [3], WHO established a guideline value of 1.0 µg/L in drinking water [4], limit also adopted by the Portuguese legislation (DL 306/2007). Nevertheless, most of the other ECs, particularly pharmaceuticals, are not yet legislated due to the lack of ecotoxicity data (studies not yet performed or not conclusive) and analytical limitations. Besides the risk, these contaminants share a resistance, partial or total, to conventional treatments at the water treatment plants (WTPs) and urban wastewater treatment plants (WWTPs) since they are often water soluble, polar to semipolar, organic compounds, of intermediate to low molar mass, commonly present in very low concentrations (pg/L to µg/L range).

The control of ECs in WTPs and WWTPs is therefore a priority goal that requires the assessment of the risks involved, the improvement of the current barriers and, if necessary, the (W)WTP rehabilitation with advanced treatment technologies [2]. In this context, in Water Quality and Treatment Laboratory (UQTA) of LNEC several treatment studies pursuing eco-efficient barriers against microcontaminants are being conducted, namely the optimization of the current sedimentation steps in wastewater treatment and the development of advanced treatment essentially based on adsorption, hybrid adsorption/membrane processes and/or biodegradation. The studies are integrated in several European Projects which will be presented in the following sections. Although these projects contain several complementary actions, they will be purposely presented in the perspective of activated carbon interest.

2. Activated carbon for improving conventional



Figure 1. LNECs lamellar sedimentation prototype which will be adapted for pilot trials in two WWTPs (LIFE Impetus).

Figura 1. Prototipo lamelar de sedimentación que será adaptado para ensayos piloto en duas plantas de depuração de águas (LIFE Impetus).

wastewater treatment - LIFE Impetus

LIFE Impetus “Improving current barriers for controlling pharmaceutical compounds in urban wastewater treatment plants” started in January 2016 and will be developed during 3.5 years. It is coordinated by LNEC and has the participation of two wastewater management entities - Águas do Algarve, S.A. and EPAL, SA., one company – EHS Environment and Regional Development Consulting, Lda., and three universities – Algarve University and Science and Pharmacy Faculties of Lisbon University (FCUL and FFUL).

The project aims at demonstrating feasible improvement measures to enhance the removal of pharmaceuticals (PhCs) removal in urban WWTPs with conventional activated sludge (CAS) treatment, the most common biological process in urban WWTPs. The project was developed in the logic of resource efficiency, developing cost-effective solutions based on the existing infrastructures (many of them recently built), as new investments are probably limited in the near future due to economic constraints.

LIFE Impetus involves a 3-year field test in two Portuguese CAS-WWTPs in water stressed regions (Lisbon and Algarve) for demonstrating improved operation strategies and the chemical enhancement of existing barriers for PhC control. Concerning this last one, different clarification strategies will be demonstrated, at pilot scale, including the use of absorbents and coagulants for improving the clarification process, comparing commercial and newly developed materials using natural wastes and plants.

In an early phase, the project includes the preparation and characterization of new adsorbents prepared from local vegetal wastes, cork and carob, and their lab testing to assess the adsorption kinetics and capacity for a short list of target PhCs in synthetic waters. The activated carbons will be prepared and characterized at FCUL, where the screening and the lab-scale assays will also be carried out. Adsorbent(s) with adequate performance will be further tested by LNEC team at lab-scale for the target PhC removal from real wastewaters and used in demonstration trials at pilot-scale.



Figure 2. PAC/MF prototype designed by LNEC and installed in Alcantarilha WTP (LIFE Hymemb).

Figura 2. Prototipo PAC/MF instalado en la planta de tratamiento de agua de Alcantarilha (LIFE Hymemb).

Pilot scale tests will be conducted with 3 sedimentation prototypes which will be constructed or adapted (Figure 1) and installed in Beirolas WWTP (Lisbon) and Faro Noroeste WWTP (Faro-Algarve): one rapid mixer/ lamellar sedimentation prototype for the primary clarification step in Beirolas WWTP, and two conventional sedimentation prototypes for the secondary clarification steps in both WWTPs. Pilot trials will be performed during 18 months in several operating conditions allowing to demonstrate the impact of coagulant and activated carbon addition in the quality of the wastewater resulting from primary and secondary clarification.

3. Activated carbon for hybrid adsorption/membrane processes – LIFE Hymemb and LIFE aWARE

LIFE Hymemb Project (2014-2016) “Tailoring hybrid membrane process for sustainable drinking water production” is coordinated by LNEC and has the partnership of the water company, Águas do Algarve S.A. The project involves a 2-year field test of a powdered activated carbon/ceramic microfiltration (PAC/MF) prototype (Figure 2), designed by UQTA team, in Alcantarilha WTP, to demonstrate the process effectiveness, reliability and efficiency, and ensure a meaningful benchmarking between the advanced and the conventional water treatment processes.

Figure 3 shows the target contaminants of this project as well as the concept of the hybrid PAC/MF process, which integrates the advantages of both low pressure membrane processes and PAC adsorption, and minimizes some of their disadvantages. Low-pressure membranes are not able, unless by adsorption onto the membrane, to retain microcontaminants (e.g. pharmaceuticals, cyanotoxins), but are a safe barrier against (oo)cysts and bacteria and allow a total removal of particles (< 0.1 NTU), including PAC of smaller size (< 10 µm) than usual and thus with faster adsorption kinetics. On the other hand, PAC is able to improve the removal of microcontaminants while enabling to control the irreversible membrane fouling [5].

Adsorption to activated carbon is therefore the key-step of adsorption/membrane processes for the removal of low molar mass (< 300 Da) and intermediate molar

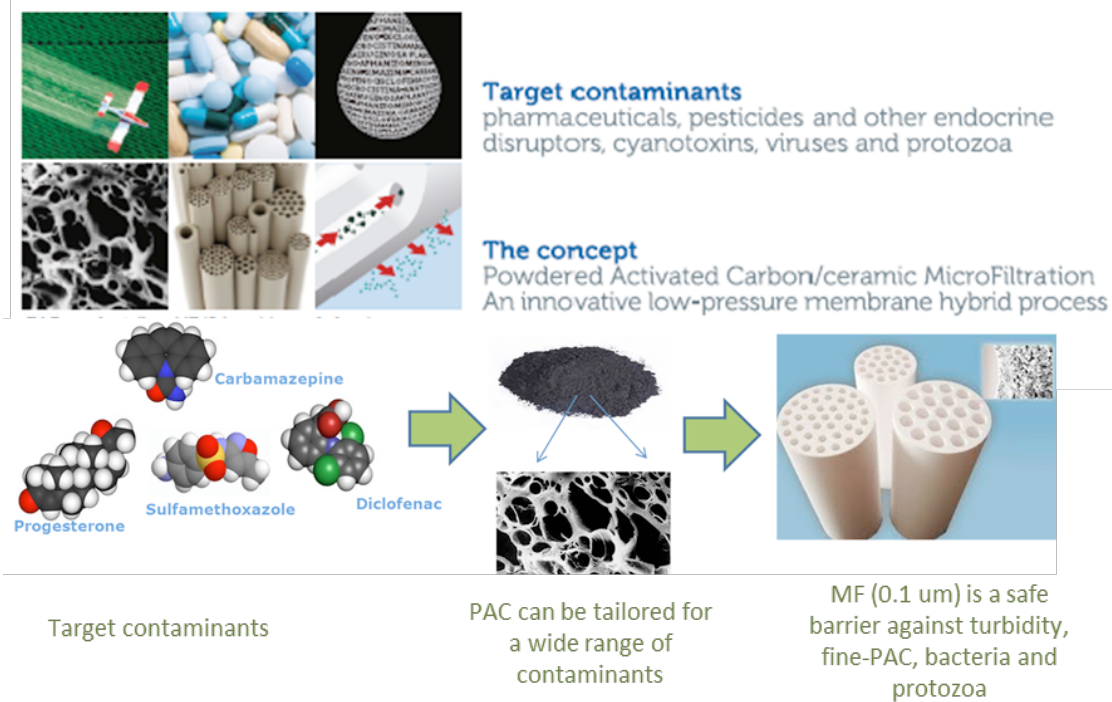


Figure 3. The target contaminants and the concept of LIFE Hymemb project.
Figura 3. Los contaminantes objetivo y lo concepto de proyecto LIFE Hymemb.

mass contaminants (300-1000 Da), and also for viruses, and should allow the adaptation to space-time specificities, presenting solutions for a wide range of applications. For such purpose, one of the innovation pillars of this project is the “tailoring”, i.e. the adjustment of PAC type and dosing to specific contaminants and the high flexibility of membrane process. Therefore, pretreatment is easily adjustable to water quality (PAC and/or coagulant addition and pH adjustment), low-pressure membranes may work

with or without PAC addition, in dead-end operation, minimizing the operating costs, or in cross-flow when/ if necessary (semi dead-end operation).

The selection of the powdered activated carbons adequate to control the project’s target contaminants through PAC conventional addition and the hybrid PAC/MF process followed a 3-step methodology developed in UQTA/LNEC [6]: i) selection of a short-list of ECs representative of the target contaminants;

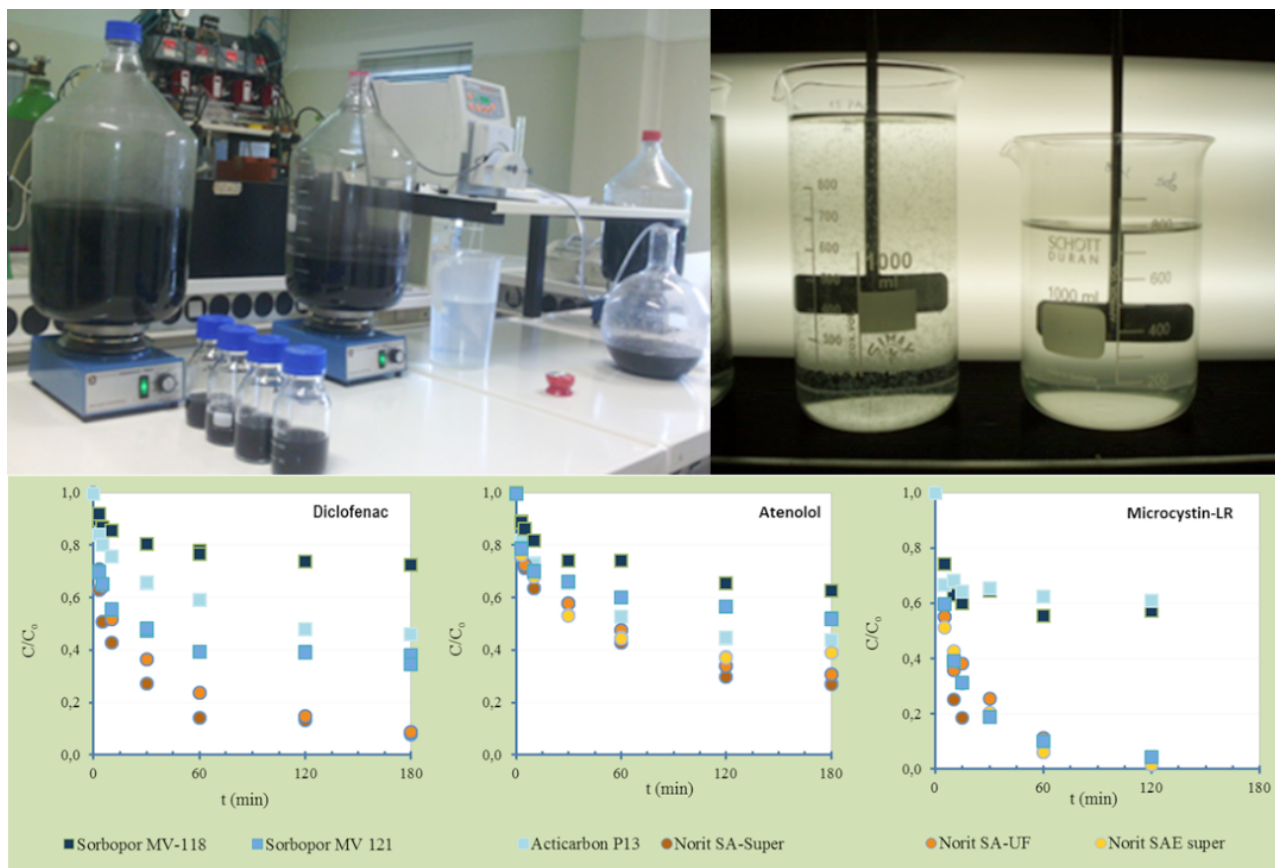


Figure 4. Laboratory tests for selecting PACs and optimizing PAC dosing.
Figura 4. Ensayos de laboratorio para selección de los PAC y la optimización de la dosificación.

ii) pre-selection of commercial PACs with the adequate chemical and textural properties for each application (classification/elimination process based on average particle size, surface charge and pore volume distribution); iii) performance of adsorption kinetics (Figure 4) with the selected PACs and a short-list of ECs in model waters and in natural waters from Alcantarilha WTP.

The preselected PACs were characterized, including their elemental analysis, porosimetry and point of zero charge (pH_{pzc}). Adsorption kinetic assays were performed with the short-list of ECs (5 pharmaceuticals, 1 pesticide and 4 microcystins, natural organic matter). Four PACs were tested for PAC conventional addition and five for PAC/MF application. This methodology allowed selecting one PAC for each application – PAC conventional addition and PAC/MF – which are being tested/demonstrated at pilot scale for EC removal.

PAC/MF prototype is working at Alcantarilha WTP since July 2015. The membrane module (KleanSep, Orelis) contains three tubular ceramic membranes with a total area of 0.75 m² and a pore diameter of 0.1 μm. One of the main objectives of the project is to identify PAC/MF optimal pre-treatment and optimize the PAC/MF operating conditions under different feed water qualities. Up to this moment very promising results have been obtained in terms of treated water fluxes and quality.

LIFE aWARE (2013-2016) “Innovative hybrid MBR-(PAC-NF) systems to promote Water Reuse” is being developed in El Prat WWTP (Barcelona, Spain), combining the technology of membrane bioreactors (MBR) with the hybrid adsorption/membrane process of PAC/nanofiltration (PAC/NF). The project is coordinated by CETAqua (Barcelona), and the UQTA team was responsible for: i) selecting the adequate PAC for controlling ECs and ii) evaluating, at lab scale, of different PAC/NF configurations to be implemented at a pilot scale in El Prat WWTP.

PAC selection followed the methodology developed by UQTA/LNEC and already presented in this section. For the short-list of ECs, the starting point was the contaminants previously detected in campaigns in El Prat WWTP and Llobregat river [7] and afterwards a classification according to the properties that are important for PAC adsorption, namely size, charge and hydrophobicity. Four classes were identified and a compound representative of each class was chosen.

Two activated carbons were preselected for performing the adsorption kinetics until equilibrium of the target pharmaceuticals and, through the analysis of the PAC capacity and removal rate, one activated carbon was chosen to perform the lab PAC/NF trials. For the evaluation of the adsorption capacity complementary adsorption isotherms of the 4 target PhCs in mineral matrix were performed, as well as kinetics and isotherms with micro screened secondary effluent of El Prat WWTP. Adsorption isotherms were modeled with the Freundlich model, for single solutes, or with the Fritz & Schlünder model in competition scenario [8], and the adsorption kinetics were modeled with the Homogeneous Surface Diffusion Model – HSDM [9]. Combining the calibrated models of competitive adsorption isotherms and kinetics batch numeric simulations of the PhC removal vs PAC dose and contact time were performed for predicting removals for different PAC concentrations and contact times.

The PAC/NF configuration tests were performed in a laboratorial unity dimensioned and built by UQTA team. Two configurations were tested: i) one with a single PAC dose at the beginning of the filtration cycle (pulse dosing) and ii) other with continuous PAC dosing (step dosing). The membrane (X-FLOW HFW 1000 da Pentair) has a molecular weight cut-off of 1000 Da, which is high for nanofiltration, allowing to remove dissolved organic compounds of intermediate-high molecular weight (e.g. natural organic matter), but working at a relatively low pressure (around 1 bar) with relatively high fluxes (20- 25 L/m².h). The tests included NF trials (no PAC addition) and PAC/NF trials (single and step PAC dosing) with the evaluation of the removal of the four pharmaceuticals supplemented to the micro screened secondary effluent of El Prat WWTP. No pressure increase was observed with PAC addition and the higher removals (between 68-98%) were observed for a pulse dosing of 100 mg/L PAC [10].

4. Biological activated carbon (BAC) filtration

Due to MC-LR chemical stability and the strong competition with natural organic matter (NOM) (μg MC-LR/L vs mg NOM/L) for adsorbents and oxidants, conventional drinking water treatment may not guarantee the absence of MC-LR in the distributed water [4]. Adsorption-based processes, as hybrid adsorption/ low-pressure processes [5] or biological activated carbon (BAC) filtration [11] are promising

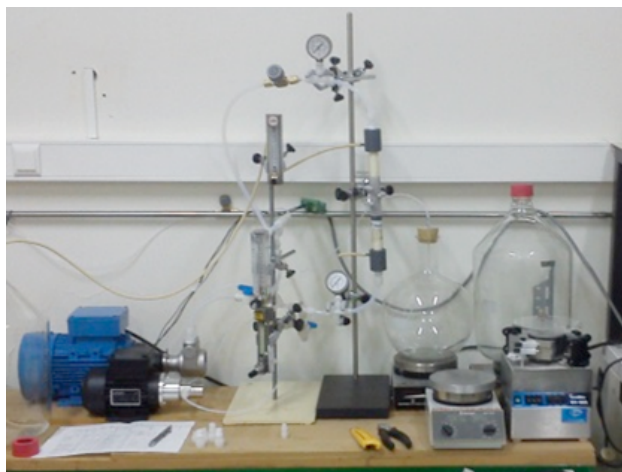


Figure 5. Laboratory unit of PAC/NF
Figura 5. Unidad PAC/NF de laboratorio

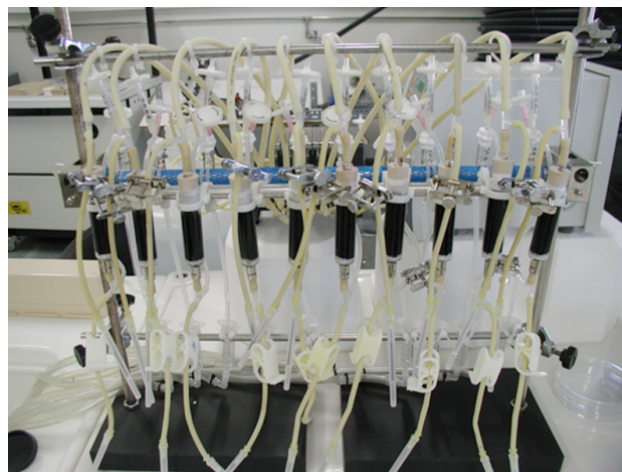


Figure 6. BAC filters assembly.
Figura 6. Ensamblaje de filtros BAC

options for upgrading the water treatment plants. BAC filters are typically robust systems, simple to assemble and with low energy requirements, representing an interesting alternative technology for controlling NOM MC-LR [12] and other microcontaminantss [13].

Granular activated carbon (GAC), besides being an excellent adsorbent material, is a good support media for the attachment and growth of microorganisms and biofilm development. Activated carbon biofilters take advantage of the accumulation of substrates in the GAC particle surface and of the roughness the carbon granules which protects microbial cells from the fluid shear stress. Microorganisms established therein can biodegrade the adsorbed compounds. The synergy of the adsorption, desorption, biodegradation and filtration processes determines the effectiveness of these systems. Biodegradation also promotes continuous bioregeneration of activated carbon and consequently increases filter lifetime. Furthermore, it allows removing assimilable and biodegradable organic carbon and thus controlling the undesirable development of biofilms in the water supply networks [14]. The efficacy of BAC filters depends on the quality of water to be treated (eg., concentration and type of NOM, pH, temperature, ionic strength), the operating conditions (eg., contact time, filtration flow rate and filter back washing frequency), on GAC characteristics (textural properties and surface chemistry), and on the composition and density of the microbial community installed. When operated under optimum conditions, BAC filters can be effective in the removal of biodegradable contaminants such as the cyanotoxins.

A bench-scale study on MC-LR removal by BAC filters was performed at UQTA, focusing the effects of i) organic matter of different absorbability and biodegradability and ii) the filter empty bed contact time (EBCT) on filter performance (Figure 6). This study was carried out with colonised F400 (Chemviron) columns fed with synthetic water that mimicked surface raw water after ozonation and, therefore, able to sustain biological activity in BAC filters (DOC 5 mg C/L as tannic acid, sodium acetate and benzaldehyde, pH 7.2, electrical conductivity 280 μ S/cm). The main results were the following [14]:

- The establishment of biological activity is inevitable in activated carbon filters, provided biodegradable organic matter is present in feed water.
- The biological activity in BAC filters extended the filter lifetime - BAC removal efficiency of tannic acid after 4 months of operation was identical to the removal observed by virgin GAC filter with only one week of operation, in identical conditions.
- Adsorption and biodegradation processes contribute to microcystin-LR removal by BAC filters.
- BAC microbiota is able to biodegrade microcystin-LR in the presence of other carbon and energy sources.
- Lower EBCT values (10 min) favor the biological activity in BAC filters better than higher EBCTs (15 or 20 min) - higher EBCTs provided higher intake rates of dissolved oxygen and nutrients, which favored the uptake/removal rates of dissolved oxygen and tannic acid.

5. Acknowledgements The investigation projects herein presented have received funding from European

Union LIFE programme under grant agreement LIFE14 ENV/PT/000739 (www.life-impetus.eu), LIFE12 ENV/PT/001154 (www.life-hymemb.eu) and LIFE11 ENV/ES/000606 (www.life-aware.eu).

BAC investigation work was supported by the Portuguese Foundation for Science and Technology (FCT - Fundação para a Ciência e Tecnologia) through the project PTDC/ECM/69610/2006 and the PhD fellowship SFRH/BD/21941/2005. FCT is also acknowledged for the Post-Doctoral research grant SFRH/BPD/91875/2012 provided to R.M.C. Viegas.

6. References

- [1] Snyder S, Wert E, Lei H, Westerhoff P, Yoon Y. Removal of EDCs and pharmaceuticals in drinking and reuse treatment processes. Report of AWWA Research Foundation 2007.
- [2] Rosa MJ, Vieira P, Menaia J. O tratamento de água para consumo humano face à qualidade de água na origem. Guia Técnico 13, IRAR/LNEC, Lisboa, ISBN: 978-989-95392-7-3, 2009.
- [3] Codd GA, Morrison LF, Metcalf JS. Cyanobacterial toxins: risk management for health protection. *Toxicology and Applied Pharmacology* 2005; 203: 264-272.
- [4] WHO. Cyanobacterial toxins: Microcystin-LR in drinking-water. Background document for preparation of WHO Guidelines for drinking-water quality. Geneva (WHO/SDE/WSH/03.04/57) 2003.
- [5] Campinas M, Rosa MJ. Removal of microcystins by PAC/UF. *Separations and Purification Technology* 2010;71: 114-120.
- [6] Campinas M, Mesquita E, Viegas RMC, Napier V, Rosa MJ. Seleção de carvão ativado em pó para tratamento de água para consumo humano: aplicação convencional e processo híbrido PAC/MF. In *Anais do Encontro Nacional de Entidades Gestoras de Água e Saneamento - ENEG 2015*. Porto, 1 – 4 December 2015.
- [7] Viegas RMC, Mesquita E, Campinas M, Rosa MJ. Contaminantes emergentes em águas residuais: melhoria do tratamento convencional e opções de tratamento avançado. 13^o Congresso da Água, Lisboa, 7-8 April 2016.
- [8] Campinas M, Viegas RMC, Rosa MJ. Modelling and understanding the competitive adsorption of microcystins and tannic acid. *Water Research* 2014; 47: 5690-5699.
- [9] Viegas RMC, Campinas M, Costa H, Rosa MJ. How do the HSDM and Boyd's model compare for estimating intraparticle diffusion coefficients in adsorption processes. *Adsorption* 2014; 20: 737746.
- [10] Viegas RMC, Mesquita E, Campinas M, Almeida CMM, Rosa MJ. Aplicação da tecnologia híbrida adsorção/nanofiltração no tratamento de águas residuais para reutilização. In *Anais do Encontro Nacional de Entidades Gestoras de Água e Saneamento - ENEG 2015*, 1 – 4 December 2015.
- [11] Newcombe G, Nicholson BC. Water treatment options for dissolved cyanotoxins. *Journal of Water Supply: Research and Technology – Aqua* 2004; 53.4: 227239.
- [12] Wang H, Ho L, Lewis DM, Brookes JD, Newcombe G. Discriminating and assessing adsorption and biodegradation removal mechanisms during granular activated carbon filtration of microcystin toxins. *Water Research* 2007; 41: 4262–4270.
- [13] Reungoat J, Escher BI, Macova M, Keller J. Biofiltration of wastewater treatment plant effluent: Effective removal of pharmaceuticals and personal care products and reduction of toxicity. *Water Research* 2011; 45 (9): 2751276.
- [14] Mesquita E. Remoção de cianotoxinas da água para consumo humano em filtros de carvão ativado com actividade biológica. Algarve University, Faro, Portugal PhD thesis 2012 (portuguese language).

Critical discussion on activated carbons from bio - wastes - environmental risk assessment

Un análisis crítico del uso de carbones activados obtenidos a partir de bioresiduos – evaluación de riesgos medioambientales

M. Bernardo^{1*}, N. Lapa², I. Matos¹, I. Fonseca¹

¹ LAQV/REQUIMTE, Departamento de Química, Faculdade de Ciências e Tecnologia, Universidade Nova de Lisboa, 2829-516 Caparica, Portugal.

² LAQV/REQUIMTE, Departamento de Ciências e Tecnologia da Biomassa, Faculdade de Ciências e Tecnologia, Universidade Nova de Lisboa, 2829-516 Caparica, Portugal.

*Corresponding author: maria.b@fct.unl.pt

Abstract

The use of bio-wastes as precursor materials to prepare porous activated carbons have gained much attention in recent years, mainly due to their abundance and low cost. Particularly, it has been registered an increasing interest in these waste-derived materials for environmental applications, particularly as adsorbents for water treatment. Activated carbons may retain the mineral matter initially present in the precursors as well as the chemical agents used in the activation process; therefore, it is important to assess the potential environmental impact associated to their use, in order to avoid problems related with secondary environmental pollution.

This review intends to give an insight and provide discussion about the environmental risk assessment of activated carbons derived from bio-wastes.

Resumen

La utilización de bio-residuos como materiales precursores de carbones activados porosos ha ganado mucha atención en los últimos años, principalmente por su abundancia y bajo costo; en particular, sus aplicaciones ambientales adsorbentes para tratamiento de aguas. No obstante, estos carbones activados pueden conservar la materia mineral inicialmente presente en los precursores y también los agentes químicos usados en el proceso de activación. Por lo tanto, es importante evaluar el

potencial impacto ambiental asociado a su utilización para evitar problemas de contaminación secundaria.

Esta revisión intenta proporcionar una discusión crítica sobre la evaluación del riesgo ambiental del uso de carbones activados derivados de bio-residuos.

1. Introduction

In the last years, the number of publications concerning the conversion of bio-waste to activated carbon (AC) has significantly increased [1]. Any bio-waste material with a high carbon and low inorganic contents can be used as precursor of AC [2]. Therefore, bio-waste, particularly lignocellulosic wastes, have proved to be suitable, low-cost and abundant alternatives to the conventional raw materials for AC production such as petroleum residues, wood, coal, peat and lignite, which are expensive and the majority non-renewable [1]. Moreover, the use of bio-wastes for the production of AC is a potential pathway to solve the waste management problems of several industries dealing with these type of wastes.

There are two main processes for AC preparation: physical or chemical activation (Figure 1). Physical activation is a two-step process, which means that the raw material is first carbonized in the absence of oxygen in a process named as pyrolysis (usually at temperatures between 400-850 °C) followed by activation of the resulting char from the carbonization step with oxidant gases such as steam or CO₂ (around

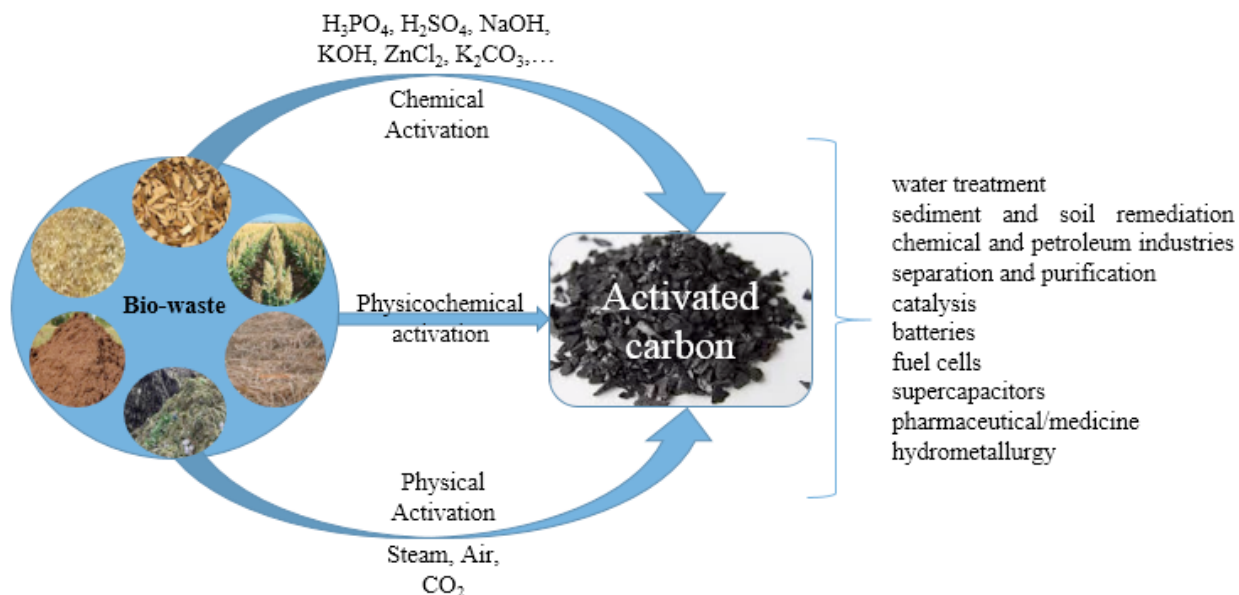


Figure 1. Schematic illustration of bio-wastes-derived activated carbon process and the possible applications.

Figura 1. Ilustración esquemática del proceso de producción de carbones activados derivados de bio-residuos y sus diferentes aplicaciones.

600-1000 °C) [1-2]. Chemical activation can be a one-step or two-step method for the preparation of AC; it involves the impregnation of the precursor (the biomass or the resulting char from the first step of carbonization) with the chemical agent (dehydrating agents and/or oxidants) followed by heating under inert atmosphere at temperatures between 400-800 °C) [1-2]. Also, physical and chemical activation can be used simultaneously.

Chemical activation has the advantage of producing AC with high surface area, but the washing of the resulting carbons in order to remove the residuals of reactants and inorganic matter (ash) from the precursor makes the process time and energy consuming, expensive and environmentally non-friendly [3]. On the other hand, physical activation presents some disadvantages: the ACs are obtained in two steps, higher temperatures of activation and poorer control of the porosity [4].

The high adsorption capacity of AC as a result of the high available area due to an extensive internal pore structure, makes them useful materials in several industries and applications: water treatment [5], sediment and soil remediation [6], chemical and petroleum industries [7], separation and purification [8], catalysis [9], energy storage [10], batteries [11], fuel cells [12], supercapacitors [3], pharmaceutical/medicine [13], hydrometallurgy [14], among others.

The valorisation of AC through the application routes described above requires the knowledge of their composition, properties and risk assessment, mainly due to environmental and economic reasons. Specially, the increasing interest in these waste-derived ACs for environmental applications, particularly those related to soil and water remediation, requires studies on the potential environmental impact associated with their use in order to avoid problems of secondary environmental pollution.

2. Environmental risk assessment of ACs derived from bio-wastes

2.1 The concept of ecotoxicity

According to the European Waste Framework Directive [15], an ecotoxic material presents or may present immediate or delayed risks for one or more compartments of the environment. Therefore, ecotoxicity tests must be applied to identify the potential hazardous properties of a particular material with respect to the environment or to assess the risk related to a site-specific exposure scenario.

Ecotoxicity can be estimated using two approaches: a chemical-specific approach and a toxicity-based approach. In the former case, chemical analyses are compared to quality criteria or threshold values to estimate toxicity. In the latter case, toxicity is measured directly using bioassays [16].

The determination of chemical contaminants in complex materials of unknown composition is an extremely difficult task and does not allow a proper prediction of the global ecotoxic effects. On the other hand, bioassays integrate the effects of all contaminants including additive, synergistic and antagonistic effects [16], and are sensitive to the bioavailable fraction of the contaminants only. Therefore, combining chemical analyses with ecotoxicological tests, as an integrated

strategy to characterize the environmental impact of a given sample, has the advantage of providing a more complete set of information about its global toxic effect [17].

The evaluation of the ecotoxicity of a sample can be made by applying both chemical analyses and biological tests to the raw materials or to their aqueous extracts (eluates). Assays on the aqueous eluate of the sample are the most commonly employed method for ecotoxicity assessment, particularly for materials directly exposed to water (fresh and salted water environments) or to compartments in which the water is an important component (soil). Indeed, the release of soluble constituents upon contact with water can be regarded as a main mechanism of release, which results in a potential risk to the environment as a consequence of the use of waste-derived materials. Moreover, assessing the ecotoxicity on the aqueous soluble fraction of the material provides a more accurate risk to the environment instead of considering the sample bulk composition which would provide an overestimated prediction of the ecotoxic risk [18].

Lapa et al. [19] proposed a methodology to assess the ecotoxicity of a given material: both chemical and ecotoxicological characterizations are performed on the resulting eluates and both are used as positive criteria, i.e., the presence of at least one pollutant in a concentration higher than the threshold values or if at least one of the biological tests is positive, the material shall be classified as ecotoxic. The negative criterion presumes that only the negative response to all of the ecotoxicological tests, and if only all the chemical parameters are below the limit values allows the classification as non-ecotoxic. An adaptation of this methodology to the materials focused in this review is presented on Figure 2.

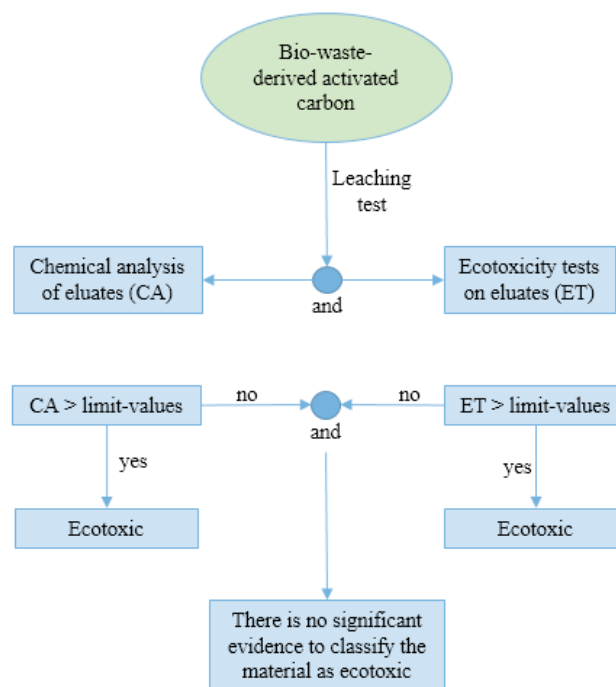


Figure 2. Possible criterion to assess the ecotoxicity of bio-waste-derived ACs.

Figura 2. Criterio posible para evaluación de la ecotoxicidad de carbonos activados derivados de bio-residuos.

There is a significant lack of studies dealing with the ecotoxicological characterization of bio-waste-based

ACs through bioassays. To the authors' knowledge, there is only the work of Yeung et al. [20] that prepared AC from coffee wastes by phosphoric acid and potassium hydroxide activation; all the AC samples produced by those authors showed no ecotoxicity towards the bacterium *Escherichia coli*.

2.2 Leaching behaviour

In order to generate a water extract from a solid material, several leaching methods have been developed and a wide variety of test protocols is available in literature [21-22].

Even with a washing step, ACs may retain the mineral matter initially present in the precursors, as well as the chemical agents used in the activation process or in carbons surface modification. Therefore, the release of potential environmental contaminants is a possibility that might restrict their applications. The use of leaching tests on bio-waste-derived ACs will allow the prediction of contaminants mobility.

In spite of the importance of leaching tests, there is a lack of studies dealing with the application of these methodologies for environmental risk analysis of AC materials.

Rozada et al. [23] produced sewage sludge ACs for liquid phase adsorption through $ZnCl_2$ activation; the authors investigated the amount of Zn from the activating agent leached to the liquid phase from the produced ACs and found that it was significant ($176 \text{ mg L}^{-1} \text{ g}^{-1}$). As Bernardo et al. [17] showed, there is a relationship between Zn concentration in eluates from carbon materials and their ecotoxicity behaviour suggesting the necessity of controlling zinc mobility.

Fitzmorris et al. [24] converted municipal sludge and poultry manure into ACs by steam activation. The resulting ACs presented high ash fraction and were washed with 0.1 M HCl solution. The authors submitted the washed ACs to a leaching step (L/S ratio of 100 L kg^{-1} , stirring for 4 hours) with solutions at different pHs and monitored the release of several metals such as As, Cr, Cu, Ni, Pb, Se and Zn. Under acidic conditions (0.1 M HCl, pH = 1), all the metals were released, but particularly Cu ($1000 - 1600 \text{ mg kg}^{-1}$) and Zn ($400 - 1800 \text{ mg kg}^{-1}$) were leached in higher amounts, also because they were the metals present with high concentrations on ACs. Poultry derived ACs also released considerable amounts of Ni (300 mg kg^{-1}) under acidic pH. At pH 5 (water adjusted with 2% HNO_3), a much smaller amount of each metal was released. The highest concentration determined was for Zn in the municipal sludge-based carbon (300 mg kg^{-1}) and Ni (200 mg kg^{-1}) in the poultry litter-based carbon. Only residual amounts of the other metals were quantified in solution. At pH 7, only some residual Zn was still released from the sludge-based carbon ($<200 \text{ mg kg}^{-1}$). In almost cases, no metals were detected in solution.

Guo et al. [25] studied the leaching of inorganic constituents (dissolved nitrogen, dissolved phosphorus, Cu, Pb, Zn, Cd and As) from poultry litter ACs also produced by steam activation. The produced ACs were washed with 0.1 M HCl solution and then rinsed with water. The washed ACs were then leached (L/S ratio of 10 L kg^{-1} , stirring for 24 h) with deionised water, hot water and HCl 0.1 M solution. All the chemical elements analysed were more readily

extracted with hot water, but especially with the acidic solution. Dissolved nitrogen ($10.66 - 22.35 \text{ mg kg}^{-1}$) and dissolved phosphorus ($74.02 - 1326.9 \text{ mg kg}^{-1}$) were released from the poultry litter derived ACs. The release of heavy metals such as Cu, Pb, Zn and Cd was negligible for all leaching agents, however, As was leached in considerable amounts ($5.36 - 9.71 \text{ mg kg}^{-1}$).

These studies demonstrated that the pH of the liquid medium played a significant role in the amount of metal and non-metal ions that can be released from these type of bio-waste-derived ACs. The mobility of inorganic contaminants is, in general, significantly higher for acidic conditions. Therefore, if these ACs would be considered for environmental applications, the control of pH conditions could be critical.

2.3 Life Cycle Assessment (LCA)

The potential environmental impacts associated with AC production process from bio-wastes can be evaluated through the life cycle assessment (LCA) tool. LCA allows to assess the environmental impacts during the entire life of a product (from the raw material extraction and energy production and use, up to the treatment, recycling and final disposal of the wastes generated)[26], in terms of inputs of energy and natural resources and of outputs of wastes and emissions to the different environmental compartments (air, water and soil) [27].

Hjaila et al. [26] applied the LCA tool to assess the environmental impact associated with activated carbon preparation from olive-waste cake in Tunisia by chemical activation using phosphoric acid. The authors considered the steps of impregnation, pyrolysis, cooling and drying the final AC product. The steps involving transport, raw material drying, crushing, and washing the final AC were excluded from the impact assessment. The results showed that the environmental impacts are dominated by impregnation, followed by pyrolysis of the impregnated precursor, and finally by drying the washed AC. The global warming potential impact was found to be $11.10 \text{ kg CO}_2 \text{ eq/kg AC}$. If transportation, raw material drying, crushing, and AC washing would be included, the environmental impact could be higher than those quantified by authors.

Arena et al. [27] used LCA to quantify all the interactions with the environment across all stages of the life cycle of steam activated coconut shell AC in Indonesia. The boundaries of this study included processes and transportations from raw material acquisition to the delivery of the product, but the use and final disposal of the AC have not been taken into account, which could affect the final results. The authors concluded that the overall environmental performance of the manufacturing process is dominated by the stages of crushing and tumbling (where the coconut, or the AC product, are crushed to obtain powdered or granulated material) and that of heat recovery and steam generation, mainly due to the high consumptions of electrical energy.

No studies were identified on LCA taking into account the entire life of ACs, being possible to conclude that there is a lack of information about the environmental performance of the overall chain of bio-waste-derived activated carbons.

Conclusions

From the survey literature, it became clear that there is a significant lack of studies dealing with the assessment of the ecotoxic properties of bio-waste-based ACs. Particularly, the evaluation of the AC ecotoxicity through the application of biological assays with test organisms representing different ecological chain levels needs more attention in order to prove their value and sustainability.

LCA of these waste-derived materials has to be much more applied to understand all the environmental aspects involved from raw biomass waste through production, use, disposal and/or recycling. LCA results will allow to indicate the operations with the greatest effects on the environmental performance of ACs production and hence where improvements are necessary.

Acknowledgments

The authors would like to acknowledge the Portuguese Foundation for Science and Technology (FCT) for the financial support with the Post-Doc grants SFRH/BPD/93407/2013. I. Matos thanks FCT for project Investigador FCT contract IF/01242/2014/CP1224/CT0008. This work was also supported by the Associate Laboratory for Green Chemistry LAQV which is financed by national funds from FCT/MEC (UID/QUI/50006/2013) and co-financed by the ERDF under the PT2020 Partnership Agreement (POCI-01-0145-FEDER – 007265).

References

- [1] Yahya MA, Al-Qodah Z, Ngah CWZ. Agricultural bio-waste materials as potential sustainable precursors used for activated carbon production: A review. *Renew Sustain Energy Rev* 2015; 46:218–235.
- [2] Ioannidou O, Zabaniotou A. Agricultural residues as precursors for activated carbon production—A review. *Renew Sustain Energy Rev* 2007; 11:1966–2005.
- [3] Abioye AM, Ani FN. Recent development in the production of activated carbon electrodes from agricultural waste biomass for supercapacitors: A review. *Renew Sustain Energy Rev* 2015; 52:1282–1293.
- [4] Hernández-Montoya V, García-Servín J, Bueno-López JI. Thermal Treatments and Activation Procedures Used in the Preparation of Activated Carbons. In: Virginia Hernández Montoya (Ed.). *Lignocellulosic Precursors Used in the Synthesis of Activated Carbon - Characterization Techniques and Applications in the Wastewater Treatment*, InTech, 2012.
- [5] Dias JM, Alvim-Ferraza MCM, Almeida MF, Rivera-Utrilla J, Sánchez-Polo M. Waste materials for activated carbon preparation and its use in aqueous-phase treatment: A review. *J Environ Manage* 2007; 85:833–846.
- [6] Hilber I, Buchelli TD. Activated carbon amendment to remediate contaminated sediments and soils: a review. *Global NEST J* 2010; 12 (3):305–317.
- [7] Zhao C, Gu P, Zhang G. A hybrid process of powdered activated carbon countercurrent two-stage adsorption and microfiltration for petrochemical RO concentrate treatment. *Desalination* 2013; 330:9–15.
- [8] Kacem M, Pellerano M, Delebarre A. Pressure swing adsorption for CO₂/N₂ and CO₂/CH₄ separation: Comparison between activated carbons and zeolites performances. *Fuel Process Technol* 2015; 138: 271–283.
- [9] Matos I, Silva MF, Ruiz-Rosas, Vital J, Rodríguez-Mirasol J, Cordero T, Castanheiro JE, Fonseca IM. Methoxylation of α -pinene over mesoporous carbons and microporous carbons: A comparative study. *Microporous Mesoporous Mater* 2014; 199:66–73.
- [10] Bader N, Ouederni A. Optimization of biomass-based carbon materials for hydrogen storage. *J Energy Storage* 2016; 5:77–84.
- [11] Liu E, Shen H, Xiang X, Huang Z, Tian Y, Wu Y, Wu Z, Xie H. A novel activated nitrogen-containing carbon anode material for lithium secondary batteries. *Mater Lett* 2012; 67:390–393.
- [12] Santoro C, Artyushkova K, Babanova S, Atanassov P, Ieropoulos I, Grattieri M, Cristiani P, Trasatti S, Li B, Schuler AJ. Parameters characterization and optimization of activated carbon (AC) cathodes for microbial fuel cell application. *Bioresour Technol* 2014; 163:54–63.
- [13] Rosinski S, Lewinska D, Piaztkiewicz W. Application of mass transfer coefficient approach for ranking of active carbons designed for hemoperfusion. *Carbon* 2004; 42:2139–2146.
- [14] Seo SY, Choi WS, Yang TJ, Kim MJ, Tran T. Recovery of rhenium and molybdenum from a roaster fume scrubbing liquor by adsorption using activated carbon. *Hydrometall* 2012; 129–130:145–150.
- [15] Directive 2008/98/EC of the European Parliament and of the Council of the European Union of 19 November 2008 on waste and repealing certain Directives, OJ L 312, 22.11.2008, p. 3–30.
- [16] European Standard 14735:2005. Characterisation of waste – Preparation of waste samples for ecotoxicity tests, European Committee for Standardization, Brussels, Belgium, 2005.
- [17] Bernardo M, Mendes S, Lapa N, Gonçalves M, Mendes B, Pinto F, Lopes H. Leaching behaviour and ecotoxicity evaluation of chars from the pyrolysis of forestry biomass and polymeric materials. *Ecotoxicol Environ Saf* 2014; 107:9–15.
- [18] Bernardo M, Study of the valorisation of the solid by-products obtained in the co-pyrolysis of different wastes. Universidade Nova de Lisboa, PhD thesis 2013.
- [19] Lapa N, Barbosa R, Morais J, Mendes B, Méhu J, Oliveira JFS. Ecotoxicological assessment of leachates from MSWI bottom ashes. *Waste Manage* 2002; 22:583–593.
- [20] Yeung P, Chung P, Tsang H, Tang JC, Cheng GY, Gambari R, Chui C, Lam K. Preparation and characterization of bio-safe activated charcoal derived from coffee waste residue and its application for removal of lead and copper ions. *RSC Adv* 2014; 4:38839–38847.
- [21] Kalemekiewicz J, Sitarz-Palczak E. Efficiency of leaching tests in the context of the influence of the fly ash on the environment. *J Ecol Eng* 2015;16(1):67–80.
- [22] Hansen JB, Gamst J, Laine-Ylijoki J, Wahlström M, Larsson L, Hjelmar O. A framework for using leaching test for non-volatile organic compounds. NT Technical Report 585, Nordic Innovation Centre project number: 04050, Oslo, Norway, 2005.
- [23] Rozada F, Otero M, Morán A, García AI. Activated carbons from sewage sludge and discarded tyres: Production and optimization. *J Hazard Mater B* 2005; 124:181–191.
- [24] Fitzmorris KB, Lima IM, Marshall WF, Reimers RS. Anion and Cation Leaching or Desorption from Activated Carbons from Municipal Sludge and Poultry Manure as Affected by pH. *Water Environ Res* 2006; 78:2324.
- [25] Guo M, Qiu G, Song W. Poultry litter-based activated carbon for removing heavy metal ions in water. *Waste Manage* 2010; 30:308–315.
- [26] Hjalila K, Baccar R, Sarrà M, Gasol CM, Blázquez P. Environmental impact associated with activated carbon preparation from olive-waste cake via life cycle assessment. *J Environ Manage* 2013; 130:242–247.
- [27] Arena N, Lee J, Clift R. Life Cycle Assessment of activated carbon production from coconut shells. *J Clean Prod* 2016; in press.

Micropore size distribution of activated carbons: a key factor for a deeper understanding of the adsorption mechanism of pharmaceuticals

Distribución de tamaño de microporos en carbones activados: un factor clave para una comprensión más profunda del mecanismo de adsorción de productos farmacéuticos

A. S. Mestre*, M. Galhetas, M. A. Andrade

Centro de Química e Bioquímica, Faculdade de Ciências, Universidade de Lisboa, 749-016 Lisboa, Portugal.

*Corresponding author: asmestre@fc.ul.pt

Abstract

The elucidation of the pore structure of activated carbons requires complementary adsorption data and is of fundamental importance for the comprehension of the adsorption mechanism of organic molecules, as is the case of pharmaceutical compounds. The present work reports studies developed in the Adsorption and Adsorbent Materials Group highlighting the contribution of the micropore size distribution (MPSD), obtained from the fitting of CO₂ adsorption data, for the deeper understanding of kinetic and equilibrium adsorption data of pharmaceutical compounds with distinct dimensions and behaviours in solution.

Resumen

La elucidación de la estructura porosa de carbones activos requiere datos de adsorción complementarios y es de importancia fundamental para la comprensión del mecanismo de adsorción de moléculas orgánicas, como es el caso de compuestos farmacéuticos. El presente estudio reporta los trabajos desarrollados en el Grupo de Adsorción y Materiales Adsorbentes de la Universidad de Lisboa destacando la contribución de la distribución del tamaño de microporos, obtenida mediante el ajuste de los datos de adsorción de CO₂, para la comprensión más profunda de los datos cinéticos y de equilibrio de la adsorción de compuestos farmacéuticos con distintas dimensiones y comportamientos en solución.

1. Introduction

The detailed characterization of activated carbons (texture, chemical composition, morphology) is quite a challenging task, given the extreme complexity regarding size and shape of pores, and variety of structures and surface functionalities.

The most effective experimental approach for obtaining information on the adsorption process is the experimental determination of an isotherm, which contains information on the adsorption process. On the other hand, knowledge of the surface chemistry of carbon materials is also of fundamental importance, since their behaviour is strongly influenced by the presence of chemical species at the surface that will allow their use in various technological fields. Regardless the unquestionably importance of the surface chemistry characterization, in this paper, we will focus on the key role of the textural characterization of the materials to allow deeper insights on the adsorption mechanism of pharmaceutical compounds (Figure 1).

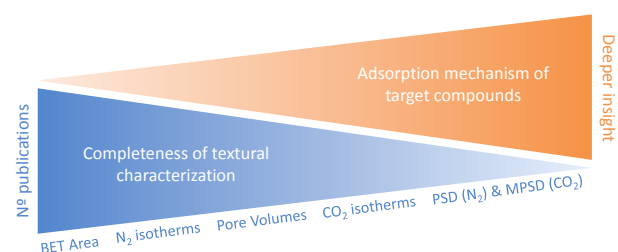


Figure 1. Relationship between the degree of completeness of activated carbons' textural characterization and the deeper comprehension of the adsorption mechanism of pharmaceutical compounds (PSD – pore size distribution; MPSD – micropore size distribution).

Figura 1. Relación entre el grado de exactitud de la caracterización textural carbones activados y la comprensión más profunda del mecanismo de adsorción de compuestos farmacéuticos (PSD - distribución del tamaño de poros; MPSD - distribución del tamaño de microporos).

The textural characterization of activated carbon consists on the determination of N₂ and CO₂ isotherms and on the use of mathematical models for the quantification of the specific surface area, pore volume and pore size distribution. However, the great majority of studies reporting the use of activated carbon materials for the removal of contaminants presents only few information regarding the porous network of the adsorbents, which consequently limits a thorough analysis of the collected data and the comparison with other literature studies.

As illustrated in Figure 1, , the most often reported textural parameter is, by far, the specific surface area (BET area), determined by the model proposed by S. Brunauer, P. H. Emmett and E. Teller, in 1938, which aimed to quantitatively describe the physical adsorption of vapor in non-porous solids [1]. Yet, there is a general awareness of the shortcomings in relation to the underlying theory of this model, and in the particular case of microporous adsorbents, such as activated carbons, there is also a lack of a real physical meaning. So, the comparison of the textural properties of different samples based only on the BET area value can therefore be misleading, and further characterization of the texture is advised.

The simple analysis of the shape of experimental isotherms according to the IUPAC classification [2] enables to gather qualitative information about the type and fraction of pores of an activated carbon. However, beyond the analysis of the shape of the curves, isotherms must also be interpreted quantitatively, so that comparisons between materials can be made. This quantitative analysis of the micro, meso and

total pore volumes can be performed by numerous analytical methods that can be applied to the N_2 adsorption data, as is the case of Gurvich rule for total pore volume or the Dubinin-Radushkevich equation, t -method or a_s method for the micropore volume [3-7].

Even with the information gathered from all the above mentioned methods, it is not possible to justify some results regarding adsorption processes in liquid or gas phase, when the effect of the surface chemistry is ruled out. In these cases the pore size distribution assessment from the N_2 and CO_2 adsorption data stands as an additional tool for the textural characterization of carbon materials. A correct assessment of the micropore size distribution (MPSD) of the materials can be crucial to explain, for example, the maximum capacity, affinity and more complex phenomena, such as two-step isotherms, or the influence of the temperature in the adsorption process, as it will be further demonstrated in section 3.

2. Micropore size distribution assessment

A detailed characterization of activated carbons should include pore size analysis in the entire range of pores, and for this it is important to combine data from N_2 and CO_2 adsorption at, respectively, $-196^\circ C$ and $0^\circ C$. Since the micropore volume constitutes the most important fraction of the surface area of activated carbons, the use of CO_2 instead of N_2 adsorption data has been repeatedly proposed as a better alternative due to the well-known diffusion limitations of N_2 in carbons with narrow micropores [4,8]. In fact, the assessment of the MPSD from CO_2 adsorption data is a key information, particularly when the adsorption of molecules of small dimensions is envisaged, since it may allow a deeper understanding of the diffusion and adsorption mechanism.

There are many methods to calculate the MPSD, most of them based on classical methods, *i.e.*, Horvath-Kawazoe, t -plot, and methods based on the theory of micropore volume filling (TMVF), namely the models of Dubinin-Radushkevich (DR), Dubinin-Radushkevich-Astakhov (DA) and Dubinin-Radushkevich-Stoeckli (DRS) [3-5]. The distribution of mesopores is generally made by methods based on the Kelvin equation, such as Barrett, Joyner and Halenda (BJH) or Broekhoff and de Boer (BdB), and their modifications, being however out of the scope of the present manuscript

In the 80's considerable progress was made on the understanding of fluid behaviour constrained by the presence of walls, which led to the application of the Density Functional Theory (DFT) to the adsorption phenomena [9-11]. From a mathematical approach, the DFT method applied to the calculation of the pore size distribution (PSD) is based on the integral of the individual isotherms of defined given sizes.

The most advanced form of this theory is called the non-local approach (NLDFIT) that is based on calculating model isotherms that may be used to determine pore size distribution from gas adsorption data. Nowadays, the advanced methods based on NLDFIT succeed in determining the pore size distribution in the entire range of pore sizes accessible to the adsorptive molecule [12,13].

However, the determination of the micropore size distribution remains a difficult problem for most activated carbons, given their highly developed

micropore network. In fact, only few studies in the literature report the assessment of MPSD of activated carbons by the use of the more sophisticated NLDFIT method applied to CO_2 adsorption data [14]. Moreover, these methods are difficult to implement due to their mathematical complexity, so, the majority of studies only present MPSDs assessed from the application of DRS equation what, as it will be discussed in the following, can lead to an inaccurate information.

In a study developed by Pinto and coworkers [15], the application of two variations of the DR equation to assess the micropore size distribution of carbon samples was discussed. The methodologies used for the fitting of the CO_2 adsorption data were the conventional DRS equation and a novel approach for fitting the integral adsorption equation for which the MPSDs are not constrained to a particular preassumed shape.

From the comparison of MPSD data obtained by these approaches for laboratory-made and commercial samples, the authors concluded that the results are highly dependent on the method used to make the adjustment of the experimental data, as it is clearly illustrated in Figure 2. Although the plots for samples AC1 and AC2 are relatively similar, significant differences were found between the results obtained by the two methods for the other two samples.

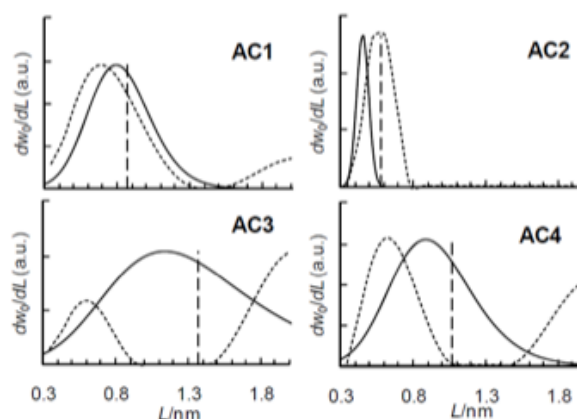


Figure 2. Micropore size distributions (MPSDs) of activated carbons obtained by fitting the DRS equation (solid line) and by the methodology proposed by Pinto *et al.* [15] (broken line). The vertical dashed line represents the weighted average micropore size of the distribution obtained by fitting the integral adsorption equation. Reprinted with permission from Ref. [15]. Copyright 2010 American Chemical Society.

Figura 2. Distribuciones del tamaño de microporos de carbonos activos obtenidos mediante el ajuste de la ecuación DRS (línea continua) y por la metodología propuesta por Pinto *et al.* [15] (línea discontinua). La línea vertical discontinua representa el tamaño de microporo medio ponderado de la distribución obtenida mediante el ajuste de la ecuación de adsorción integral. Reimpreso con el permiso de la referencia. [15]. Copyright 2010 American Chemical Society.

The DRS equation gives a micropore size distribution that is a Gaussian average of the actual distribution, and it is only expected to give a good description of the actual distribution in cases where the activated carbons have relatively narrow and symmetric distributions, as in samples AC1 and AC2. So, the Gaussian-shaped distribution obtained from the DRS equation is not a suitable description for the MPSD of activated carbons for all cases.

From the practical point of view, it is preferable to use the fitting of the integral adsorption equation for

the determination of the MPSTDs of carbon materials, since it does not assume a Gaussian distribution, and consequently allows to obtain more accurate pore size distributions. This method has been increasingly used in our group for the assessment of the MPSTDs of activated carbons, and has enable us to interpret results of the adsorption of pharmaceuticals from liquid phase in a very straightforward way, as it will be highlighted in the following section.

The importance of using complementary data, and particularly the determination of MPSTD, to assure a deeper characterization of activated carbons is exemplified in Figure 3 and Table 1 for three microporous carbons with similar type I(a) N₂ adsorption isotherms. Following the most common approach for characterizing porous materials, it is clear that carbons B and C have similar BET areas, while carbon A presents a slightly higher value, which are in accordance with the isotherms depicted in Figure 3(a). The type I(a) isotherms reveal the presence of a narrow micropore distribution and the quantification of the pore volumes presented in Table 1 corroborates this analysis. The volumes of micropores assessed from the application of the a_s method to the N₂ adsorption data allows, however, to gather more information regarding the amount of ultra and supermicropores in each sample. This volumes are also in agreement with the micropore volumes assessed by the DR method to both N₂ and CO₂ adsorption data. In fact, samples A and B present a higher volume of narrower micropores ($W_{DR\ CO_2} > W_{DR\ N_2}$), while sample C has a higher percentage of larger micropores.

Although all this discussion already points out the differences between these three microporous activated carbons, the further determination of the MPSTD is even more informative, since the amount of micropores with different pore widths is clearly quantified (Figure 3(c)). In fact, this analysis reveals striking differences between these samples, with carbon A and B presenting monomodal distributions, centered at, respectively, 0.72 nm and 0.62 nm, and carbon C presenting a bimodal distribution with micropores with widths between 0.4 and 0.9 nm, and also higher than 1.2 nm. Regarding the samples with a monomodal distribution, carbon B has a sharper distribution (0.5 to 0.8 nm), characteristic of materials with molecular sieve properties, while carbon A has a wider micropore size distribution (0.5 to 1.4 nm).

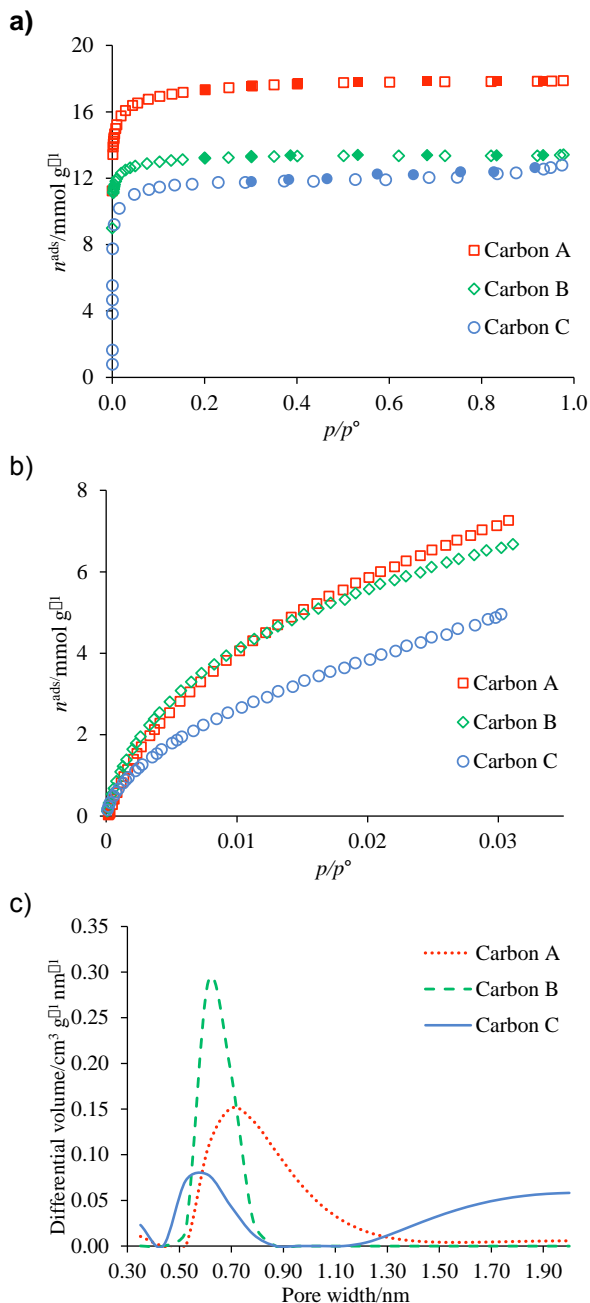


Figure 3. Textural characterization of three activated carbon samples: (a) N₂ adsorption-desorption isotherms at -196 °C, closed symbols are desorption points; (b) CO₂ adsorption isotherms at 0 °C; (c) micropore size distributions according to [15].

Figura 3. Caracterización textural de tres muestras de carbón activado: (a) isoterma de adsorción-desorción de N₂ a -196 °C, símbolos cerrados son puntos de desorción; (B) isoterma de adsorción de CO₂ a 0 °C; (c) distribuciones del tamaño de microporos de acuerdo con [15].

Table 1. Nanotextural properties of three microporous activated carbons.

Tabla 1. Propiedades nanotexturales de tres carbones activos microporosos.

Materials	<i>a_s method</i>						<i>DR equation</i>	
	A_{BET} (m ² g ⁻¹)	V_{total} (cm ³ g ⁻¹)	V_{meso} (cm ³ g ⁻¹)	$V_{\alpha total}$ (cm ³ g ⁻¹)	$V_{\alpha ultra}$ (cm ³ g ⁻¹)	$V_{\alpha super}$ (cm ³ g ⁻¹)	$W_{DR\ N_2}$ (cm ³ g ⁻¹)	$W_{DR\ CO_2}$ (cm ³ g ⁻¹)
Carbon A	1375	0.63	0.01	0.62	0.35	0.27	0.58	0.65
Carbon B	1053	0.47	0.00	0.47	0.30	0.17	0.46	0.52
Carbon C	907	0.43	0.03	0.40	0.16	0.24	0.40	0.27

A_{BET} - Apparent surface area, estimated from the N₂ isotherms, applying the BET equation in the range 0.05 < p/p° < 0.15 [3]; V_{total} - Total pore volume, evaluated at $p/p^\circ = 0.975$ in the N₂ adsorption isotherms at -196 °C [6]; V_{meso} - Mesopore volume, obtained from the difference between V_{total} and $V_{\alpha total}$; $V_{\alpha total}$, $V_{\alpha ultra}$, $V_{\alpha super}$ - Total micropore volume, ultramicropore volume (width less than 0.7 nm), and supermicropore volume (width between 0.7 and 2 nm), obtained from the application of the a_s method applied to the N₂ adsorption data, taking as reference the isotherm reported by Rodríguez-Reinoso *et al.* [7]; $W_{DR\ N_2}$ and $W_{DR\ CO_2}$ - Micropore volume analyzed using the Dubinin–Radushkevich formulism to the N₂ and CO₂ adsorption data [3].

3. MPSPD for deeper insights into the adsorption of pharmaceuticals onto activated carbons

In this section, examples illustrating the importance of MPSPD as a tool for obtaining a deeper insight into the adsorption mechanism of pharmaceutical compounds by activated carbons, will be presented. In all the cases, the MPSPD of the porous carbons was obtained from CO₂ adsorption data, according to the method described by Pinto *et al.* [15]. The molecular structure and information regarding the critical dimensions of the pharmaceutical compounds for which the adsorption mechanism onto activated carbons will be discussed in the following sections are displayed in Figure 4.

3.1 Ibuprofen

Regarding the ibuprofen adsorption onto activated carbons prepared from industrial pre-treated cork, a deeper characterization of the microporosity revealed to be necessary for the interpretation of the obtained results [17], since the correlation of the different ibuprofen uptakes for samples with similar microporous volumes ($V_{\alpha \text{ total}}$) was not so straightforward. For example, for three activated carbons with $V_{\alpha \text{ total}}$ between 0.27 and 0.32 cm³ g⁻¹, removal efficiencies ranging from 16 % to 69 % were obtained, being the higher removal attained for the sample with the intermedium $V_{\alpha \text{ total}}$ value. The surface chemistry of two of these samples assessed by the determination of the pH at the point of zero charge (pH_{PZC}) is similar – $\text{pH}_{\text{PZC}} \sim 5$ – but samples presented distinct removal efficiencies (16% and 33%).

Given the critical dimension of ibuprofen, 0.72 nm, and that no restriction to the diffusion of ibuprofen

into larger micropores is likely to occur, the diffusion towards the adsorption active sites has proved to be dependent of the presence of larger micropores. The uptake trend was also dependent on the MPSPDs of the samples, pointing out that ibuprofen adsorption occurs mainly in pores with widths between 0.72 and around 1.40 nm. Besides, according to the MPSPDs, the sample with the higher percentage of micropores between these widths (44%), *i.e.*, close to the ibuprofen critical dimensions, presents the higher value for the Langmuir constant (K_L), a measure of the adsorption affinity.

The effect of surface chemistry was also considered, but no enhanced adsorption was observed for samples presenting the most favorable electrostatic interaction (neutral carbons surface or positively charged – solution pH > pH_{PZC} – and ibuprofen in the anionic form), being then possible to conclude that for the adsorption of ibuprofen onto this set of carbons, texture stands as the determinant parameter controlling the process.

3.2 Caffeine

On the opposite of what was observed for ibuprofen adsorption, to justify the adsorption mechanism of caffeine onto activated carbons, both texture and surface chemistry have to be taken into account [18,19].

Caffeine is a compound with a critical dimension of ~ 0.45 nm, so, it will have less steric constrains to the diffusion than ibuprofen. In fact, literature data reveals higher adsorption capacity for activated carbons with higher micropore volume, particularly if large

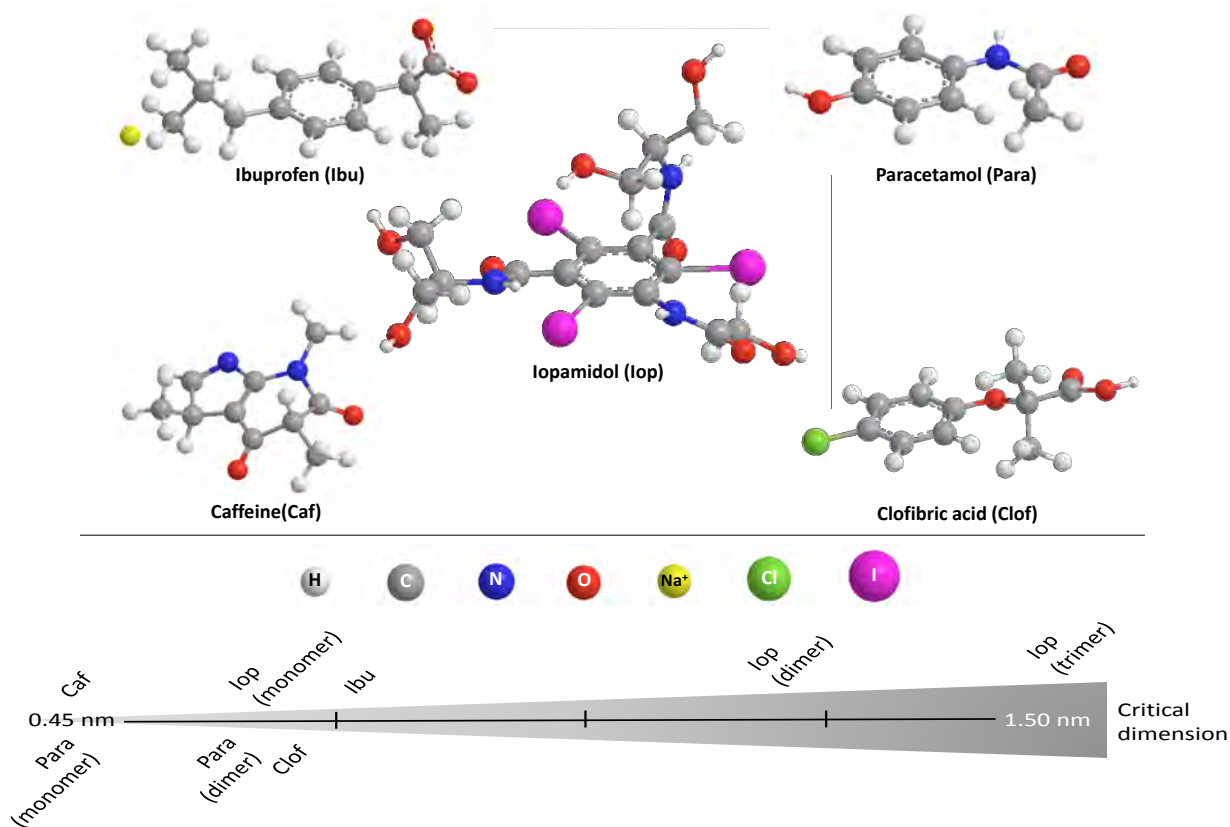


Figure 4. Molecular structure and scale highlighting the trend of the critical dimensions of the mentioned pharmaceutical compounds (see ref. [16] and references cited in the following topics for more detailed data). For paracetamol and iopamidol, the critical dimensions of their aggregates are also presented.

Figura 4. Estructura molecular y escala que destaca la tendencia de las dimensiones críticas de los compuestos farmacéuticos mencionados (véase la ref. [16] y las referencias citadas en los siguientes temas para obtener información más detallada). Para el paracetamol y el iopamidol, se presentan también las dimensiones críticas de sus agregados.

amounts of pores with apertures close to the critical dimensions of caffeine are present, and consequently a more efficient packing of the molecules is possible. The adsorption affinity values obtained for caffeine adsorption onto char-derived, rapeseed-derived and commercial activated carbons cannot be explained considering only the MPSPD of the samples. Actually, besides the textural parameters, the adsorption affinity of caffeine seems to be also controlled by the surface chemistry of the carbons, most possible due to the high percentage of lone electron pairs in the caffeine molecule.

3.3 Paracetamol

The influence of the MPSPD of carbons obtained from a residue produced from pine gasification (fly ash), in the adsorption process of paracetamol was also demonstrated [18,20], and allowed to rationalize the unexpected lower adsorption affinities of the lab-made carbons.

In these works the authors obtained lower adsorption affinities for the activated carbons presenting the maximum of the MPSPDs aligned with the critical dimensions of paracetamol molecule (~0.46 nm), what is not commonly observed. However, if considering also the existence of paracetamol dimers in solution, with slightly higher critical dimensions (~0.66 nm), both maximum adsorption capacities and affinities could be related with the MPSPD of the materials. In another study, sucrose-derived activated carbons were also tested for paracetamol adsorption [16] and once again the MPSPD allowed to justify the adsorption capacities. As it is clearly illustrated in Figure 5, the maximization of the adsorption capacity for paracetamol occurs in the materials presenting a larger volume of micropores with dimensions between 0.5 and 1.1 nm.

Following this research topic the authors investigated the influence of the temperature (20–40 °C) in the adsorption process of paracetamol onto activated carbons with distinct MPSPD [21] and proved that paracetamol oligomers were formed in the presence of the activated carbon. Once again the MPSPD of

the adsorbents allowed to explain the temperature dependence observed. The sample presenting a continuous MPSPD obeys to the expected thermodynamic behaviour for a simple adsorption process (higher adsorption capacity at lower temperature), while for materials with the maximum of the MPSPD centered near the critical dimensions of the species or when the MPSPD is not continuous, the maximum adsorption capacity increases when temperature changes from 20 °C to 40°C. This finding was rationalized considering stronger adsorbent–adsorbate interactions that promote changes in the oligomers conformations, allowing better diffusion and packing of these larger species during adsorption. This results could not be explained just considering the energy gain associated with the temperature increase.

3.4 Iopamidol

Iopamidol is a voluminous molecule for which more steric hindrance during the adsorption process onto microporous activated carbons can be expected. In order to elucidate the parameters controlling the adsorption of this molecule, activated carbons with different pore network were already tested [16,22].

The results obtained with two sets of samples were very distinct and unexpected, since two-step isotherms were obtained for lab-made samples, while commercial materials presented type I curves [22]. These results could only be explained correlating the MPSPDs of the carbons with theoretical and experimental data that revealed the existence of iopamidol aggregates in solution, with obviously increasing critical dimensions (i.e. monomer ~ 0.6 nm, dimer ~ 1.2 nm and trimer ~ 1.5 nm), and the dependence of this aggregation with concentration. The two-step isotherms were only observed for lab-made samples where micropores with widths between 1.2 and 2 nm are absent, and consequently the diffusion of larger species towards the adsorption site is hindered. The second step of the isotherms corresponds to the adsorption of the dimer and trimer species in larger porosity.

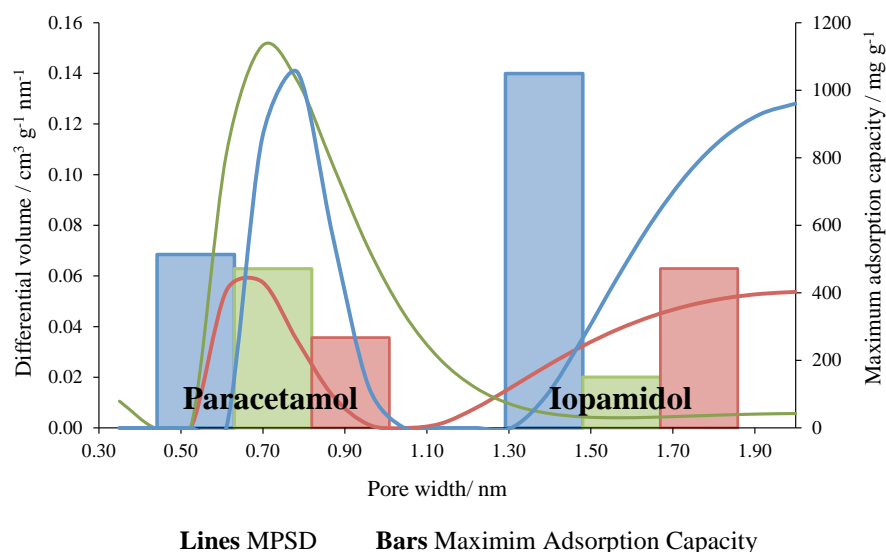


Figure 5. Relation between the micropore size distribution (MPSPD) of three activated carbons and their maximum adsorption capacity for paracetamol and iopamidol. Lines represent the micropore size distribution while bars correspond to the maximum adsorption capacity for each pharmaceutical compounds.

Figura 5. Relación entre la distribución del tamaño de microporos (MPSPD) de tres carbones activados y su capacidad de adsorción máxima de paracetamol y iopamidol. Las líneas representan la distribución del tamaño de microporo mientras que las barras corresponden a la capacidad máxima de adsorción para cada un compuesto farmacéutico.

The importance of the MPSPD in the adsorption of iopamidol is also clearly illustrated in the results obtained with sucrose-derived activated carbons [16]. The initial adsorption rate is higher for the material with a well-developed mesopore network, a trend also observed in the previous example. On the other hand, the adsorption capacity of the carbon presenting the higher volume of pores with widths higher than 1.3 nm overcomes by far the performance of the other tested carbons, as it is shown in Figure 5. Thus, to maximize iopamidol adsorption, activated carbons must present a MPSPD with a high percentage of pores with apertures larger than 1.3 nm.

3.5 Clofibrac acid

In a work that aimed to evaluate the effect of solution pH and water hardness in clofibrac acid adsorption onto two commercial activated carbons, the MPSPDs also contributed to explain the results in hard water at pH 8 [23].

Independently of the water hardness degree, the increase of solution pH from 3 to 8 lead in all cases to a lower removal of clofibrac acid, since the deprotonated clofibrac acid specie present at pH 8 has a much higher solubility. However, at pH 8, when changing from deionized water to hard water, the maximum adsorption capacity increases, being the most pronounced effect observed for the carbon presenting the larger volume of wider micropores. These data were reasoned considering calcium complexation with clofibrate anion, as exposed by molecular modeling and conductivity studies, that allows the adsorption of clofibrac acid entities as CaClO_2 or CaClO^- . The most noticeable effect, observed for the carbon with the larger volume of micropores with apertures higher than 1.1 nm, was related with the possibility of accommodating more entities, thus amplifying the enhancement of clofibrac acid adsorption in hard water.

5. Acknowledgments

The work reported here was supported by the Portuguese Science and Technology Foundation (FCT) through the financial to the Center of Chemistry and Biochemistry (UID/MULTI//00612/2013). ASM also thanks FCT for a Post-doc grant (SFRH/BPD/86693/2012) and MG thanks CNPq for Post-doc grant (15794/2015-7). Professor Ana Paula Carvalho is kindly acknowledged for her critical revision of the manuscript.

6. References

- [1] Brunauer S; Emmett PH and Teller E. Adsorption of gases in multimolecular layers. *Journal of the American Chemical Society* 1938; 60:309-319.
- [2] Thommes M, Kaneko K, Neimark AV, Olivier JP, Rodríguez-Reinoso F, Rouquerol J and Sing KSW. Physisorption of gases, with special reference to the evaluation of surface area and pore size distribution (IUPAC Technical Report). *Pure and Applied Chemistry* 2015; 87:1051-1069.
- [3] Gregg SJ, Sing KSW. *Adsorption, Surface Area and Porosity*. 2nd ed. London: Academic Press Inc.; 1982.
- [4] Rouquerol F; Rouquerol J; Sing K, Llewellyn P and Maurin G. *Adsorption by Powders and Porous Solids - Principles, Methodology and Applications* (2nd ed). Academic Press 2014.
- [5] Marsh, H and Rodríguez-Reinoso, F. *Activated Carbon*, Elsevier 2006.
- [6] Gurvich L, *J. Soc. Phys.-Chim. Russe*, 1915; 47:805-827.
- [7] Rodríguez-Reinoso F, Martín-Martínez JM, Prado-Burguete C and McEnaney B. A standard adsorption isotherm for the characterization of activated carbons. *J. Phys. Chem.*, 1987; 91:515-516.
- [8] Choma J and Jaroniec M. Characterization of Nanoporous Carbons by Using Gas Adsorption Isotherms. In: Bandosz TJ. Ed. *Activated Carbon Surfaces in Environmental Remediation*, Volume 7, Elsevier 2006, p 107-118.
- [9] Tarazona P, Marconi UMB and Evans R. Phase equilibria of fluid interfaces and confined fluids. Non-local versus local density functionals. *Mol Phys* 1987; 60:573-595.
- [10] Seaton NA, Walton JPRB and Quirke N. A New Analysis Method for the Determination of the Pore Size Distribution of Porous Carbons from Nitrogen Adsorption Measurements. *Carbon* 1989; 27:853-861.
- [11] Lastoskie C, Gubbins KE and Quirke N. Pore Size Distribution Analysis of Microporous Carbons: A Density Functional Theory Approach. *J Phys Chem* 1993; 97:4786-4796.
- [12] Jagiello J and Olivier JP. 2D-NLDFT Adsorption Models for Carbon Slit-Shaped Pores with Surface Energetical Heterogeneity and Geometrical Corrugation. *Carbon* 2013; 55:70-80.
- [13] Jagiello J and Olivier JP. Carbon Slit Pore Model Incorporating Surface Energetical Heterogeneity and Geometrical Corrugation. *Adsorption* 2013; 19:777-783.
- [14] Falco C, Marco-Lozar JP, Salinas-Torres D, Morallón E, Cazorla-Amorós D, Titirici MM and Lozano-Castelló D. Tailoring the porosity of chemically activated hydrothermal carbons: Influence of the precursor and hydrothermal carbonization temperature. *Carbon* 2013; 62(0):346-355.
- [15] Pinto ML, Mestre AS, Carvalho AP and Pires J. Comparison of methods to obtain micropore size distributions of carbonaceous materials from CO_2 adsorption based on the Dubinin-Radushkevich isotherm. *Ind Eng Chem Res* 2010; 49:4726-4730.
- [16] Mestre AS, Tyszko E, Andrade MA, Galhetas M, Freire C and Carvalho AP. Sustainable activated carbons prepared from a sucrose-derived hydrochar: remarkable adsorbents for pharmaceutical compounds. *RSC Adv* 2015; 5:19696-19707.
- [17] Mestre AS, Pires RA, Aroso I, Fernandes EM, Pinto ML, Reis RL, Andrade MA, Pires J, Silva SP and Carvalho AP. Sustainable carbons prepared from industrial pre-treated cork: Sustainable adsorbents for pharmaceutical compounds removal. *Chem Eng J* 2014; 253:408-417.
- [18] Galhetas M, Mestre AS, Pinto ML, Gulyurtlu I, Lopes H and Carvalho AP. Chars from gasification of coal and pine activated with K_2CO_3 : Acetaminophen and caffeine adsorption from aqueous solutions. *J Colloid Interface Sci* 2014; 433: 94-103.
- [19] Batista MKS, Mestre AS, Matos I, Fonseca IM and Carvalho AP. Biodiesel production waste as promising biomass precursor of reusable activated carbons for caffeine removal. *RSC Adv* 2016; 6:45419-45427
- [20] Galhetas M, Mestre AS, Pinto ML, Gulyurtlu I, Lopes H and Carvalho AP. Carbon-based materials prepared from pine gasification residues for acetaminophen adsorption. *Chem Eng Journal* 2014; 240:344-351.
- [21] Galhetas M, Andrade MA, Mestre AS, Kangni-fofi E, Villa de Brito MJ, Pinto ML, Lopes H and Carvalho AP. The influence of the textural properties of activated carbons on acetaminophen adsorption at different temperatures. *Phys Chem Chem Phys* 2015; 17:12340-12349.
- [22] Mestre AS, Machuqueiro M, Silva M, Freire R, Fonseca IM, Santos MSCS, Calhorda MJ, Carvalho AP. Influence of activated carbon porous structure on iopamidol adsorption. *Carbon* 2014; 77:607-615.
- [23] Mestre AS, Nabico A, Figueiredo PL, Pinto ML, Santos MSCS and Fonseca IM. Enhanced clofibrac acid removal by activated carbons: Water hardness as a key parameter. *Chem Eng Journal* 2016; 286:538-548

When carbon meets light: synergistic effect between carbon nanomaterials and metal oxide semiconductors for photocatalytic applications

Cuando el carbón conoce la luz: efecto sinérgico entre nanomateriales de carbón y semiconductores de óxidos metálicos para aplicaciones fotocatalíticas

C. G. Silva*, L. M. Pastrana-Martinez, S. Morales-Torres

Laboratory of Separation and Reaction Engineering - Laboratory of Catalysis and Materials (LSRE-LCM). Department of Chemical Engineering, Faculty of Engineering, University of Porto, Rua Dr. Roberto Frias, 4200-465 Porto, Portugal.

*Corresponding author: cgsilva@fe.up.pt

Abstract

Activated carbon based materials and more recently, nanostructured carbon materials namely, fullerenes, nanotubes, nanodiamonds and graphene, have been the focus of intensive research for application in nanotechnology. In the field of photocatalysis, carbon materials have been combined with conventional semiconductors as carbon/inorganic composites seeking for synergies resulting from the coupling of both phases. This overview paper aims at exploring some important aspects that influence the photocatalytic activity of hybrid carbon/metal oxide materials such as the synthesis method, the nature and the surface chemistry of the carbon phase as well as their use immobilized in membranes or as films.

Resumen

Los materiales basados en carbón activado y más recientemente, materiales nano-estructurados de carbón, concretamente, fullerenos, nanotubos, nanodiamantes y grafeno, han sido el foco de una amplia investigación para su aplicación en nanotecnología. En el campo de la fotocatalisis, los materiales de carbón han sido combinados con semiconductores convencionales formando materiales compuestos carbón/material inorgánico con el fin de buscar sinergias del acoplamiento entre ambas fases. Este artículo de revisión tiene como objetivo explorar algunos aspectos importantes que afectan a la actividad fotocatalítica de los compuestos carbón/óxido metálico, tales como el método de síntesis, la naturaleza y la química superficial del carbón, así como su uso inmovilizado en membranas o películas.

1. Introduction

Photocatalytic technologies have been gaining increasing commercial interest worldwide mostly in the fields of environmental cleanup (water/air purification/disinfection), architecture (self cleaning surfaces), energy (photovoltaics and solar fuels) and organic synthesis. One of the most challenging research lines in photocatalysis consists in the development of highly active catalysts for solar applications. The effectiveness of solar-driven photocatalytic processes is dictated to a great extent by the semiconductor's capability of absorbing visible light, as well as its ability to suppress the rapid combination of photo-generated electrons and holes.

Titanium dioxide (TiO_2) is the most widely used semiconductor in photocatalytic applications. Nevertheless, due to its relatively high bandgap

(3.2eV corresponding to a wavelength of 388 nm), TiO_2 is marginally activated under solar irradiation, since UV light represents less than 5% of the overall solar energy reaching Earth's surface.

Carbon materials are widely employed to couple with conventional semiconductors due to properties such as large specific surface area, inertness, stability in both acid and basic media, and tunable surface chemistry. They have demonstrated to induce some beneficial effects on the photocatalytic performance of semiconductor metal oxides by creating synergies between both metal oxide and carbon phases. Generally, this effect is attributed to the decrease of the bandgap energy of the composite catalysts, to an enhancement of the adsorptive properties as well as charge separation and transportation properties.

The great diversity of carbon nanomaterials namely, fullerenes, carbon nanotubes (CNT), graphene related materials (e.g., reduced graphene oxide, rGO, and graphene oxide, -GO) and nanodiamonds (NDs), among others, have stimulated the interest in the design of high-performance hybrid photocatalysts [1-4]. Since their discovery by Iijima [5], CNT have been the focus of various studies in catalysis due to their unique structural, electronic and mechanical properties. CNT have shown the potential to contribute to the increase of the photocatalytic activity of metal oxide semiconductors [6-9]. The high surface area, semiconducting properties and the possibility of tailoring the surface chemistry make CNT a very attractive option for producing carbon- TiO_2 photocatalysts. Recently, graphene is making a deep impact in many areas of science and technology as consequence of its unique electronic, optical, mechanical, and thermal properties. GO is an exciting precursor of graphene because oxygen-containing functional groups attached on the graphene surface can be partly removed, resulting in the partial restoration of the sp^2 hybridization of carbon [10]. The exfoliation of graphite oxide, followed by a reduction process to yield rGO, offers important advantages, namely the possibility to obtain a tailored hydrophilic surface of graphene, decorated with oxygenated functionalities, by a cost-effective approach. These surface groups can be used to facilitate the anchoring of semiconductor and metal nanoparticles, or even the assembly of macroscopic structures, which are relevant to develop highly efficient photocatalysts [11, 12]. Furthermore, the chemical reduction of GO is a promising route towards the large scale production of graphene for different applications [13]. NDs are being increasingly used for a wide range of applications due to their remarkable

thermal conductivity, biocompatibility and tailored chemical properties. NDs can be obtained on a large scale at low cost by detonation of carbon-containing explosives, exhibiting a uniform distribution of particle sizes (typically 4-5 nm) together with specific surface areas around $250 \text{ m}^2 \text{ g}^{-1}$.

In this overview paper some key aspects involved in photocatalytic processes using carbon nanomaterials/metal oxide hybrid materials will be presented namely the catalysts' synthesis route, the type of carbon and metal oxide materials, the influence of carbon materials' surface chemistry and the immobilization of such composite photocatalysts, with a special focus in the work which is being developed in our group in this field. More emphasis will be put in composite materials based on TiO_2 , while some examples using ZnO will be also addressed.

2. Routes for the synthesis of carbon-metal oxide photocatalysts

The synthesis of carbon-metal oxide photocatalysts can be carried by different methods, such as mixing and/or sonication, sol-gel process, liquid phase deposition, hydrothermal and solvothermal methods [14].

The easiest technique used for coupling carbon nanomaterials with metal oxide semiconductors is by simply mixing both phases. This can be carried out by mechanical mixing of the powder materials or by suspending them in a solvent (normally water). In the first work by our group on the use of carbon materials in photocatalytic reactions, physical mixtures of different activated carbons (AC) with different surface chemistries and TiO_2 Evonik P25 (former Degussa) were successfully used for the degradation of an azo dye (solophenyl green BLE 155). The simple addition of powdered activated carbon to TiO_2 under UV irradiation induced a beneficial effect on the photocatalytic degradation of the organic dye, which has been attributed to the capacity of AC to work as a co-adsorbent and as photosensitizer since the best results were obtained with the AC sample with a more basic surface (higher electron availability). The research work was then extended to the degradation of mono-, di- and tri-azo dyes, an increase in the efficiency of the photocatalytic process being observed for the abatement of all dyes when AC was introduced in the TiO_2 slurry [15]. In another work, CNT were combined with different types of TiO_2 by a hydration-dehydration method, which consisted in mixing CNT and TiO_2 in water under sonication followed by heating at 353 K until complete evaporation of water [16, 17]. The resulting materials were used for the photocatalytic degradation of caffeine, methylene blue (MB) and several phenolic compounds. In all cases the pre-functionalization of the CNT' surface with oxygen-containing groups, such as carboxylic acids and phenols was fundamental for the enhancement of the photocatalytic activity of the hybrid materials in relation to neat TiO_2 . The simple mixing and sonication method was also used to synthesize GO- TiO_2 composites but using P25 photocatalyst as TiO_2 nanoparticles [18]. The resulting composites presented narrower band gaps than that for P25 as consequence of the intimate contact between both TiO_2 and carbon phases facilitated by the formation of C-O-Ti bonds between the hydroxy groups of P25

and the oxygen-containing surface groups of GO.

The sol-gel technique is one of the most used techniques for the production of TiO_2 , having many advantages over other production routes including the formation of very pure and homogeneous materials. This technique also allows the introduction of other solid phases during the TiO_2 synthesis process to form composites. It involves a hydrolysis step during which the carbon material is added, followed by the polycondensation of titanium alkoxides. The final materials are obtained after calcination for the removal of TiO_2 precursor and formation of the metal oxide. AC and CNT have been applied for the synthesis of TiO_2 -based materials by an acid catalyzed sol-gel route and used for the photocatalytic degradation of azo dyes and phenolic compounds [6, 7, 9, 19-21].

Another technique used in our group for the production of carbon- TiO_2 composites is the liquid phase deposition method (LPD), which is normally followed by a thermal treatment of the obtained materials in N_2 atmosphere [3]. In particular, graphene based- TiO_2 composites were prepared using different GO contents and treatment temperatures. The photocatalytic efficiency was evaluated for the degradation of diphenhydramine (DP) pharmaceutical and methyl orange (MO) azo-dye under both near-UV/Vis and visible light irradiations [3]. The GO- TiO_2 composite with the best photocatalytic activity was that prepared with a 4.0 wt.% GO and treated at 473 K (hereafter referred as GOT). The superior performance of GOT exceeded that of the benchmark P25 photocatalyst for both DP and MO pollutants and was attributed to the optimal assembly and interfacial coupling between the GO layers and TiO_2 nanoparticles. The photocatalytic efficiency of GOT has been also tested in the degradation of other pollutants such as microcystin-LR (the most common and toxic variant of the group of microcystins) and off-odor compounds (Geosmin and 2-methylisoborneol) in water under UV-A and solar light [22], the variant microcystin-LA (MC-LA) [23], 17-beta-estradiol under simulated solar light [24], estradiol under simulated solar light [24], endocrine disruptor [25], and EU/EPA priority pollutant pesticides [26], among others. Nanodiamonds- TiO_2 composites (ND_{ox} T-15, containing 15.0 wt.% of NDs) were also synthesized by using the LPD method and a thermal treatment at 473 K [2, 4]. The photocatalytic activity of these materials will be presented below when discussing the effect of the surface chemistry in the activity of carbon-metal oxide materials.

3. The role of the carbon materials' surface chemistry

Carbon materials' surface groups take an important role in the way they link to metal oxide semiconductors and consequently, in the electronic and photocatalytic performance of the composite materials. Liquid-phase functionalization of CNT with nitric acid leads to the creation of large amounts of carboxylic acid and phenol groups at the surface of the CNT (referred as CNT_f); these functionalities are accountable for promoting the dispersion of TiO_2 particles in the CNT- TiO_2 composites and also contribute to the formation of C-O-Ti bonds, as in esterification reactions between the carboxylic acid groups of CNT and the hydroxy groups existent at the surface of TiO_2 [6, 16, 17]. The functional groups present at the surface of

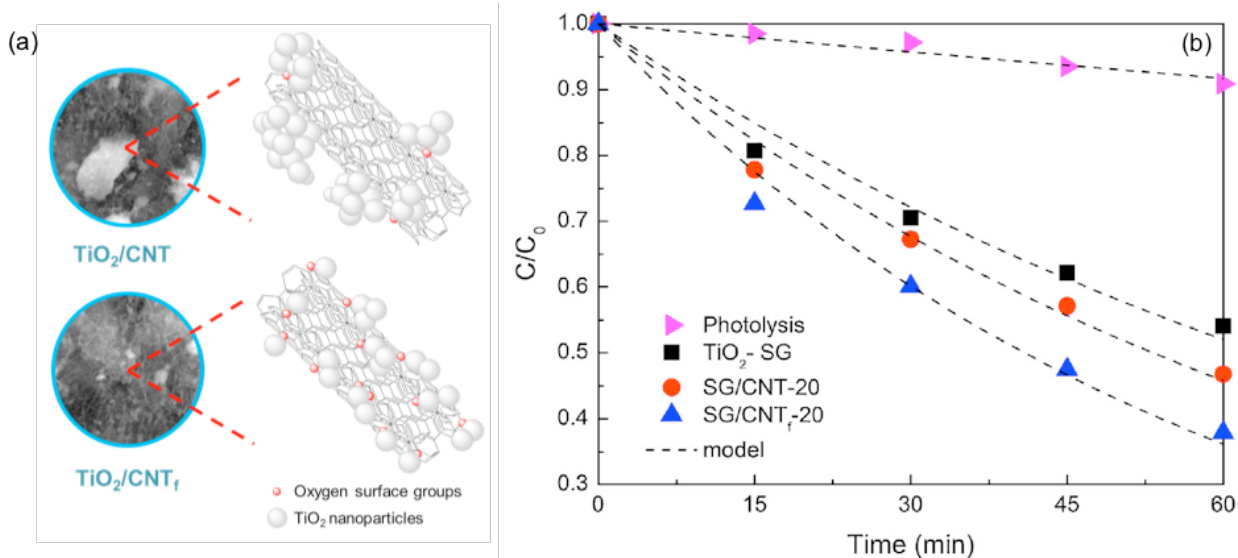


Figure 1. (a) Dispersion of TiO₂ at the surface of CNT_f and pristine CNT in composite materials prepared by SG; (b) evolution of the normalized concentration (C/C_0) of MB during photolysis and photocatalytic degradation using TiO₂, and CNT/TiO₂ composites. Figures adapted with permission from ref. [17]. Copyright 2015, Elsevier.

Figura 1. (a) Dispersión de partículas de TiO₂ sobre la superficie de CNT puros y funcionalizados en materiales compuestos preparados por el método SG; (b) evolución de la concentración normalizada (C/C_0) de MB durante la degradación por fotólisis y fotocatalisis usando TiO₂, y materiales compuestos CNT/TiO₂. Figuras adaptadas con permiso de ref. [17]. Copyright 2015, Elsevier.

CNT_f promote the anchoring of the TiO₂ particles as well as their dispersion, avoiding agglomeration and subsequently increasing the surface area of the resulting materials (Fig. 1a). It was found that for the composites prepared by sol-gel (SG) method, the introduction of CNT leads to a slight increase in the photocatalytic efficiency towards the degradation of MB under near UV to visible irradiation (Fig. 1b), which is attributed to a synergy effect due to the creation of an electronic interphase interaction between CNT and TiO₂ phases. In addition, a marked increase of the films photocatalytic activity was observed when CNT_f were used to prepare the composites as compared to pristine CNT (Fig. 1b).

The effect of CNT' surface oxygen functionalities was also explored for CNT-TiO₂ composites (loaded with Pt, acting as co-catalyst) for the photocatalytic production of H₂ from methanol and from saccharides [8]. In that case, the photocatalytic efficiency of composite materials produced by mixing and sonication of TiO₂ and oxidized (with HNO₃ 10 M at boiling temperature)

CNT (CNTox-TiO₂) was compared with a composite prepared by introduction of TiO₂ during the CNT' oxidation process [(CNT-TiO₂)ox]. Infrared analysis of the two materials show that in the case of (CNT-TiO₂)ox, there is a decrease in the intensity of the bands corresponding to O-H and C-O groups when compared to the spectra of CNTox-TiO₂, which suggests that TiO₂ may be attached to CNT' surface groups such as phenols and carboxylic acids (Fig. 2a). Also, the bands originated from C-C and C-H, due to aromatic ring vibrations, are less intense in (CNT-TiO₂)ox compared to CNTox-TiO₂, which indicates a better dispersion of the TiO₂ particles at the surface of CNT in the (CNT-TiO₂)ox composite. This observation is in line with the higher intensity of the Ti-O band in the (CNT-TiO₂)ox composite, revealing that the TiO₂ particles are better distributed over the surface of CNT for this composite. Fig. 2b shows a schematic representation of the mechanism of photocatalytic production of H₂ from methanol using CNT-TiO₂ composites under irradiation of $\lambda \geq 365$ nm. At these

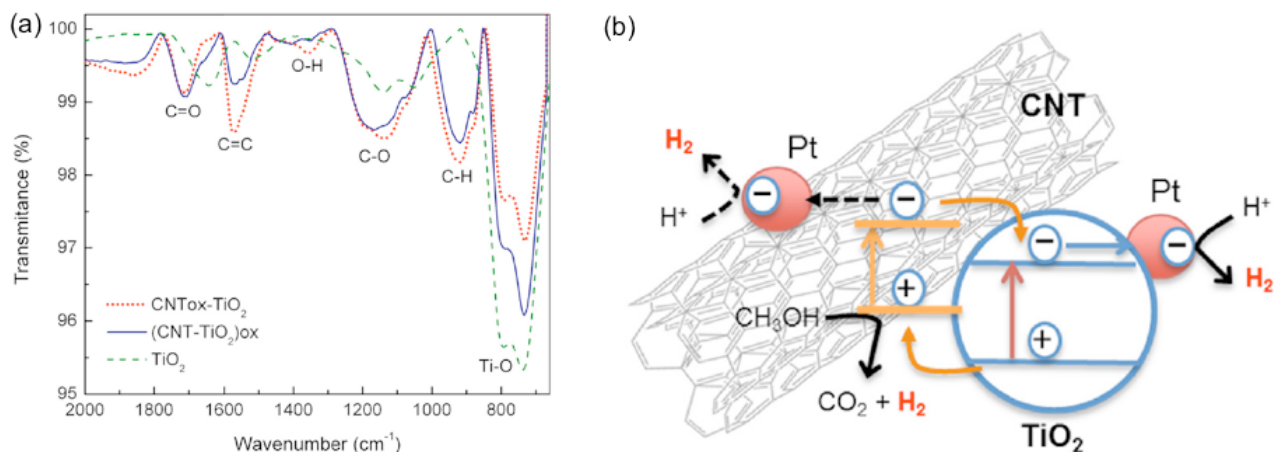


Figure 2. (a) Infrared ATR spectra of bare TiO₂, CNTox-TiO₂ and (CNT-TiO₂)ox composites; (b) schematic representation of the photocatalytic mechanism of H₂ generation from water/methanol solutions under near irradiation at $\lambda \geq 365$ nm using Pt/(CNT-TiO₂)ox catalyst. Figures adapted with permission from ref. [8]. Copyright 2015, Elsevier.

Figura 2. (a) Espectros de infrarrojos (ATR) de TiO₂ puro, CNTox-TiO₂ y materiales compuestos (CNT-TiO₂)ox; (b) representación esquemática del mecanismo fotocatalítico de producción de H₂ a partir de disoluciones agua/metanol con irradiación $\lambda \geq 365$ nm usando el catalizador Pt/(CNT-TiO₂)ox. Figuras adaptadas con permiso de ref. [8]. Copyright 2015, Elsevier.

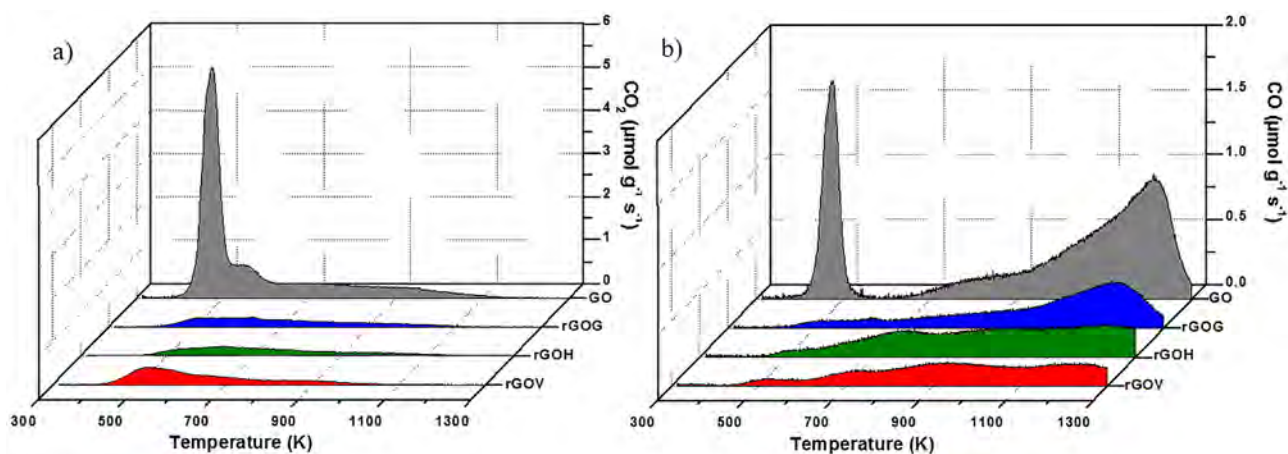


Figure 3. TPD profiles for GO and reduced samples (rGOG, rGOV and rGOH): (a) CO_2 and (b) CO release. Figures adapted with permission from ref. [27]. Copyright 2014, Elsevier.

Figura 3. Perfiles de TPD para GO y muestras reducidas (rGOG, rGOV y rGOH): formación de (a) CO_2 y (b) CO. Figuras adaptadas con permiso de ref. [27]. Copyright 2014, Elsevier.

conditions it is expected that both TiO_2 and CNT could be photo-excited. Electrons from the valence band of TiO_2 are excited to the conduction band of the semiconductor and transferred to Pt nanoparticles reducing protons and generating H_2 . On the other hand, positively charged holes may migrate to the CNT phase to oxidize methanol. Simultaneously, due to the strong interphase interaction between CNT and TiO_2 , photo-excited electrons in the CNT phase may migrate to the conduction band of TiO_2 , increasing the availability of these species in the TiO_2 phase and therefore enhancing H_2 production. Since Pt particles could also be found in CNT, electrons may also migrate to those particles, which act as active sites for H_2 generation.

In another work [27], GO was chemically reduced using vitamin C (rGOV) and glucose (rGOG), both environmental friendly reducing agents, as well as hydrazine (rGOH), and the evolution of the graphene oxygen-containing surface groups was systematically analysed. Furthermore, the reduced GO samples (rGO)- TiO_2 composites were prepared in order to assess the effect of the nature and amounts of oxygenated groups on the photocatalytic performance of composites under near-UV/Vis and visible irradiation. The evolution of oxygen functionalities of GO, during the chemical reduction processes can be systematically analysed using different characterization techniques [27]. The UV-Vis absorption spectra of the GO suspension as well as the chemically reduced rGO suspensions can be used as a quick probe for the degree of GO reduction. After the chemical treatment with different reducing agents (rGOG, rGOV and rGOH), the absorption band at 231 nm presented a red shift to ~ 260 nm, corresponding to deoxygenation of the GO suspensions by the reduction processes. The reduction of GO is also indicated by the colour change of the solution, i.e. from light brown to black after the reduction process. The black colour observed for the rGO dispersion has been related to the partial restoration of the π network and electronic conjugation. X-ray photoelectron spectroscopy (XPS) measurements are also a valuable technique for the determination of the oxygen functionalities. Indeed, after the chemical reduction, the contribution of the C_{1s} region associated with oxygenated species decreased for all the rGO samples, indicating considerable deoxygenation by the reduction process. The degree

of deoxygenation of GO by chemical reduction was also observed in the oxygen content of the samples. The lowest O/C ratio for the rGO samples was obtained by treatments performed with glucose and vitamin C, a better reducing character being observed than that obtained with the toxic hydrazine compound.

Concerning the Raman spectra of the rGO samples, at 514.5 and 785 nm laser excitations, all samples exhibit the graphitic G band arising from the bond stretching of sp^2 carbon atoms and the dispersive, defect-activated D band together with the high frequency modes, including the 2D band, the defect activated combination mode (D+D') and the 2G overtone that could be best resolved at 514.5 nm. Temperature programmed desorption (TPD) technique has been used to calculate the amounts of different types of oxygenated groups, which evolve as CO and CO_2 . The TPD profiles for CO_2 and CO are shown in Figs. 3a and b, respectively. The high oxygen content and larger CO_2 and CO evolution, detected for the GO sample correspond to the presence of a larger amount of oxygenated groups in comparison with the rGO samples. The thermal stability of oxygenated functional groups depends on the type of group and on the surroundings to which they are bounded. The deconvolution methodology was applied considering the temperatures at which the different groups evolved as CO_2 and CO upon heating. These results showed the complex chemical composition of GO that contains mainly epoxy and hydroxyl groups on the basal planes as well as minor content of carbonyls, carboxyls, ethers, quinones, lactones, and phenols attached at vacancy and edge sites [27] (Fig. 4).

Different graphene- TiO_2 composites were prepared with the pristine GO and rGO samples by the liquid phase deposition method. The materials were tested for the photocatalytic degradation of diphenhydramine under both UV/Vis and visible light irradiation. A lower photocatalytic activity observed for the composites containing rGO, in comparison with that prepared with GO, which is attributed to the very low amount of oxygenated surface groups that leads to a weak interaction between TiO_2 and rGO during the preparation method employed. The affinity of surface hydroxyl groups on TiO_2 to undergo charge transfer interaction with carboxylic acid functional groups on GO is reported in literature [13]. These effects can be

responsible for the optimal assembly and interfacial coupling between GO sheets and TiO₂ nanoparticles during the preparation of the composite (consisting of GO platelets embedded into TiO₂), as well as for the higher photocatalytic performance of the GO-TiO₂ composite.

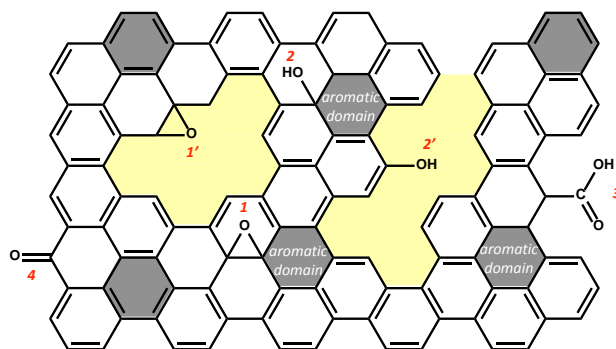


Figure 4. Schematic of oxygen-containing groups placed in the aromatic domain of GO: (1), epoxy groups located at the interior; (1'), epoxy groups located at the edge; (2), hydroxyl located at the interior; (2'), hydroxyl at the edge; (3) carboxyl and (4) carbonyl at the edge. Figure adapted with permission from ref. [27]. Copyright 2014, Elsevier.

Figura 4. Esquema de los grupos oxigenados situados en la estructura aromática de GO: (1), grupos epóxidos localizados en el interior; (1'), grupos epóxidos situados en el eje; (2), hidroxilos localizados en el interior; (2'), hidroxilos en el eje; (3) carboxílicos y (4) carbonilos en el eje. Figura adaptada con permiso de ref. [27]. Copyright 2014, Elsevier.

Concerning the NDs, the introduction of surface functional groups on the nano-sized diamond particles also plays an important role in the photocatalytic activity of the composites (Fig. 5). It is significant to refer that the oxidation treatment in air at 703 K produces not only oxygen-containing surface species but also is known to purify the nanodiamond powders (i.e. eliminating non-diamond carbon in the detonation product by a selective oxidation) [28, 29]. Therefore, the marked enhancement on the photodegradation rate for the ND_{ox}-T-15 could be attributed to the significant amount of oxygen surface species on ND_{ox} (mainly carboxylic anhydrides, lactones, phenols and, to a lower extent, carbonyl/quinone groups), which are known to be beneficial for the preparation of TiO₂ nanostructured carbon composites [6, 16] and to the increased purity of the nano-sized diamond constituent after the

oxidation treatment. For comparison purposes, the GO-TiO₂ composite prepared in our previous study (GOT) [3] and ND_{ox}-T-15 were tested under the same conditions. The pseudo-first order rate constants were very similar for ND_{ox}-T-15 ($91 \cdot 10^{-3} \text{ min}^{-1}$) and GOT ($92 \cdot 10^{-3} \text{ min}^{-1}$) both presenting slightly higher efficiency than P25 ($79 \cdot 10^{-3} \text{ min}^{-1}$) for DP degradation.

4. The nature of carbon materials

The photocatalytic activity of GO-TiO₂ composites was compared to that obtained for other carbon-TiO₂ materials but containing CNT or fullerenes (C₆₀) and thereby, the effect of the nature of the nanostructured carbon material was studied for the photodegradation of MO and DP under both near-UV/Vis and visible light irradiation [30]. The activity of the materials depended on the nature (GO, CNT or C₆₀) and content (4 or 12wt.%) of the carbon used. Although all carbon-TiO₂ composites were more active than P25 and bare TiO₂ under Vis light irradiation, GO-TiO₂ exhibited the highest photocatalytic activity under near-UV/Vis and Vis light irradiation and thereby, it was a superior nanostructured carbon material than CNT and C₆₀ to develop active composite photocatalysts.

ZnO is considered as an alternative to TiO₂ in photocatalytic applications due to its similar band gap (3.3 eV), its versatile morphology and lower cost. Since it also requires excitation in the near UV region, carbon materials have been used for increasing its activity under solar light irradiation. In a recent study by our group, ZnO synthesized by chemical vapor deposition (CVD) was combined by mixing and sonication with different carbon nanomaterials namely CNT, nanofibers (CNF), NDs, fullerene (C₆₀) and few-layers graphene (FLG)[31]. The composite materials were successfully used for phenol degradation under simulated solar light. It was found that the efficiency of the photocatalytic process depended on the nature of the carbon material used. The composites prepared from CNT (NC-CNT, AK-CNT and PYG-CNT) were less active when compared to other catalysts containing ND, fullerene, CNF and FLG, Fig. 6).

The highest photocatalytic activity was observed for the composite prepared with N-doped CNT (N-CNT). An increase of c.a. 100% in the k_{app} for phenol

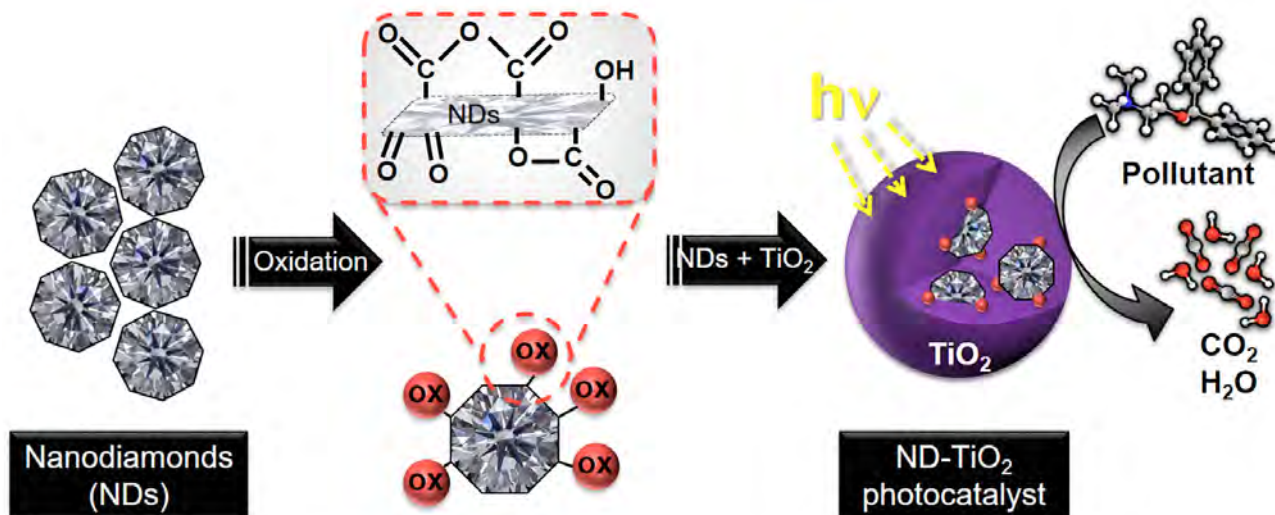


Figure 5. Schematic representation on the synthesis of ND-TiO₂ photocatalysts. Figure adapted with permission from ref. [2]. Copyright 2013, WILEY-VCH Verlag GmbH & Co.

Figura 5. Representación esquemática de la síntesis de fotocatalizadores ND-TiO₂. Figura adaptada con permiso de ref. [2]. Copyright 2013, WILEY-VCH Verlag GmbH & Co.

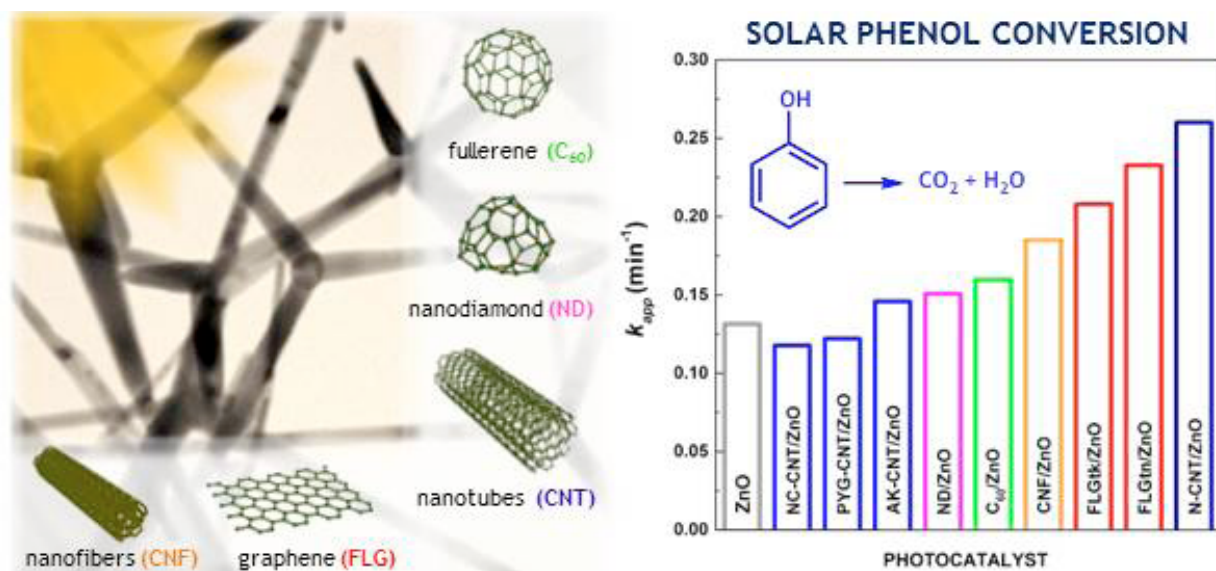


Figure 6. Apparent first order rate constants (k_{app}) for the photocatalytic reactions using ZnO and carbon/ZnO materials. Figure adapted with permission from ref. [31]. Copyright 2015 Elsevier.

Figura 6. Constantes de velocidad aparentes de primer orden (k_{app}) para las reacciones fotocatalíticas usando materiales ZnO y carbón/ZnO. Figura adaptada con permiso de [31]. Copyright 2015, Elsevier.

degradation was obtained when using N-CNT/ZnO compared to the bare material (ZnO).

For comparison purposes, composites using undoped CNT and oxidized CNT (CNT/ZnO and CNT_o/ZnO, respectively) were also prepared and tested in the degradation of phenol. As expected, the results demonstrate that CNT' functionalization promotes an increase in the efficiency of the resulting carbon/ZnO catalysts (around 10%), much lower than the effect promoted by nitrogen doping. A photocatalytic experiment using bare N-CNT was also performed and no phenol conversion was observed under these conditions, suggesting that the activity of the composite material results from cooperative interactions between the metal oxide and the carbon phase. Among the photocatalysts tested, the composite prepared using N-doped CNT as carbon phase (N-CNT/ZnO) showed the highest photocatalytic activity, which was attributed to the presence of electron rich nitrogen-containing groups on the CNT' surface. Photoluminescence analysis confirmed that N-CNT act as an effective electron scavenger for ZnO, inhibiting the recombination of photoexcited electron-hole pairs, thus improving the photoactivity.

4. Composites' immobilization

The use of photocatalysts in powder form has been associated with many drawbacks including the difficult separation of the catalyst from the treated effluent. The immobilization and deposition of the photocatalyst in supports intend to overcome the trouble of recovering the material from the treated media, as well as to improve the contact between the pollutant molecules and the photocatalyst particles. An ideal support should satisfy criteria such as to be stable during the photocatalytic process, to offer a high specific surface area and a strong adherence for the photocatalyst and to have an affinity towards pollutant molecules. In our group, several materials such as glass substrates, inorganic porous and polymer membranes, as well as fibres have been employed to immobilize highly active photocatalysts.

CNT-TiO₂ composites immobilized in glass substrates

have been successfully used for the degradation of MB dyes and phenolic compounds [17, 32]. The materials were immobilized as thin films on glass slides by using the so-called doctor blade method, which can be easily employed as a fast and non-energy consuming technique for mass production of thin films with good uniformity and reproducible properties. The photoefficiency of the immobilized catalysts appeared to be related to the inherent properties of the materials and to the characteristics of the resulting films such as homogeneity, thickness, roughness and resistance to mechanical stress. Results show that in most cases, there is an increase in the photoefficiency of the hybrid materials when CNT are present in the films. For composite materials containing TiO₂ P25 and commercial TiO₂ anatase powder from Sigma Aldrich (SA), this increase in the activity for MB removal was proportional to the amount of CNT in the composite materials. The composites produced with TiO₂-SA have shown the highest efficiencies, which were attributed to both the homogeneity of the obtained films and to the photocatalytic properties of the composite materials.

In our group, the highly active GOT composite, bare TiO₂ and P25 catalysts were immobilized into three types of membranes: alginate porous hollow fibres [2], ultrafiltration (UF) mono-channel alumina monoliths [33] and flat sheet membranes [34]. The immobilization of GOT into a matrix of alginate allowed to obtain porous fibres with a rough external surface and high activity and stability in the photodegradation of DP under UV/Vis irradiation after consecutive continuous light-dark cycles [2]. In general, polymer membranes and fibres may be decomposed by the UV irradiation over long reaction times. In this context, GOT and bare TiO₂ were deposited on UF and nanofiltration (NF) alumina membranes to be tested in a hybrid photocatalysis/ultrafiltration process for the removal of typical synthetic dyes, such as MO and MB [33]. The catalytic/filtration behaviour of GOT was much better than that for the membrane with bare TiO₂, in particular under Vis light irradiation. Furthermore, the performance of the membrane with GOT was

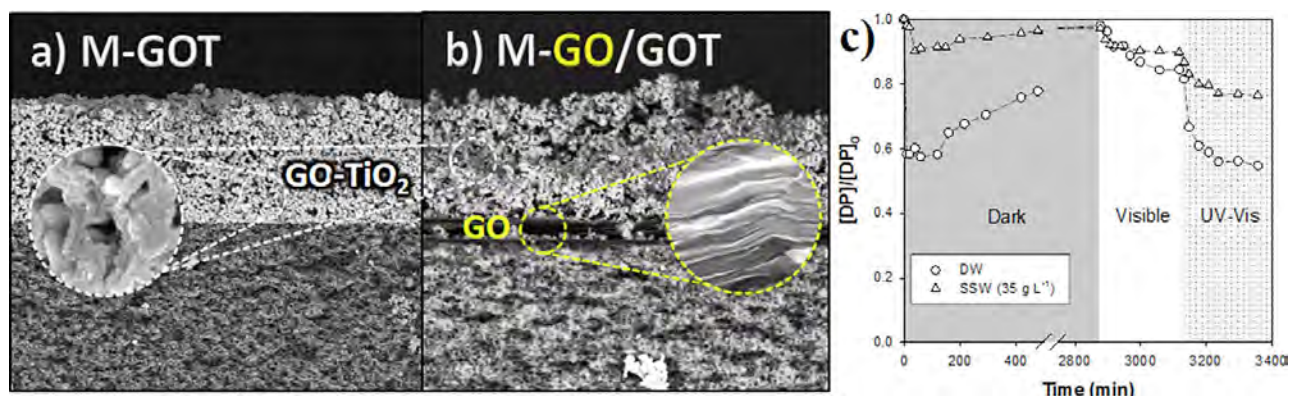


Figure 7. Cross-sectional SEM micrographs of (a) M-GOT and (b) M-GO/GOT (insets corresponds to the GOT composite or the freestanding GO membrane: M-GO, respectively); (c) DP removal in DW and SSW (35 g L⁻¹) with the M-GO/GOT membrane under dark conditions, near-UV/Vis and visible light irradiation. Figures adapted with permission from ref. [34]. Copyright 2015, Elsevier.

Figura 7. Micrografías de SEM de (a) M-GOT y (b) M-GO/GOT (las figuras pequeñas corresponden al material GOT o la membrana de GO: M-GO, respectivamente); (c) Eliminación de DP en DW y SSW (35 g L⁻¹) con una membrana M-GO/GOT en ausencia de luz, con irradiación UV cercano/Vis y luz visible. Figuras adaptadas de ref. [34]. Copyright 2015, Elsevier.

superior than that of a standard NF process in regard to the overall dye removal capacity and to the dye concentration reduction in the permeate effluent.

The deposition of photocatalysts onto flat sheet membranes was carried out by using a simple filtration method and mixed cellulose ester (MCE) membranes as supports [34]. The membranes prepared with GOT, TiO₂ and P25 were labelled as M-GOT, M-TiO₂ and M-P25, respectively. The membrane presenting the highest photocatalytic activity (M-GOT) was also modified by intercalating a freestanding GO membrane between the MCE membrane and the GOT photocatalyst layer. For that, a GO dispersion was filtered through a M-GOT membrane, and a homogeneous GO layer was obtained above the MCE membrane and the layer of GOT (labelled as M-GO/GOT, Figs. 7a and b).

The prepared membranes were compared in terms of photocatalytic activity using distilled water (DW), simulated brackish water and (SSW) seawater. The photocatalysts were homogeneously deposited without appreciable presence of cracks, holes or another defects. The M-GO/GOT membrane showed higher pollutant removal under dark conditions and good performance under visible and near-UV/Vis irradiation (Fig. 7c). However, the M-GOT membrane performed better, probably due to the higher compactness in the case of M-GO/GOT as a consequence of the synthesis conditions required for its preparation.

5. Conclusions and future perspectives

Carbon-metal oxide semiconductor materials have been widely investigated and are promising materials for photocatalytic applications. The synergic effect induced by the presence of carbon materials in the hybrid photocatalysts is mainly attributed to the decrease of electron/hole recombination, bandgap tuning and increase in the adsorptive active sites. The great morphological and electronic versatility of carbon nanomaterials offers the possibility of designing novel photocatalytically-active materials for a wide variety of applications. The full understanding of the synergies created between carbon nanomaterials and metal oxide semiconductors is crucial for the development of highly active photocatalysts. While the existence of high amounts of carbon-containing contaminants in the environment (greenhouse gases, organic

water pollutants, etc) is of major concern, nanoscale carbon materials can be considered an outstanding solution towards the development of photocatalytic technologies.

Acknowledgements

This work was financially supported by Project POCI-01-0145-FEDER-006984 – Associate Laboratory LSRE-LCM funded by FEDER through COMPETE2020 - Programa Operacional Competitividade e Internacionalização (POCI) – and by national funds through FCT - Fundação para a Ciência e a Tecnologia. S.M.T. acknowledges FCT for the post-doctoral grant with reference SFRH/BPD/74239/2010. C.G.S. and L.M.P.M. acknowledge the FCT Investigator Programme (IF/00514/2014 and IF/01248/2014, respectively) funded by the European Social Fund and the Human Potential Operational Programme.

References

- [1] Morales-Torres S, Pastrana-Martínez LM, Figueiredo JL, Faria JL, Silva AMT. Design of graphene-based TiO₂ photocatalysts - A review. *Environ Sci Pollut Res* 2012; 19: 3676-3687.
- [2] Pastrana-Martínez LM, Morales-Torres S, Carabineiro SAC, Buijnsters JG, Faria JL, Figueiredo JL, Silva AMT. Nanodiamond-TiO₂ Composites for Heterogeneous Photocatalysis. *ChemPlusChem* 2013; 78 (8): 801-807.
- [3] Pastrana-Martínez LM, Morales-Torres S, Likodimos V, Figueiredo JL, Faria JL, Falaras P, Silva AMT. Advanced nanostructured photocatalysts based on reduced graphene oxide-TiO₂ composites for degradation of diphenhydramine pharmaceutical and methyl orange dye. *Appl Catal B* 2012; 123-124: 241-256.
- [4] Sampaio MJ, Pastrana-Martínez LM, Silva AMT, Buijnsters JG, Han C, Silva CG, Carabineiro SAC, Dionysiou DD, Faria JL. Nanodiamond-TiO₂ composites for photocatalytic degradation of microcystin-LA in aqueous solutions under simulated solar light. *RSC Adv* 2015; 5 (72): 58363-58370.
- [5] Iijima S. Helical microtubules of graphitic carbon. *Nature* 1991; 354 (6348): 56-58.
- [6] Silva CG, Faria JL. Photocatalytic Oxidation of Benzene Derivatives in Aqueous Suspensions: Synergic Effect Induced by the Introduction of Carbon Nanotubes in a TiO₂ Matrix. *Applied Catalysis B: Environmental* 2010; 101 (1-2): 81-89.
- [7] Silva CG, Faria JL. Photocatalytic oxidation of phenolic compounds by using a carbon nanotube-titanium dioxide composite catalyst. *ChemSusChem* 2010; 3 (5): 609-618.

- [8] Silva CG, Sampaio MJ, Marques RRN, Ferreira LA, Tavares PB, Silva AMT, Faria JL. Photocatalytic production of hydrogen from methanol and saccharides using carbon nanotube-TiO₂ catalysts. *Appl Catal B* 2015; 178 82-90.
- [9] Silva CG, Wang W, Faria JL. Nanocrystalline CNT-TiO₂ composites produced by an acid catalyzed sol-gel method, in: *Materials Science Forum*, 2008, pp. 849-853.
- [10] Pei S, Cheng H-M. The reduction of graphene oxide. *Carbon* 2012; 50 (9): 3210-3228.
- [11] Du J, Lai X, Yang N, Zhai J, Kisailus D, Su F, Wang D, Jiang L. Hierarchically Ordered Macro-Mesoporous TiO₂-Graphene Composite Films: Improved Mass Transfer, Reduced Charge Recombination, and Their Enhanced Photocatalytic Activities. *ACS Nano* 2010; 5 (1): 590-596.
- [12] Kamat PV. Graphene-Based Nanoarchitectures. Anchoring Semiconductor and Metal Nanoparticles on a Two-Dimensional Carbon Support. *J Phys Chem Lett* 2009; 1 (2): 520-527.
- [13] Chua CK, Pumera M. Chemical reduction of graphene oxide: a synthetic chemistry viewpoint. *Chem Soc Rev* 2014; 43 (1): 291-312.
- [14] Morales-Torres S, Pastrana-Martínez LM, Figueiredo JL, Faria JL, Silva AMT. Design of graphene-based TiO₂ photocatalysts-a review. *Environ Sci Pol Res* 2012; 19 (9): 3676-3687.
- [15] Silva CG, Wang W, Faria JL. Photocatalytic and photochemical degradation of mono-, di- and tri-azo dyes in aqueous solution under UV irradiation. *J Photochem Photobiol A* 2006; 181 (2-3): 314-324.
- [16] Marques RRN, Sampaio MJ, Carrapiço PM, Silva CG, Morales-Torres S, Dražić G, Faria JL, Silva AMT. Photocatalytic degradation of caffeine: Developing solutions for emerging pollutants. *Catal Today* 2013; 209 108-115.
- [17] Sampaio MJ, Marques RRN, Tavares PB, Faria JL, Silva AMT, Silva CG. Tailoring the properties of immobilized titanium dioxide/carbon nanotube composites for photocatalytic water treatment. *J Environ Chem Eng* 2013; 1 (4): 945-953.
- [18] Morales-Torres S, Pastrana-Martínez LM, Figueiredo JL, Faria JL, Silva AMT. Graphene oxide-P25 photocatalysts for degradation of diphenhydramine pharmaceutical and methyl orange dye. *Appl Surf Sci* 2013; 275 361-368.
- [19] Silva CG, Wang W, Selvam P, Dapurkar S, Faria JL. Structured TiO₂ based catalysts for clean water technologies, in: *Studies in Surface Science and Catalysis*, 2006, pp. 151-158.
- [20] Wang W, Serp P, Kalck P, Silva CG, Faria JL. Preparation and characterization of nanostructured MWCNT-TiO₂ composite materials for photocatalytic water treatment applications. *Mater Res Bull* 2008; 43 (4): 958-967.
- [21] Wang W, Silva CG, Faria JL. Photocatalytic degradation of Chromotrope 2R using nanocrystalline TiO₂/activated-carbon composite catalysts. *Appl Catal B* 2007; 70 (1-4): 470-478.
- [22] Fotiou T, Triantis TM, Kaloudis T, Pastrana-Martínez LM, Likodimos V, Falaras P, Silva AMT, Hiskia A. Photocatalytic Degradation of Microcystin-LR and Off-Odor Compounds in Water under UV-A and Solar Light with a Nanostructured Photocatalyst Based on Reduced Graphene Oxide-TiO₂ Composite. Identification of Intermediate Products. *Ind Eng Chem Res* 2013; 52 (39): 13991-14000.
- [23] Sampaio MJ, Silva CG, Silva AMT, Pastrana-Martínez LM, Han C, Morales-Torres S, Figueiredo JL, Dionysiou DD, Faria JL. Carbon-based TiO₂ materials for the degradation of Microcystin-LA. *Appl Catal B* 2015; submitted.
- [24] Mboula VM, Héquet V, Andrès Y, Gru Y, Colin R, Doña-Rodríguez JM, Pastrana-Martínez LM, Silva AMT, Leleu M, Tindall AJ, Mateos S, Falaras P. Photocatalytic degradation of estradiol under simulated solar light and assessment of estrogenic activity. *Appl Catal B* 2015; 162 437-444.
- [25] Maroga Mboula V, Héquet V, Andrès Y, Pastrana-Martínez LM, Doña-Rodríguez JM, Silva AMT, Falaras P. Photocatalytic degradation of endocrine disruptor compounds under simulated solar light. *Water Res* 2013; 47 (12): 3997-4005.
- [26] Cruz M, Gomez C, Duran-Valle CJ, Pastrana-Martínez LM, Faria JL, Silva AMT, Faraldos M, Bahamonde A. Bare TiO₂ and graphene oxide TiO₂ photocatalysts on the degradation of selected pesticides and influence of the water matrix. *Appl Surf Sci in press*.
- [27] Pastrana-Martínez LM, Morales-Torres S, Likodimos V, Falaras P, Figueiredo JL, Faria JL, Silva AMT. Role of oxygen functionalities on the synthesis of photocatalytically active graphene-TiO₂ composites. *Appl Catal B* 2014; 158-159 329-340.
- [28] Mochalin VN, Shenderova O, Ho D, Gogotsi Y. The Properties and Applications of Nanodiamonds. *Nat Nanotechnol* 2012; 7 (1): 11-23.
- [29] Schrand AM, Hens SAC, Shenderova OA. Nanodiamond Particles: Properties and Perspectives for Bioapplications. *Crit Rev Solid State Mat Sci* 2009; 34 (1-2): 18-74.
- [30] Pastrana-Martínez LM, Morales-Torres S, Papageorgiou SK, Katsaros FK, Romanos GE, Figueiredo JL, Faria JL, Falaras P, Silva AMT. Photocatalytic behaviour of nanocarbon-TiO₂ composites and immobilization into hollow fibres. *Appl Catal B* 2013; 142-143 101-111.
- [31] Sampaio MJ, Bacsa RR, Benyounes A, Axet R, Serp P, Silva CG, Silva AMT, Faria JL. Synergistic effect between carbon nanomaterials and ZnO for photocatalytic water decontamination. *J Catal* 2015; 331 172-180.
- [32] Sampaio MJ, Silva CG, Marques RRN, Silva AMT, Faria JL. Carbon nanotube-TiO₂ thin films for photocatalytic applications. *Catal Today* 2011; 161 (1): 91-96.
- [33] Athanasekou CP, Morales-Torres S, Likodimos V, Romanos GE, Pastrana-Martínez LM, Falaras P, Dionysiou DD, Faria JL, Figueiredo JL, Silva AMT. Prototype composite membranes of partially reduced graphene oxide/TiO₂ for photocatalytic ultrafiltration water treatment under visible light. *Appl Catal B* 2014; 158-159: 361-372.
- [34] Pastrana-Martínez LM, Morales-Torres S, Figueiredo JL, Faria JL, Silva AMT. Graphene oxide based ultrafiltration membranes for photocatalytic degradation of organic pollutants in salty water. *Water Res* 2015; submitted.

Development of carbon materials as metal catalyst supports and metal-free catalysts for catalytic reduction of ions and advanced oxidation processes

Desarrollo de materiales de carbono como soporte de catalizadores metálicos o catalizadores libres de metal para la reducción catalítica de iones o procesos de oxidación avanzada

O. Salomé G. P. Soares

Laboratory of Separation and Reaction Engineering - Laboratory of Catalysis and Materials (LSRE-LCM), Department of Chemical Engineering, Faculty of Engineering, University of Porto, Rua Dr. Roberto Frias, 4200-465 Porto, Portugal.

*Corresponding author: salome.soares@fe.up.pt

Abstract

The versatility of carbon materials as metal supports as well as metal-free catalysts for environmental applications is presented, highlighting some of the work carried out at the Laboratory of Catalysis and Materials (LCM), which focuses on carbon materials and catalysis as its main research areas. Carbon materials with appropriate surface and textural properties to act as supports for the active phases or as catalysts on their own have been successfully developed for catalytic processes such as the catalytic reduction of ions and advanced oxidation processes.

Resumen

El presente trabajo pretende destacar la versatilidad de los materiales de carbono tanto como soporte de catalizadores metálicos como catalizadores libres de metal para aplicaciones ambientales. Con este objetivo se presentan algunos de los trabajos realizados en el Laboratory of Catalysis and Materials (LCM), cuyas principales líneas de investigación se centran en la preparación de materiales de carbono y en la aplicación de los mismos en catálisis. Estos materiales de carbono, con propiedades superficiales y texturales adecuadas para actuar como soporte de las fases activas o como catalizadores en sí mismos, han sido aplicados con éxito en procesos catalíticos tales como la reducción catalítica de iones o procesos de oxidación avanzada.

1. Introduction

Carbon materials are currently used in heterogeneous catalysis both as supports or as catalysts on their own, due to their specific properties, namely: resistance to acid and basic media, possibility to tune their textural and surface properties, and easy recovery of precious metals by burning the carbon support [1, 2]. In particular, their use as metal-free catalysts is attracting a great deal of attention [2], being a good alternative to the traditional metal and metal oxide catalysts in several gas and liquid phase reactions [3].

Textural properties of the carbon materials can be tailored for specific applications by adequate preparation methods. The nature and concentration of the surface functional groups may be modified by appropriate thermal or chemical post-treatments. The presence of heteroatoms, such as oxygen, nitrogen and sulphur, bound to the edges of the graphene layers in the carbon material originates several surface functional groups. Such elements are either present in

the starting material or become chemically bound to the structure during the preparation [4]. Oxygenated groups can be introduced onto the carbon materials surface by oxidative treatments, either in the gas or liquid phase [5], which can be selectively removed by thermal treatments under inert atmosphere. The introduction of heteroatoms on the carbon structure allows to control the electronic properties by introducing electron acceptors or donors, which can enhance π bonding, leading to improved stability and electron transfer rate, and consequently, improved performance and durability of the catalysts during the processes [6, 7].

Carbon materials have demonstrated to be good supports for the catalytic reduction of ions over metallic catalysts in the presence of a reducing agent [8-13]. The presence of metals is mandatory for this reaction, but the carbon materials by themselves do not present any activity, their role being the promotion of a high metal dispersion. In contrast, it has been demonstrated that carbon materials are able to enhance the removal of organic pollutants as catalysts in catalytic wet air oxidation [14-16] and catalytic ozonation [17, 18] due to their outstanding textural and chemical properties. Therefore, here we describe some of the work carried out on the development of carbon materials with appropriate surface and textural properties to act as supports for the active phases or as catalysts on their own for catalytic processes such as the reduction of ions and advanced oxidation processes.

2. Carbon materials as catalyst supports

Carbon materials have a great potential as catalyst supports, especially when expensive noble metals are used, since a high metal loading and dispersion can be achieved. However, it is well known that the role of the support is not simply that of a carrier; the interaction between the active phase and the support can also affect the catalytic activity [19].

Catalytic reduction is a promising technology for water treatment, where the ions are reduced over metal catalysts in the presence of hydrogen without the formation of solid or liquid wastes. Metallic catalysts supported on carbon materials have been developed for the selective reduction of nitrate ions to nitrogen [8, 9, 20-23]; and more recently for the reduction of bromate to bromide [12, 13], showing significant advances in these catalytic processes using carbon materials as catalyst supports.

We have studied in detail several mono and bimetallic catalysts supported on commercial activated carbon (ACo) in order to optimize their composition [8, 9], and then we have studied the activities and selectivities of the best catalysts, Pd-Cu and Pt-Cu, evaluating the effect of the support [10, 24]. Therefore, different carbon materials (activated carbons with different surface chemistries (AC1, AC2, AC3), multiwalled carbon nanotubes (CNT) and carbon xerogels (CXG)) were used as supports for the bimetallic catalysts [24]. Table 1 shows the main properties of these supports. Activated carbons present the highest BET surface areas and the CNTs present the lowest values and absence of micropores. The CXG sample has a mesopore surface area higher than the activated carbon samples. Among the activated carbons, no major differences in their textural properties were observed after oxidation with HNO_3 (AC1) or thermal treatments (AC2 and AC3 were obtained by thermally treating AC1 during 1 h at 700 °C under N_2 or H_2 flow, respectively). The surface areas of the supported metal catalysts are not significantly different from the original supports.

Table 1. Textural characterization and pH_{pzc} values of the supports. Adapted from [24] with permission from Springer.

Tabla 1. Caracterización textural y valores pH_{pzc} de los soportes. Adaptado de [24] con permiso de Springer

Sample	S_{BET} (m^2/g)	S_{meso} (m^2/g)	V_{micro} (cm^3/g)	pH_{pzc}
ACo	968	177	0.346	8.3
AC1	886	162	0.322	3.1
AC2	947	164	0.342	9.0
AC3	1001	165	0.349	9.9
CNT1	320	320	0	7.0
CNT2	196	196	0	7.2
CXG	687	287	0.110	7.8

The amounts of CO and CO_2 released from the carbon supports during TPD experiments are shown in Figure 1. Among the activated carbon samples, it can be observed that sample AC1 (oxidised with HNO_3 6 M) presents the highest amount of oxygen surface groups, containing a large amount of carboxylic acid groups and lactones, which confer acid properties to this sample. Some carboxylic anhydrides, phenol and carbonyl/quinone groups are also present [25, 26]. The thermally treated samples (AC2 and AC3) present a relatively low content of oxygen surface groups, since the CO_2 releasing groups (carboxylic acid groups, lactones, carboxylic anhydrides) have been completely removed and only some of the CO releasing groups still remain on the carbon surface at high temperatures. These groups can be carbonyl/quinones that have not been decomposed by the treatment at 700 °C and pyrone groups, which have basic properties and decompose at high temperatures, conferring to these samples basic properties. Sample AC3 shows a lower amount of CO releasing groups than sample AC2 due to the treatment with hydrogen that leads to stable basic surfaces by forming C–H bonds, avoiding further adsorption of oxygen, whereas the thermal treatment under nitrogen leads to a carbon surface with reactive sites able of reincorporating oxygen when exposed to atmospheric air, leading to the formation of some of the previously removed groups. Carbon nanotube samples (CNT1 and CNT2 - commercial CNT with different proveniences) do

not have significant amounts of oxygenated surface groups and the carbon xerogel sample (CXG) presents only a few groups.

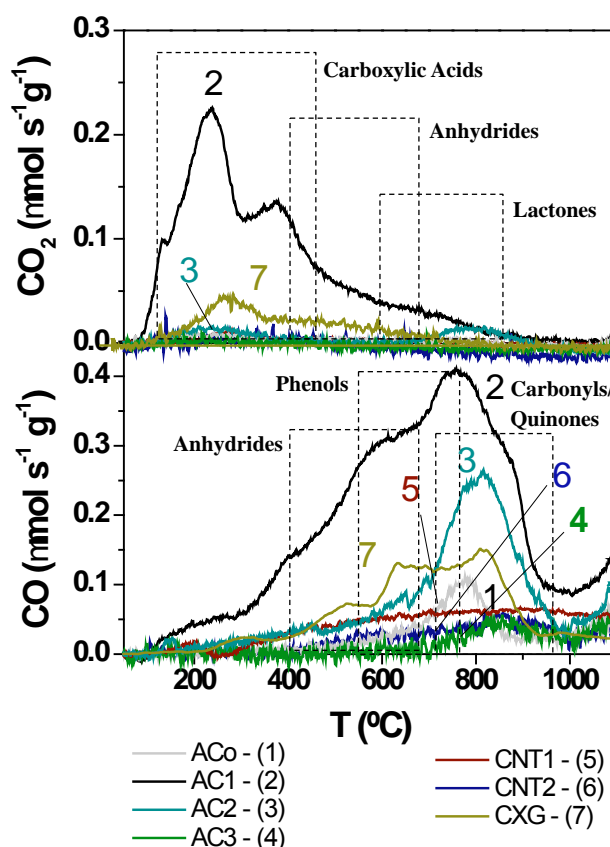


Figure 1 - TPD profiles of carbon materials: CO_2 and CO evolutions (adapted from [24] with permission from Springer).

Figura 1 - Perfiles de DTP de los materiales de carbono: evolución de CO_2 y CO (adaptado de [24] con permiso de Springer).

The surface chemistry of the support has an important role in the catalyst activity and selectivity during the nitrate reduction reaction. Figure 2 shows the results obtained with 2%Pd-Cu catalysts (wt.%), for which a nitrate conversion of 100% is always achieved, independently of the support; the time required to obtain this value being the main difference. When Pt-Cu catalysts are used this effect is much more marked [24]. Independently of the metals, catalysts supported on basic carbon materials and on carbon nanotubes (that present a neutral/basic character) are more active and selective for this reaction. TEM images revealed that the catalysts supported on AC1 and CXG present the largest metal particle sizes, showing that the surface groups of the support determine the metals dispersion. Thus, metal surface dispersion is promoted in supports without significant amounts of oxygenated surface groups, which could act as anchoring sites for the metal precursors, leading, under the condition used, to the agglomeration of the metal particles during the calcination/reduction step.

Carbon nanotubes revealed to be good supports not only due to their surface chemistry, which does not present significant amounts of surface groups, but also due to their high surface area and absence of microporosity. Therefore, this support was studied in detail. These studies demonstrate that the reduction of nitrate is quite different depending on the noble metal, the preparation conditions and the surface chemistry of the CNTs used as support [27]. The nitrogen selectivity experimentally obtained with

Pd-Cu catalysts supported on CNT is close to the maximum selectivity predicted by a mechanistic model developed for this catalytic system at the best operating conditions due to the absence of any mass transfer limitations [28].

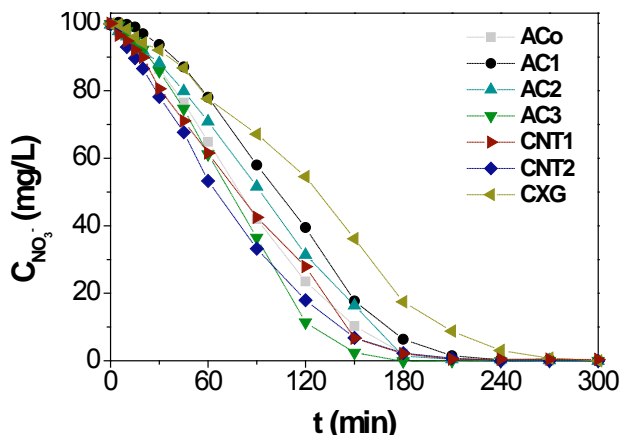


Figure 2 - NO_3^- concentration as a function of time during nitrate reduction in the presence of 2%Pd-1%Cu catalysts (adapted from [24] with permission from Springer).

Figura 2 - Evolución de la concentración de NO_3^- en función del tiempo durante la reducción de nitrato en presencia de los catalizadores 2%Pd-1%Cu (adaptado de [24] con permiso de Springer).

($C_{\text{NO}_3^-} = 100 \text{ mg/L}$, catalyst = 0.5 g/L, pH = 5.5, $Q_{\text{H}_2} = 100 \text{ Ncm}^3/\text{min}$, $Q_{\text{CO}_2} = 100 \text{ Ncm}^3/\text{min}$, $T = 25 \text{ }^\circ\text{C}$).

3. Carbon materials as metal-free catalysts

The use of CNT as metal-free catalysts is a novel approach that has been applied in heterogeneous liquid phase catalytic systems, in particular in advanced oxidation processes, as catalytic wet air oxidation (CWAO) and catalytic ozonation (COz). Briefly, wet air oxidation (WAO) is a technology that can play a major role as primary treatment for highly concentrated wastewaters that are refractory to biological treatments, operating at high reaction temperatures and pressures (200–320 °C and 20–200 bar), which can become milder in the presence of catalysts. Recent studies [14, 15] carried out in the LCM group demonstrate that carbon materials can be applied successfully as metal-free catalysts in CWAO, replacing the catalysts based on noble metals or metal oxides avoiding the leaching of the metals to the liquid

phase. COz is another promising technology for the treatment of organic pollutants, operating at room conditions. Single ozonation shows low reactivity towards specific types of recalcitrant compounds and usually leads to an incomplete degradation of the organic pollutants, but significant enhancements can be obtained in the presence of carbon materials [17]. In general, basic carbons are normally the best catalysts in these AOPs [15, 17].

Ball milling has attracted much attention as a promising method for modifying CNTs, namely to adjust their lengths and to open the closed ends, increasing their specific surface areas. Recently, we have studied the influence of ball-milling on the texture and surface properties of multi-walled carbon nanotubes to be used as catalysts for the ozonation of oxalic acid [18]. This was the pioneering work with ball milling in the LCM group. Different milling times at constant frequency and different frequencies during constant time were used for the preparation of the modified samples. It was observed that the surface area of the CNTs increases, whereas the particle size decreases with the ball-milling time until 240 min at 15 vibrations/s (see Figure 3), but the surface chemistry does not change.

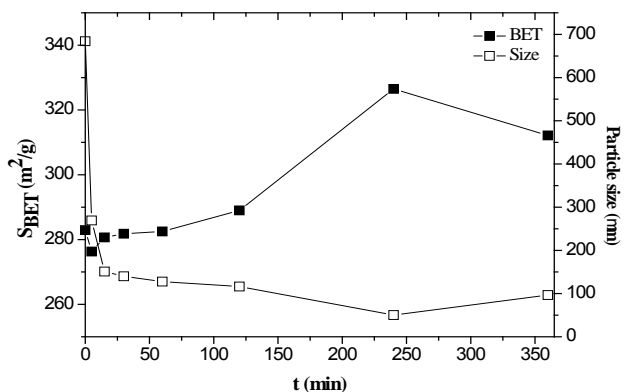


Figure 3 – Evolution of the surface area and mode of particle size distribution of CNT samples with the milling time, for the vibration frequency of 15 vibrations/s (Reprinted from [18] with permission from Elsevier).

Figura 3 – Evolución de la superficie y de la distribución de tamaño de partícula de las muestras de CNT con el tiempo de molienda, para una frecuencia de vibración de 15 vibraciones/s (Reimpreso de [18] con permiso de Elsevier).

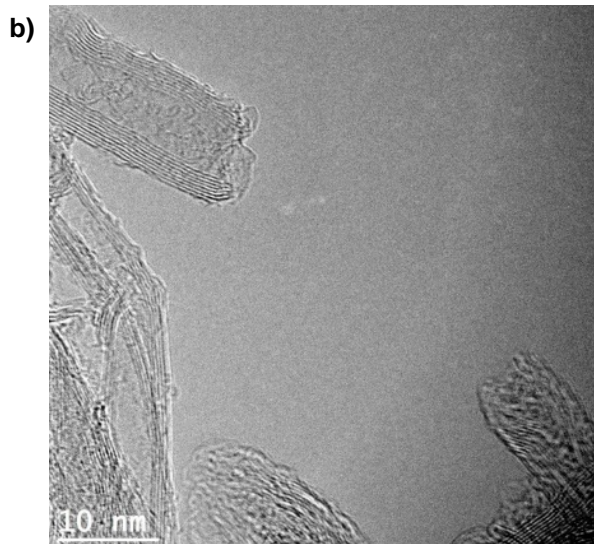
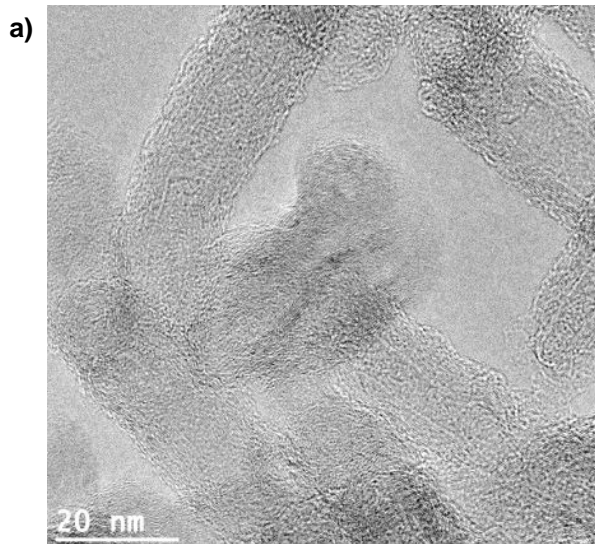


Figure 4 – Representative HRTEM images of the pristine CNT sample (a) and after 240 minutes of milling at a vibration frequency of 15 vibrations/s (b).

Figura 4 – Imágenes representativas de HRTEM de la muestra CNT original (a) y de la misma muestra tras 240 minutos de molienda a una frecuencia de vibración de 15 vibraciones/s (b).

The pristine CNT are formed by well-defined graphitic layers and is formed by several aggregates of tubes highly entangled, curved and twisted with each other (Figure 4a)). Ball-milling is highly effective in disentangling and shortening the CNT by breaking up the tubes and, due that, with the increase of the ball-milling time, the high entanglement is markedly reduced. Open tubes are present in the samples ball milled during 240 (Figure 4b)) or 360 min [18].

The catalytic performance of the ball-milled samples in CO₂ increased significantly when compared to the unmilled CNTs, as shown is Figure 5. Through this work it was concluded that ball-milling is an effective and simple method to increase the surface area of CNTs without significant changes of their structural properties, allowing increased catalytic performance in the ozonation process.

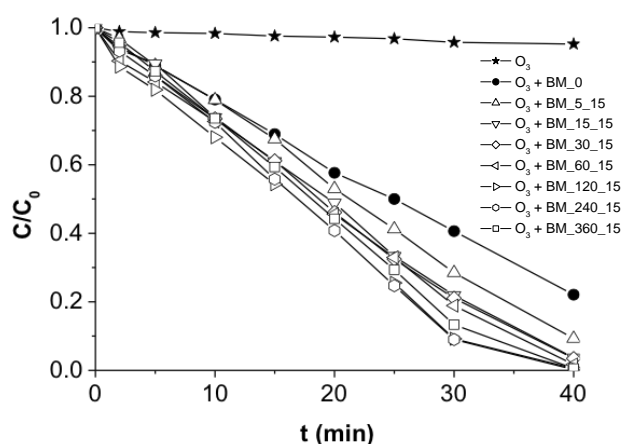


Figure 5 – Evolution of the dimensionless concentration of oxalic acid during single ozonation (O₃) and in the presence of ball-milled CNT at different times and constant vibration rate (15) (Reprinted from [18] with permission from Elsevier).

Figura 5 – Evolución de la concentración de ácido oxálico sin dimensiones durante la ozonización sola (O₃) y en presencia de CNT molino en diferentes tiempos y velocidad de vibración constante (15) (Reimpreso de [18] con permiso de Elsevier).

(C₀ = 1 mM, CNT = 0.14 mg/L)

The development of metal-free carbon materials by tailoring textural and surface chemical properties can play an important role in the catalytic performance; in particular, N-doping was demonstrated to increase the activity of carbon catalysts in oxidation reactions [7, 15]. The main benefit of using N-doped carbons when compared to traditional catalysts (noble metals or metal oxides) is that the N-species are well anchored into the catalyst structure and, as a result, the drawbacks related to active phase sintering are improbable to occur even under severe reaction conditions [29]; in addition, there is improved stability and electron transfer rate, leading to a higher durability of the catalysts during the catalytic processes [6, 7].

Nitrogen doping of carbon materials can be attained in-situ during synthesis or ex-situ using appropriate post-treatments. In recent years, several routes have been tried to modify the carbon structure, in order to develop new functional materials with enhanced properties [30]. Normally, all these methods implicate high energy consumption and multi-step processes, which raise the catalyst manufacturing cost, limiting their practical applications. Recently, we have developed an easy to handle method to prepare N-doped carbon nanotubes [31] and also N-doped graphene oxide (GO) [32] by ball milling, followed by a thermal treatment under inert atmosphere, which avoids the use of solvents and production of wastes. Melamine and urea were used as nitrogen precursors and the procedure applied leads to the incorporation of large amounts of N-groups namely pyridine (N-6), pyrrole (N-5) and quaternary nitrogen (N-Q). The thermal decomposition products of the N-precursor lead to the incorporation of the N-functionalities onto the carbon surface due to the close contact between the precursor and the CNT as a result of the previous mechanical mixture performed by ball milling. The catalysts produced by this method can be easily scalable for practical applications, since their production does not require highly specialized and expensive equipment.

N-doped samples were obtained by ball milling the commercial multi-walled carbon nanotubes with the N-precursors, using the milling conditions optimized in a previous work [18], followed by a thermal treatment under N₂ flow until 600 °C. The modified samples show small differences regarding the surface area (S_{BET}) (lower than 100 m² g⁻¹). The milling of the original CNTs leads to the largest increase of the surface area, while the incorporation of nitrogen originates samples with the lowest surface areas, as shown in Table 2. The addition of the N-precursor only slightly increases the oxygenated surface groups. On the contrary, significant amounts of nitrogen (between 0.2 and 4.8 %) can be introduced on the surface of the CNTs (see Table 2), especially when melamine was used as the N-source. The nature of the N-functionalities, identified by XPS, included pyridine-like N atoms (N-6), pyrrole-like N atoms (N-5), and quaternary nitrogen (N-Q), which are usually thermally stable on carbons.

In a subsequent work [16], it was demonstrated that this ball milling and solvent-free methodology is fairly adequate for the preparation of N-doped carbon materials with enhanced properties for the mineralization of organic pollutants in two distinct advanced oxidation processes: catalytic wet air oxidation and catalytic ozonation. Figure 6 shows that oxalic acid was completely mineralized in 5 min by CWAO and in 4 h by CO₂, under the operation conditions used.

Table 2. Textural and chemical properties of carbon nanotube samples adapted from [31] with permission from Elsevier.

Tabla 2. Textura y propiedades químicas de las muestras de nanotubos de carbono adaptado de [18] con permiso de Elsevier.

Sample	S _{BET} (m ² g ⁻¹)	(CO) _{TPD} (μmol g ⁻¹)	(CO ₂) _{TPD} (μmol g ⁻¹)	N _{XPS} (wt. %)
CNT-O	291	200	23	n.d.
CNT-BM	391	173	44	n.d.
CNT-BM-M-DT	355	338	214	4.8
CNT-BM-U-DT	353	273	112	0.8

n.d. – not determined

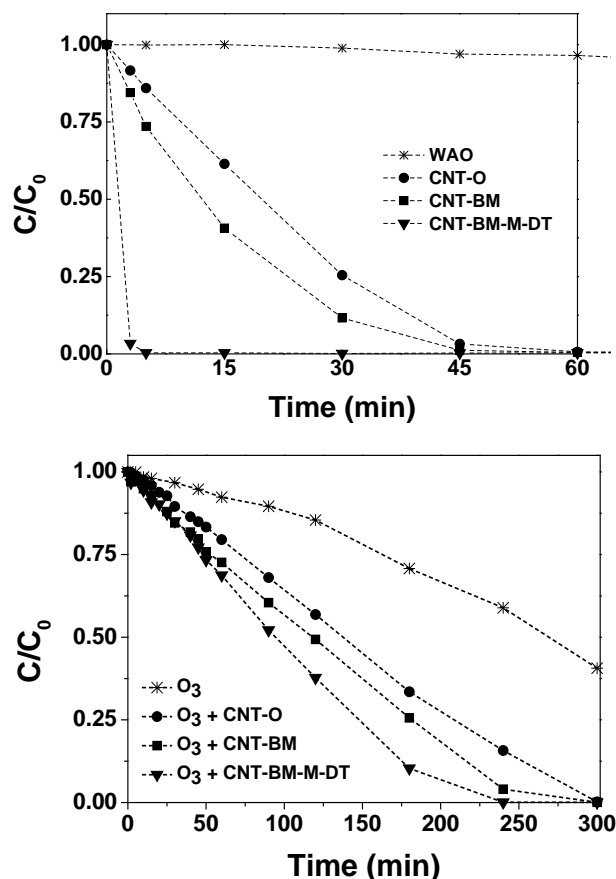


Figure 6 - Evolution of the normalized oxalic acid concentrations: a) in CWAO (140 °C and 40 bar of total pressure, 0.1 g of catalyst; $C_0 = 1000$ mg/L) and b) in COz (room temperature, 0.05 g of catalyst; $C_0 = 450$ mg/L). (non-catalytic conditions (WAO), single ozonation (O_3), original (CNT-O), ball milled (CNT-BM) and sample doped with melamine (CNT-BM-M-DT) (adapted from [16] with permission from Elsevier).

Figura 6 - Evolución de la concentración de ácido oxálico: a) en CWAO (140 °C y 40 bar de presión total, 0,1 g de catalizador; $C_0 = 1000$ mg/L) y b) en COz (temperatura ambiente, 0,05 g de catalizador; $C_0 = 450$ mg/L). (condiciones no catalíticas (WAO), ozonización (O_3), original (CNT-O), molida (CNT-BM) y la muestra dopada con melamina (CNT-BM-M-DT) (adaptado de [16] con permiso de Elsevier).

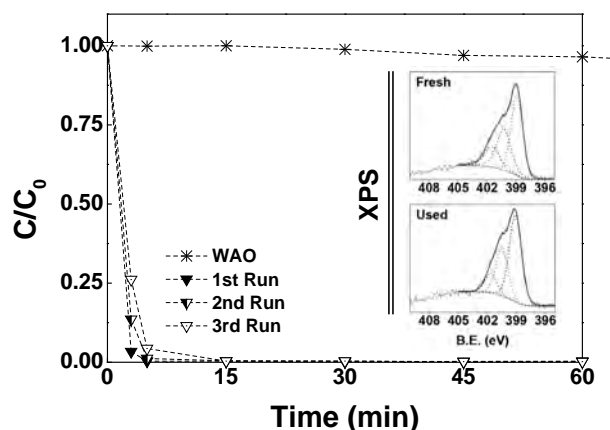


Figure 7 - Cyclic experiments and N1s XPS spectra for the fresh CNT-BM-M-DT sample and after being used in CWAO of oxalic acid (adapted from [16] with permission from Elsevier).

Figura 7 - Experimentos cíclicos y espectros de XPS N1s de la muestra CNT-BM-M-DT, antes y después de ser utilizada en la CWAO de ácido oxálico (adaptado de [16] con permiso de Elsevier).

Cyclic experiments using the same catalyst (CNT-BM-M-DT) with fresh solutions of oxalic acid show a slight deactivation of the catalyst during CWAO. Nevertheless, complete degradation of oxalic acid is observed in less than 15 min. This is frequently

observed during consecutive runs of CWAO due to a slight oxidation of the carbon surface promoted by the operating conditions used. On the other hand, the N-groups introduced on the carbon surface showed to be stable, as can be seen in Figure 7, which shows that the N1s XPS spectra of this catalyst before and after being used in CWAO of oxalic acid present similar proportions of the N-functionalities (N-6, N-5 and N-Q groups).

The novel metal-free catalyst developed by this easy and simple one-step method demonstrated to be effective, confirming that this solvent-free ball milling methodology is quite adequate for the preparation of N-doped carbon materials with enhanced catalytic properties for the AOPs studied. Among the several types of carbon materials (activated carbons, carbon xerogels, ordered mesoporous carbons and carbon nanotubes) successfully tested in CWAO and in COz in the LCM [14, 15, 17, 33-35], the N-doped CNTs prepared by this ball milling method demonstrate to be those with the most outstanding catalytic performances. Therefore, we are currently focusing our interest on the development of the ball milling methodology to prepare carbon materials doped with different heteroatoms to be used as metal catalyst supports or as catalysts on their own for environmental applications.

Conclusions

It was shown that carbon materials have a great potential as catalyst supports and also as catalysts on their own mainly due to their high versatility. Our recent studies demonstrated that the textural and chemical properties of carbon materials can be enhanced for environmental applications, namely catalytic reduction of ions and advanced oxidation processes.

Acknowledgments

This work was supported by Project POCI-01-0145-FEDER-006984 – Associate Laboratory LSRE-LCM funded by FEDER funds through COMPETE2020 – Programa Operacional Competitividade e Internacionalização (POCI) – and by national funds through FCT - Fundação para a Ciência e a Tecnologia. O.S.G.P. Soares acknowledges grant received from FCT (SFRH/BPD/97689/2013). Prof. M.F.R. Pereira, Prof. J.L. Figueiredo and R.P. Rocha are gratefully acknowledged for their assistance in the revision of the manuscript and Marina Enterria for the Spanish translations.

References

- [1] Rodriguez-Reinoso F. The role of carbon materials in heterogeneous catalysis. *Carbon* 1998; 36:159-175.
- [2] Figueiredo JL, Pereira MFR, Carbon as Catalyst, in: P. Serp, J.L. Figueiredo (Eds.), *Carbon Materials for Catalysis*, John Wiley & Sons, Inc, Hoboken, NJ, 2009, pp. 177–217.
- [3] Sun X, Wang R, Su D. Research progress in metal-free carbon-based catalysts. *Chin J Catal* 2013; 508-523.
- [4] Bandosz TJ, Surface chemistry of carbon materials, in: P. Serp, J.L. Figueiredo (Eds.), *Carbon Materials for Catalysis*, John Wiley & Sons, Inc.: Hoboken., 2009, pp. 45-92.
- [5] Figueiredo JL, Pereira MFR. The role of surface chemistry in catalysis with carbons. *Catal Today* 2010; 150:2-7.
- [6] Wong WY, Daud WRW, Mohamad AB, Kadhum AAH, Loh KS, Majlan EH. Recent progress in nitrogen-doped carbon and its composites as electrocatalysts for fuel cell applications. *Int J Hydrogen Energy* 2013; 38:9370-9386.

- [7] Boehm H-P, Catalytic Properties of Nitrogen-Containing Carbons, in: P. Serp, J.L. Figueiredo (Eds.), Carbon Materials for Catalysis, pp. 219-265, John Wiley & Sons, Inc. Hoboken, NJ, 2009, pp. 219-265.
- [8] Soares OSGP, Órfão JJM, Pereira MFR. Activated Carbon Supported Metal Catalysts for Nitrate and Nitrite Reduction in Water. *Catal Lett* 2008; 126:253-260.
- [9] Soares OSGP, Órfão JJM, Pereira MFR. Bimetallic catalysts supported on activated carbon for the nitrate reduction in water: Optimization of catalysts composition. *Applied Cat B* 2009; 91:441-448.
- [10] Soares OSGP, Órfão JJM, Pereira MFR. Pd-Cu and Pt-Cu Catalysts Supported on Carbon Nanotubes for Nitrate Reduction in Water. *Ind Eng Chem Res* 2010; 49:7183-7192.
- [11] Soares OSGP, Órfão JJM, Pereira MFR. Nitrate reduction in water catalysed by Pd-Cu on different supports. *Desalination* 2011; 279:367-374.
- [12] Restivo J, Soares OSGP, Órfão JJM, Pereira MFR. Bimetallic activated carbon supported catalysts for the hydrogen reduction of bromate in water. *Catal Today* 2015; 249:213-219.
- [13] Restivo J, Soares OSGP, Órfão JJM, Pereira MFR. Metal assessment for the catalytic reduction of bromate in water under hydrogen. *Chem Eng J* 2015; 263:119-126.
- [14] Rocha RP, Silva AMT, Romero SMM, Pereira MFR, Figueiredo JL. The role of O- and S-containing surface groups on carbon nanotubes for the elimination of organic pollutants by catalytic wet air oxidation. *Applied Cat B* 2014; 147:314-321.
- [15] Rocha RP, Sousa JPS, Silva AMT, Pereira MFR, Figueiredo JL. Catalytic activity and stability of multiwalled carbon nanotubes in catalytic wet air oxidation of oxalic acid: The role of the basic nature induced by the surface chemistry. *Applied Cat B* 2011; 104:330-336.
- [16] Soares OSGP, Rocha RP, Gonçalves AG, Figueiredo JL, Órfão JJM, Pereira MFR. Highly active N-doped carbon nanotubes prepared by an easy ball milling method for advanced oxidation processes. *Appl Catal B* 2016; 192:296-303.
- [17] Gonçalves AG, Figueiredo JL, Órfão JJM, Pereira MFR. Influence of the surface chemistry of multi-walled carbon nanotubes on their activity as ozonation catalysts. *Carbon* 2010; 48:4369-4381.
- [18] Soares OSGP, Gonçalves AG, Delgado JJ, Órfão JJM, Pereira MFR. Modification of carbon nanotubes by ball-milling to be used as ozonation catalysts. *Catal Today* 2015; 249:199-203.
- [19] Rodríguez-Reinoso F, Sepúlveda-Escribano A. Carbon as catalyst support, in: P. Serp, J.L. Figueiredo(Eds.), Carbon Materials for Catalysis, John Wiley & Sons, Inc, Hoboken, NJ, 2009, pp. 131-156.
- [20] Soares OSGP, Jardim EO, Reyes-Carmona A, Ruiz-Martinez J, Silvestre-Albero J, Rodríguez-Castellón E, Órfão JJM, Sepulveda-Escribano A, Pereira MFR. Effect of support and pre-treatment conditions on Pt-Sn catalysts: Application to nitrate reduction in water. *J Colloid Interface Sci* 2012; 369:294-301.
- [21] Soares OSGP, Órfão JJM, Pereira MFR. Nitrate reduction with hydrogen in the presence of physical mixtures with mono and bimetallic catalysts and ions in solution. *Applied Cat B* 2011; 102:424-432.
- [22] Soares OSGP, Órfão JJM, Ruiz-Martinez J, Silvestre-Albero J, Sepulveda-Escribano A, Pereira MFR. Pd-Cu/AC and Pt-Cu/AC catalysts for nitrate reduction with hydrogen Influence of calcination and reduction temperatures. *Chem Eng J* 2010; 165:78-88.
- [23] Soares OSGP, Órfão JJM, Gallegos-Suarez E, Castillejos E, Rodríguez-Ramos I, Pereira MFR. Nitrate reduction over a Pd-Cu/MWCNT catalyst: application to a polluted groundwater. *Environl Technol* 2012; 33:2353-2358.
- [24] Soares OSGP, Órfão JJM, Pereira MFR. Nitrate Reduction Catalyzed by Pd-Cu and Pt-Cu Supported on Different Carbon Materials. *Catal Lett* 2010; 139:97-104.
- [25] Figueiredo JL, Pereira MFR, Freitas MMA, Órfão JJM. Modification of the surface chemistry of activated carbons. *Carbon* 1999; 37:1379-1389.
- [26] Figueiredo JL, Pereira MFR, Freitas MMA, Órfão JJM. Characterization of active sites on carbon catalysts. *Ind Eng Chem Res* 2007; 46:4110-4115.
- [27] Soares OSGP, Órfão JJM, Pereira MFR. Pd-Cu and Pt-Cu catalysts supported on carbon nanotubes for nitrate reduction in water. *Ind Eng Chem Res* 2010; 49:7183-7192.
- [28] Soares OSGP, Fan X, Órfão JJM, Lapkin AA, Pereira MFR. Kinetic Modeling of Nitrate Reduction Catalyzed by Pd-Cu Supported on Carbon Nanotubes. *Ind Eng Chem Res* 2012; 51:4854-4860.
- [29] Cuong D-V, Ba H, Liu Y, Lai T-P, Nhut J-M, Cuong P-H. Nitrogen-doped carbon nanotubes on silicon carbide as a metal-free catalyst. *Chin J Catal* 2014; 35:906-913.
- [30] Su DS, Perathoner S, Centi G. Nanocarbons for the Development of Advanced Catalysts. *Chem Rev* 2013; 113:5782-5816.
- [31] Soares OSGP, Rocha RP, Gonçalves AG, Figueiredo JL, Órfão JJM, Pereira MFR. Easy method to prepare N-doped carbon nanotubes by ball milling. *Carbon* 2015; 91:114-121.
- [32] Rocha RP, Gonçalves AG, Pastrana-Martinez LM, Bordoni BC, Soares OSGP, Órfão JJM, Faria JL, Figueiredo JL, Silva AMT, Pereira MFR. Nitrogen-doped graphene-based materials for advanced oxidation processes. *Catal Today* 2015; 249:192-198.
- [33] Faria PCC, Órfão JJM, Pereira MFR. Mineralisation of coloured aqueous solutions by ozonation in the presence of activated carbon. *Water Res.* 2005; 39:1461-1470.
- [34] Orge CA, Sousa JPS, Gonçalves F, Freire C, Órfão JJM, Pereira MFR. Development of novel mesoporous carbon materials for the catalytic ozonation of organic pollutants. *Catal Lett* 2009; 132:1-9.
- [35] Rocha RP, Restivo J, Sousa JPS, Órfão JJM, Pereira MFR, Figueiredo JL. Nitrogen-doped carbon xerogels as catalysts for advanced oxidation processes. *Catal Today* 2015; 241:73-79.

Functional Carbon-Based Nanomaterials for Energy Storage: Towards Smart Textile Supercapacitors

Nanomateriales basados en carbones funcionalizados para almacenamiento de energía. Hacia supercapacitadores de tejidos inteligentes

C. Pereira^{1,*} and A. M. Pereira²

¹ REQUIMTE/LAQV, Departamento de Química e Bioquímica, Faculdade de Ciências, Universidade do Porto, 4169-007 Porto, Portugal.

² IFIMUP and IN – Institute of Nanoscience and Nanotechnology, Departamento de Física e Astronomia, Faculdade de Ciências, Universidade do Porto, 4169-007 Porto, Portugal.

*Corresponding author: clara.pereira@fc.up.pt

Abstract

Hybrid supercapacitors emerged as an eco-friendly technology to address the grand challenge of sustainable and efficient energy storage. Functional carbon-based nanomaterials are promising building blocks for the design of advanced electrodes for this type of supercapacitors. The boost on wearable electronics opened new market opportunities for hybrid supercapacitors integrated in textiles using carbon-based electrodes.

In this work, we will start by providing a brief introduction to the main principles of supercapacitors, followed by the importance of carbon (nano)materials as electrodes for the design of high-performance supercapacitors for energy storage. Subsequently, the progress achieved by our team in the field of hybrid carbon–metal oxide nanomaterials and smart textile supercapacitors will be highlighted.

Resumen

Los supercapacitadores híbridos surgieron como una tecnología respetuosa con el medio ambiente para dar respuesta al gran objetivo de conseguir un almacenamiento de energía eficiente y sostenible. Los nanomateriales de carbón funcionalizados presentan un gran potencial para el diseño de electrodos avanzados para este tipo de supercapacitadores. El impulso de los productos electrónicos en el vestido abre nuevas oportunidades de mercado para supercapacitadores híbridos integrados en los tejidos usando electrodos de carbón.

En este trabajo se presenta una breve introducción a los principios generales de los supercapacitadores, y la importancia de los nanomateriales de carbón como electrodos para el diseño de supercapacitadores de altas prestaciones en el almacenamiento de energía. Se resaltan los progresos de nuestro equipo en el campo de los nanomateriales híbridos carbón–óxido metálico y los supercapacitadores de tejidos inteligentes.

Keywords: carbon nanomaterials, hybrid compounds, supercapacitors, smart textile supercapacitors

Palabras clave: Nanomateriales de carbon, compuestos híbridos, supercapacitadores, supercapacitadores de tejidos inteligentes.

1. Introduction

In the era of high-tech, the development of wearable energy storage devices has been a great challenge

for Society, motivated by the escalating growth of the market of portable electronics and smart technologies [1,2]. In particular, the integration of flexible supercapacitors in textiles has been a major milestone in order to produce wearable energy storage clothing for the power supply of sensors, flexible displays, among others. In Portugal, the Textile Industry is one of the core engines for the economic growth. In 2014, the Portuguese Textile and Clothing Industry represented 10% of the total national exports, which corresponds to ~4600 M€¹. Therefore, the investment in high-tech textiles with novel functionalities is of paramount importance for this sector.

With the advances in Nanotechnology, nanomaterials emerged as potential building blocks for the design of high-performance textiles with novel functionalities (eg. super-hydrophobicity/oleophobicity, photochromism, thermochromism, antimicrobial properties), while providing improved comfort to the user [3,4]. In particular, carbon–metal oxide nanomaterials are promising electrode materials for the design of lightweight and flexible textile supercapacitors [1].

2. Supercapacitors: A General Overview

Supercapacitors (SCs) represent a versatile energy storage solution for a sustainable energy storage supply that bridges the gap between conventional capacitors and rechargeable batteries. As can be seen in the Ragone plot presented in Figure 1, SCs present higher power density than batteries but lower than that of traditional capacitors [5,6]. This ability allows fast charge, which is a key advantage when compared with batteries. Moreover, they present excellent cycling stability and a significantly longer cycle life (up to 10⁶ cycles) than traditional batteries (up to 500 times) [6]. On the other hand, when compared with conventional capacitors, SCs present higher energy density, which is one of their fingerprint features since they can power supply the devices for longer operation time.

The current challenge for SCs nowadays is to improve their energy density and lower their fabrication costs without sacrificing their high power capability. For that purpose, new electrode materials and electrolytes are being developed.

The simplified structure of a SC is composed by two electrodes (positive and negative), an electrolyte, two current collectors and a separator membrane [7]. The electrodes are constituted by conductive

¹ Data estimated by Associação Têxtil e Vestuário de Portugal (ATP) based on the indicators from Instituto Nacional de Estatística.

materials with a large specific surface area and/or by electrochemically active materials. The electrolyte is an ionically conducting medium that exists between both electrodes and has the main function of transporting ions until the surface of the electrodes. The separator is an ion-permeable electron-insulating membrane, *i.e.* it allows the migration of electrolyte ions and electrically isolates the two electrodes. The current trend in textile SCs is to replace liquid electrolytes by solid-gel ones that act both as electrolyte and separator. Finally, the current collectors are connected to the electrodes and are responsible for the electrons transport.

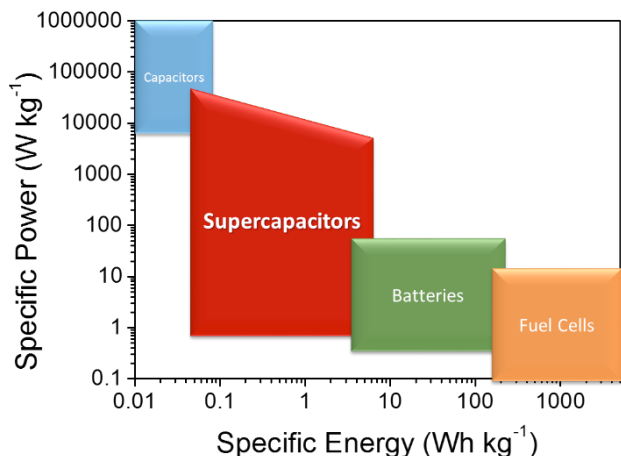


Figure 1. Ragone Plot comparing different energy storage technologies (adapted from ref. 6).

SCs taxonomy divides them in different categories depending on the electrodes type/function as well as on the energy storage mechanism. They can be classified into three large groups: *electric double-layer capacitors* (EDLCs), *pseudocapacitors* and *hybrid capacitors* (Figure 2) [7].

In **EDLCs**, the capacitive charging occurs in the electrode/electrolyte interfaces and charge is stored electrostatically by a non-Faradaic mechanism [7]. There is no charge transfer between the electrodes and the electrolyte which enables a longer cycle life. Therefore, EDLCs usually have higher power density when compared to batteries of similar dimensions. Carbon (nano)materials have been the most widely used electrode materials in EDLCs [8].

On the other hand, in **pseudocapacitors** the energy storage process involves charge transfer between the electrode and the electrolyte by means of reduction-oxidation reactions, ion intercalation/deintercalation and electrosorption (Faradaic mechanisms) [9]. The charge transfer process is similar to that of a battery, but the transfer rates are higher since in pseudocapacitors

electrochemical reactions occur at the surface and in the bulk near the surface of the electrodes instead of propagating into the bulk material [5]. Due to the nature of the storage mechanism, pseudocapacitors present higher capacitance than EDLCs, albeit their lower power density. Both cycle life and storage capability thus fall between those of batteries and EDLCs. The pseudocapacitive electrode materials most commonly used are transition metal oxides/hydroxides and electrically conducting polymers [7,9].

Hybrid capacitors emerged as a novel solution to overcome the limitations of EDLCs and pseudocapacitors, combining both abovementioned charge storage mechanisms in a single device [7]. This can be accomplished through the use of composite or hybrid materials composed by an EDLC-type and a pseudocapacitor-type component as electrodes, the so-called *composite* or *symmetric hybrids*. Hybrid capacitors can also be classified as *asymmetric hybrids* when they couple two electrodes with different storage mechanisms: in one of the electrodes, only an electrostatic process occurs, whereas in the other electrode redox reactions or a combination of non-Faradaic and Faradaic processes occur. Finally, the third type of hybrid capacitors are *battery-type hybrid capacitors*, where one of the electrodes is a material containing Li^+ ions to enable Li^+ intercalation/deintercalation similarly to battery mechanism.

3. Carbon (Nano)Materials as Electrodes in Supercapacitors

Carbon (nano)materials have been among the top choices as electrodes for energy storage applications owing to their versatile structures ranging from 0D to 3D and tunable surface chemistry [8]. In particular, activated carbon, graphene, carbon nanotubes, onion-like carbons and templated carbons have attracted great interest as EDLC-type electrodes for SCs owing to their high electrical conductivity, large specific surface area, easy handling, high chemical and thermal stability and excellent mechanical properties [8,10]. Due to these features, carbon-based SCs exhibit high power density, high charge-discharge rates, excellent cycling stability and long operation life. In Table 1 is presented a comparison between different types of carbon-based materials commonly used as EDLC-type electrodes.

Each type of carbon-based material has its unique structure and features [12]. For instance, 0D and 1D carbon nanomaterials, such as carbon onions and carbon nanotubes, allow achieving high power density due to the fast adsorption/desorption of the electrolyte ions on their surface. On the other hand,

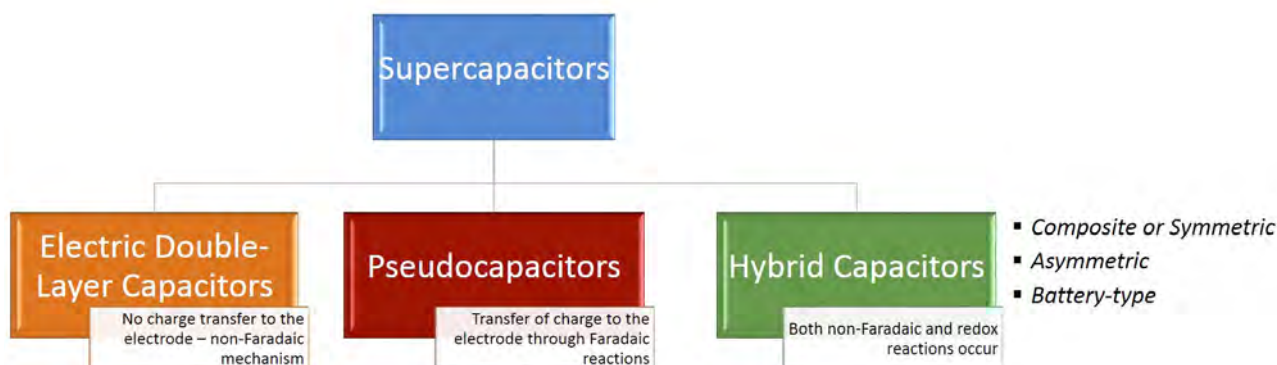



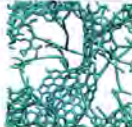
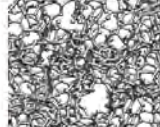



Figure 2. Flow-chart of SCs taxonomy.

Table 1. Comparison between different types of carbon-based materials used in EDLCs^a

Material	Carbon onions	Carbon nanotubes	Graphene	Activated carbon	Carbide derived carbon	Templated carbon
Dimensionality	0-D	1-D	2-D	3-D	3-D	3-D
Conductivity	High	High	High	Low	Moderate	Low
Volumetric Capacitance	Low	Low	Moderate	High	High	Low
Cost	High	High	Moderate	Low	Moderate	High
Structure						

^a Reproduced from ref. 11 with permission from The American Chemical Society.

graphene, a 2D carbon nanomaterial, can provide higher charge/discharge rate and volumetric energy density. Porous 3D carbon materials such as activated carbon, templated carbon and carbide-derived carbon present higher surface areas and pores in the Å or nm range, delivering higher energy densities if their pore dimensions matches the size of electrolyte ions [12]. Therefore, the selection of the proper type of carbon material will depend on the requirements of the target application.

In particular, in the case of the market of portable electronics, carbon nanotubes (CNTs), graphene, activated carbon and carbon fibers have attracted significant interest for the fabrication of flexible and wearable energy storage systems (eg. SC fabrics/fibers, plastic electronics, Figure 3) [10].

Despite the advantages of carbon-based SCs, they still exhibit limited specific capacitance owing to the non-Faradaic charge storage mechanism; consequently, they present lower energy density

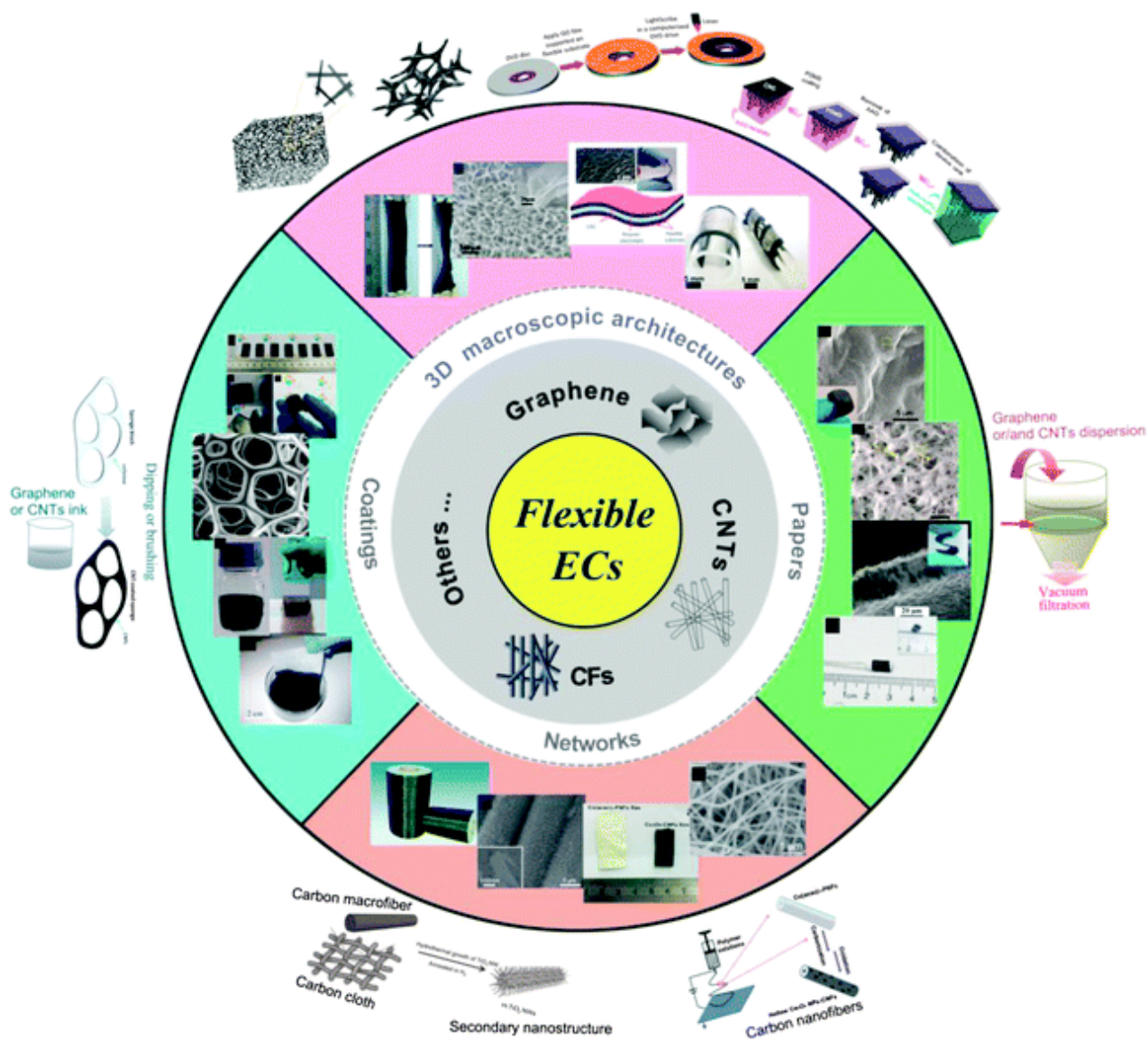


Figure 3. Fabrication of carbon-based electrode materials for flexible SCs. Reproduced from ref. 10 by permission of The Royal Society of Chemistry.

than pseudocapacitors (typically $\sim 5 \text{ Wh/kg}^{-1}$) [10]. To overcome these limitations, the performance of carbon-based electrode materials has been improved by tailoring their specific surface area, pore structure, electrical conductivity and surface chemistry [13]. To achieve this goal, several strategies have been developed, namely: (i) Design of carbon materials with hierarchical porous structure, (ii) Doping of carbon (nano)materials with heteroatoms (N, O, S, B, P) and (iii) Design of hybrids/composites combining conductive carbon (nano)materials with transition metal oxides and/or conducting polymers [13–15].

Strategy (i) allows optimizing the pore sizes and pore size distribution and simultaneously increasing the specific surface area, without compromising the electrical conductivity [14]. The high specific surface area increases the number of accessible active sites, contributing to enhanced capacitance, while the pore structure regulates the electrolyte ions diffusion and, consequently, the performance of the SC (power density and charge-discharge rate) [13].

On the other hand, the tuning of the surface chemistry of the carbon material can be achieved by strategies (ii) or (iii), which introduce an additional pseudocapacitive component to the device (Faradaic reactions) [13,14]. Furthermore, in the case of strategy (ii), the introduction of surface functionalities can improve the wettability of the carbon surface (hydrophilicity/lipophilicity), facilitating the electrolyte ions adsorption and ensuring their fast transport within the carbon material pores [13,15].

3.1 Heteroatom-Doped Carbon Nanomaterials

Heteroatom doping is an efficient method to fine-tune the structural and electronic properties of carbon electrode materials [14,15]. The presence of heteroatoms such as O, N, S and P on the surface of the carbon support may induce surface faradaic redox reactions and/or a local modification of its electronic structure besides improving the electrode-electrolyte interactions, due to a decrease of the gap between the conduction and valence bands and an increase of the number of local free electrons [7,14,15]. Among various types of heteroatoms, O-doping and N-doping have been the most extensively investigated for SC applications [16].

Oxygen-enriched carbon materials namely containing quinone groups are typically prepared by carbonization/activation of an oxygen rich precursor, liquid-phase or gas-phase post-treatment oxidation (in HNO_3 , O_2 , etc.), electrochemical oxidation and oxygen plasma treatment [14]. The oxygen-containing functional groups are usually acidic, introducing electron-acceptor properties into the carbon surface.

Nitrogen-doping can be performed by *in-situ* and post-treatment processes [14,16]. The *in-situ* route consists on the carbonization of a nitrogen-rich carbon precursor (melamine, cyanamide, polyacrylonitrile, polyaniline, etc.) followed by steam activation. The post-treatment can be performed by impregnation of porous carbon (nano)materials with N-containing reagents (NH_3 , urea, amines) followed by thermal treatment, by nitrogen plasma treatment, among others. The *in-situ* approach leads to a higher amount of nitrogen-based functional groups, while the post-treatment routes can only introduce N-functional

groups on the surface of the carbon materials. N-containing functionalities such as pyridinic N, pyrrolic N, quaternary N and N-oxide present electron-donor properties which can tailor the electrodes wettability, electrical conductivity and capacitance performance [14,16]. In this context, they contribute with additional electrons and fast electron transfer, inducing negative charges on adjacent carbon atoms and widening the electrode capacitance [17].

More recently, simultaneous co-doping of two distinct heteroatoms into carbons, namely N-/P-, B-/N-, B-/P-, emerged as a promising strategy to improve the SC performance owing to the synergistic effect between both functionalities [14]. Nevertheless, special care should be taken during heteroatom doping to avoid conductivity and structural deterioration [15]. The excessive doping may increase the number of defects on the surface of carbon materials; furthermore, the formation of multiple functional groups may lead to higher leakage current and lower cycle life (fast degradation) [14–16].

3.2 Hybrid Carbon–Metal Oxide Nanomaterials

A distinct route to improve the performance of carbon-based electrodes and overall performance of the resulting SCs consists on combining the carbon material with other components that exhibit a complementary charge storage mechanism, namely pseudocapacitive transition metal oxide/hydroxide nanoparticles (NPs) and/or conducting polymers.

In particular, hybrid carbon–metal oxide/hydroxide nanomaterials constitute a breakthrough on the design of high-performance electrodes and flexible SCs [10,18]. Through the conjugation of two distinct components with complementary physicochemical characteristics in a single electrode, a synergistical improvement of the properties of the resulting hybrid electrode can be achieved when compared with those of the individual components. The conductive carbon material is used as backbone support and conductive path for electron transport, imparting EDL capacitance. Furthermore, due to the large specific surface area and porous structure, it improves the electrolyte accessibility and contact between the electrolyte and the supported pseudocapacitive component [10]. On the other hand, the grafted metal oxide/hydroxide NPs can increase the performance of the hybrid electrode material by allowing the occurrence of reversible redox reactions upon SC charging/discharging. The most commonly used metal oxide/hydroxide nanomaterials have been RuO_2 , MnO_x , Co_3O_4 , NiO/Ni(OH)_2 , Fe_xO_y , NiCo_2O_4 , etc. [1].

Hybrid carbon–metal oxide nanomaterials can be prepared by several methods including coprecipitation, hydrothermal, electrodeposition, among others [14]. Regardless of the process, it should ensure a uniform distribution of the metal oxide NPs throughout the support surface. The presence of surface functional groups on the carbon support that act as anchoring sites is required to ensure the robust anchorage of the NPs upon their nucleation and growth and prevent particle leaching.

Nevertheless, the design of hybrid carbon–metal oxide nanomaterials with fine-tuned physicochemical properties by controllable and easily scalable routes continues to be a challenging milestone to achieve

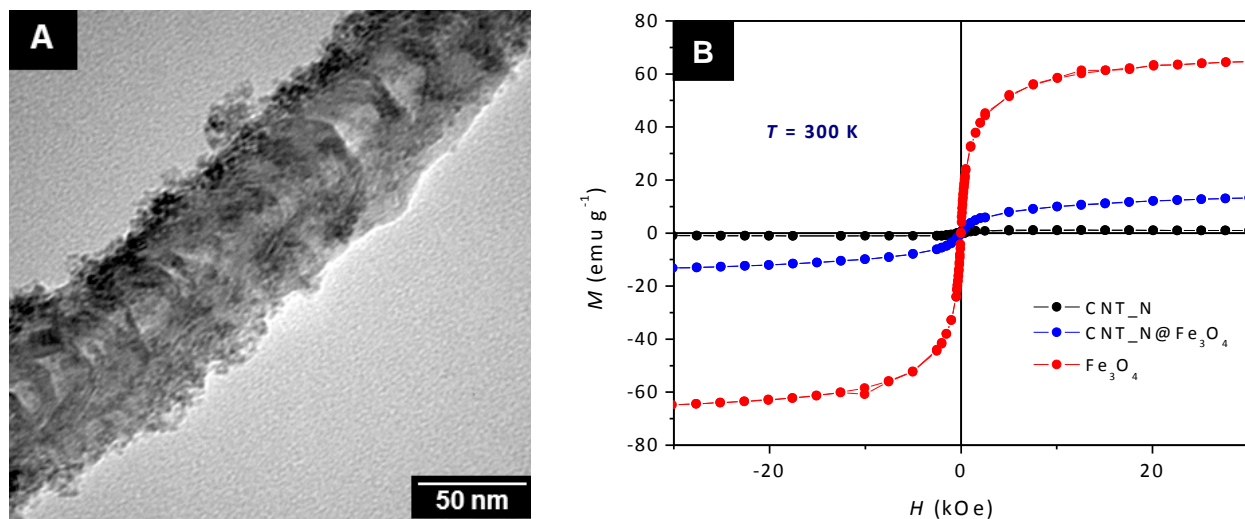


Figure 4. (A) TEM image of CNT_N@Fe₃O₄ and (B) Magnetization as a function of applied magnetic field at 300 K for CNT_N, Fe₃O₄ and CNT_N@Fe₃O₄.

high-performance SCs [18].

Our team has been fabricating novel hybrid carbon-based nanomaterials to be used as electrode materials for SCs through the immobilization of superparamagnetic transition metal ferrite NPs (MFe₂O₄ with M(II) = *d*-block transition metal cation) onto N-doped CNTs. To accomplish this goal, we have developed a one-pot *in-situ* coprecipitation process that ensures the controlled formation of NPs with reduced particle size and high crystallinity throughout the support surface [19–21]. The N-doped carbon nanotubes (CNT_N) used in this work have been prepared by the group of Prof. Dr. Antonio Guerrero-Ruiz, Instituto de Catálisis y Petroleoquímica, CSIC, Madrid, Spain through acetonitrile vapor decomposition [22].

Our main goal is to modulate the dielectric properties of CNT_N through the incorporation of MFe₂O₄ NPs with different types of M(II) cations, thus combining the high electrical conductivity arising from the CNTs support with the high specific capacitance imparted by the metal oxide NPs. As example, we have prepared a hybrid CNT_N@Fe₃O₄ nanomaterial by *in-situ* coprecipitation of iron(II) and iron(III) salt precursors in the presence of the CNT_N support induced by an alkanolamine base.

The transmission electron microscopy (TEM) images (Figure 4A) revealed the presence of ultrasmall particles with average particle size of 3.2±0.6 nm throughout the bamboo-like CNTs surface.

When it comes to hybrid nanomaterials it is vital to quantify the amount of each component. When the hybrid material has a strong magnetic component and the other constituent is magnetically weak or is non-magnetic, the measurement of the magnetic properties by magnetometry is a powerful technique to determine their loadings. In our case, the hybrid is constituted by Fe₃O₄ NPs that exhibit superparamagnetic behavior at room temperature and by CNTs that can be diamagnetic but in some cases can present weak ferromagnetic or paramagnetic properties depending on the synthesis route arising from the precursors [23].

In Figure 4B are presented the isothermal magnetization curves ($T = 300$ K) as a function of applied magnetic field for the parent CNT_N, the

unsupported superparamagnetic Fe₃O₄ NPs and the hybrid nanomaterial containing both components (CNT_N@Fe₃O₄). From Figure 4B it can be observed that the magnetization contribution arising from the CNT_N support is almost negligible when compared with that of the Fe₃O₄ magnetic nanoparticles (MNPs). On the other hand, the hybrid nanomaterial presents a similar trend to that of Fe₃O₄, albeit the lower saturation magnetization, thus confirming the presence of both CNTs and MNPs. From these curves the amount of Fe₃O₄ MNPs in the hybrid nanomaterial can be extracted with respect to that of the CNT_N support: CNT_N@Fe₃O₄ is composed by 24.5 wt% of Fe₃O₄ and 75.5 wt% of CNT_N. Moreover, the absence of magnetic hysteresis indicates that the hybrid nanomaterial is in the superparamagnetic state at room temperature, similarly to the unsupported Fe₃O₄ MNPs [19].

For the design of SCs with high performance, it is important to evaluate the electrical resistivity of the electrode since it is one of the crucial parameters to

increase the SC power density P ($P = \frac{V^2}{4R}$, where V

is the applied voltage and R is the circuit equivalent resistance) [7]. Therefore, in order to maximize the power density, the ideal electrodes should have low electrical resistivity. Another important parameter is the electrode capacitance (C), that should be high to

achieve high energy density E ($E = \frac{1}{2} C_T V^2$, where the total capacitance C_T is half of C) [7].

To determine these properties, impedance measurements in the frequency range 20 Hz – 3 MHz were performed for CNT_N, Fe₃O₄ MNPs and CNT_N@Fe₃O₄ hybrid. The electrical conductivity values as a function of frequency, presented in Figure 5, were extracted from the impedance curves by

using $\sigma = \frac{Z' t}{(Z'^2 + Z''^2) A}$, where Z' is the real part of

the impedance and Z'' is the imaginary part, A is the effective section area and t is the thickness.

Among all nanomaterials, the parent CNT_N presents the highest electrical conductivity ($\sigma \sim 0.130$ S m⁻¹ within all frequency range), with a very small Z''

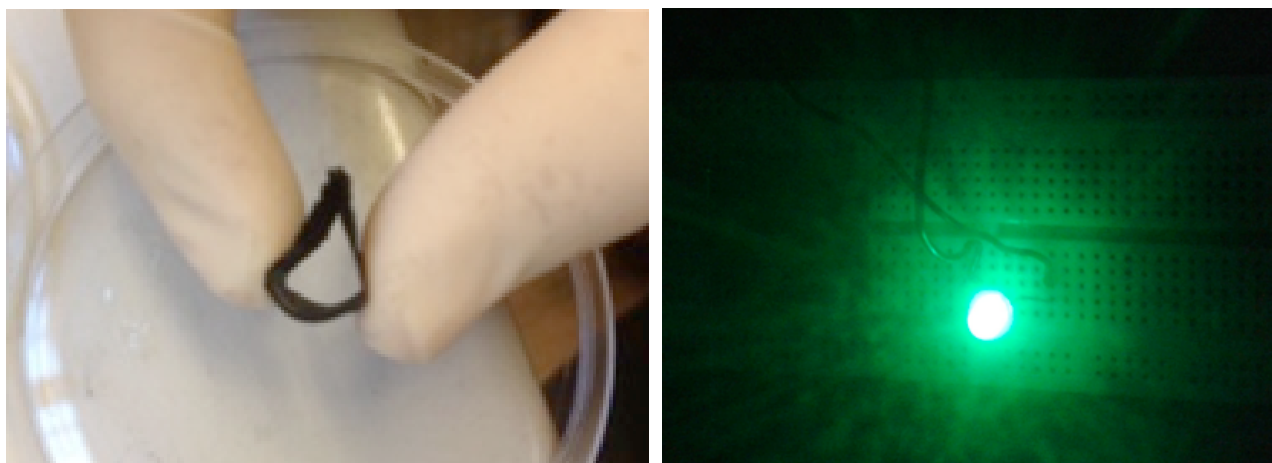


Figure 6. Flexible cotton-based SC prototype (left) and LED powered by three cotton-based prototypes connected in series (right).

(not shown), which is characteristic of a conductive material. In the case of the Fe_3O_4 MNPs, it can be observed that σ is proportional to the frequency, increasing from $\sim 10^{-8}$ to 10^{-5} S m^{-1} , showing that the material has a very small conductivity and presents an insulator behavior. Important to point out is that in the case of the $\text{CNT}_N@Fe_3O_4$ hybrid nanomaterial an intermediate electrical conductivity value was achieved of $\sigma \sim 0.043 \text{ S m}^{-1}$ within all frequency range.

Hence, through the incorporation of Fe_3O_4 MNPs onto the CNT_N support, it was possible to graft $\sim 24.5 \text{ wt}\%$ of MNPs, while preserving the typical properties of conductive materials. This is a promising achievement since the $\text{CNT}_N@Fe_3O_4$ hybrid possesses metal oxide NPs that enable the occurrence of Faradaic reactions within the SC and low resistivity arising from the support for the simultaneous occurrence of an EDLC-type mechanism. Therefore, the prepared $\text{CNT}_N@Fe_3O_4$ hybrid is a promising electrode candidate for the design of textile-based hybrid capacitors.

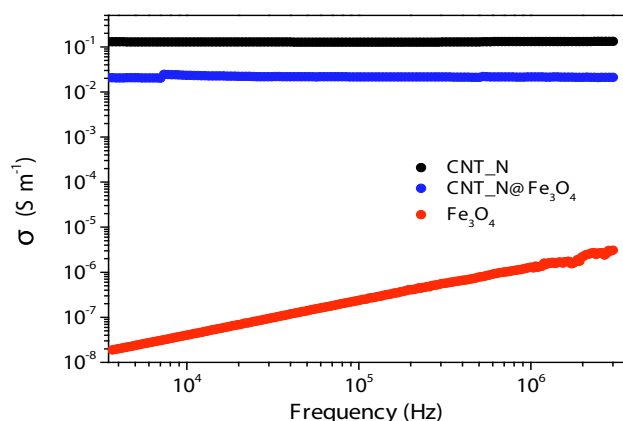


Figure 5. Electrical conductivity at room temperature as a function of frequency for CNT_N , Fe_3O_4 and $\text{CNT}_N@Fe_3O_4$.

4. Smart Textile Supercapacitors for Energy Storage

Textiles supercapacitors can be produced by different routes: (i) coating of pre-existing textile substrates, (ii) building-up fibers and yarns and (iii) designing custom woven or knitted architectures that incorporate the SC into the textile structure [2]. In strategy (i), the fabric is firstly coated with the electrode nanomaterials followed by the assembly of the resulting textile electrodes and the electrolyte/separator into the final SC textile. In this type of SC design, both electrodes

and electrolyte can be assembled in a multilayer configuration or side-by-side in a planar configuration. In route (ii), the electrode materials are incorporated during the fabrication of the fibers/yarns giving rise to electrode fibers/yarns that can then be knitted/woven directly into a garment; the fibers can be processed in different configurations and contain different coatings/multilayers or components [2].

The selected strategy should always take in mind production costs and scalability in order to become a viable solution. In this sense, our team has been developing textile SCs based on carbon–metal oxide nanomaterials through processes that can be easily scalable and implemented in Textile Industry using the available infrastructures.

We have started by fabricating novel solid-state and flexible textile SCs using composite electrodes constituted by carbon black and MnFe_2O_4 MNPs and a solid-gel electrolyte. Woven cotton substrates were dip-coated with carbon black and MnFe_2O_4 inks in order to produce the textile-based electrodes. The cotton-based SC prototype, which presented high flexibility (see Figure 6), was produced through the assembly of the textile electrodes and electrolyte in a multi-layered configuration.

The performance of the resulting SC fabric was evaluated by performing cyclic voltammetry, galvanostatic charge/discharge and electrochemical impedance spectroscopy (EIS). From the obtained current-voltage cycles, the determined specific capacitance of the SC prototype was 307 F/kg , leading to an energy density of 474 Wh/kg (per active mass loading). Furthermore, from the EIS measurements, an equivalent series resistance of $1.25 \text{ k}\Omega$ was obtained, leading to a power density of 117 W/kg . Although the energy density and capacitance of the SC fabric were promising, the equivalent series resistance was responsible for a small power density. Nevertheless, by connecting three SC fabrics with $1 \times 1 \text{ cm}^2$ in series, we were able to light a green LED for up to eight minutes (Figure 6).

Finally, the results obtained in this work demonstrated the feasibility of combining nanomaterials dispersions with dyeing processes used in the Textile Industry to design lightweight and flexible textile SCs. New processes are currently being developed by our team to fabricate high-performance textile SCs using different types of fabric substrates and hybrid carbon–metal oxide nanomaterials as electrodes.

Acknowledgments

The work was funded by Fundação para a Ciência e a Tecnologia (FCT)/MEC and FEDER under Program PT2020(project UID/QUI/50006/2013-POCI/01/0145/FEDER/007265) and through project ref. PTDC/CTM-NAN/5414/2014 in the framework of Program COMPETE. The authors thank Prof. C. Freire, MSc. student R.S. Costa, MSc. J. Valente and BSc. L. Lopes for their contribution as well as Dr. B. Bachiller-Baeza and Prof. A. Guerrero-Ruiz for providing the CNT_N nanomaterial. Prof. P. B. Tavares and MSc. L. Fernandes are also acknowledged for TEM images.

References

- [1] Lu X, Yu M, Wang G, Tong Y, Li Y. Flexible solid-state supercapacitors: design, fabrication and applications. *Energy Environ Sci* 2014; 7: 2160–2181.
- [2] Jost K, Dion G, Gogotsi Y. Textile energy storage in perspective. *J Mater Chem A* 2014; 2: 10776–10787.
- [3] Pereira C, Alves C, Monteiro A, Magén C, Pereira AM, Ibarra A, Ibarra MR, Tavares PB, Araújo JP, Blanco G, Pintado JM, Carvalho AP, Pires J, Pereira MFR, Freire C. Designing Novel Hybrid Materials by One-Pot Co-condensation: From Hydrophobic Mesoporous Silica Nanoparticles to Superamphiphobic Cotton Textiles. *ACS Appl Mater Interfaces* 2011; 3: 2289–2299.
- [4] Ribeiro LS, Pinto T, Monteiro A, Soares OSGP, Pereira C, Freire C, Pereira MFR. Silica nanoparticles functionalized with a thermochromic dye for textile applications. *J Mater Sci* 2013, 48: 5085–5092.
- [5] Hall PJ, Mirzaeian M, Fletcher SI, Sillars FB, Rennie AJR, Shitta-Bey GO, Wilson G, Cruden A, Carter R. Energy storage in electrochemical capacitors: designing functional materials to improve performance. *Energy Environ Sci* 2010; 3: 1238–1251.
- [6] Kötz R, Carlen M. Principles and applications of electrochemical capacitors. *Electrochim Acta* 2000; 45: 2483–2498.
- [7] Beguin, F, Frackowiak, E, Supercapacitors: Materials, Systems and Applications. Wiley-VCH, 1st Edition, Weinheim, Germany, 2013.
- [8] Chen T, Dai L. Carbon nanomaterials for high-performance supercapacitors. *Mater Today* 2013; 16: 272–280.
- [9] Augustyn V, Simon P, Dunn B. Pseudocapacitive oxide materials for high-rate electrochemical energy storage. *Energy Environ Sci* 2014; 7: 1597–1614.
- [10] He Y, Chen W, Gao C, Zhou J, Li X, Xie E. An overview of carbon materials for flexible electrochemical capacitors. *Nanoscale* 2013; 5: 8799–8820.
- [11] Simon P, Gogotsi Y. Capacitive Energy Storage in Nanostructured Carbon-Electrolyte Systems. *Acc Chem Res* 2013; 46: 1094–1103.
- [12] Gogotsi, Y. Not just graphene: The wonderful world of carbon and related nanomaterials. *MRS Bull* 2015; 40: 1110–1121.
- [13] Zhang LL, Zhao, XS. Carbon-based materials as supercapacitor electrodes. *Chem Soc Rev* 2009; 38: 2520–2531.
- [14] Yan J, Wang Q, Wei T, Fan Z. Recent Advances in Design and Fabrication of Electrochemical Supercapacitors with High Energy Densities. *Adv Energy Mater* 2014; 4: 1300816.
- [15] Wang G, Zhang L, Zhang J. A review of electrode materials for electrochemical supercapacitors. *Chem Soc Rev* 2012; 41: 797–828.
- [16] Hao L, Li X, Zhi L. Carbonaceous Electrode Materials for Supercapacitors. *Adv Mater* 2013; 25: 3899–3904.
- [17] Yan Y, Miao J, Yang Z, Xiao F-X, Yang HB, Liu B, Yang Y. Carbon nanotube catalysts: recent advances in synthesis, characterization and applications. *Chem Soc Rev* 2015; 44: 3295–3346.
- [18] Yuan C, Wu HB, Xie Y, Lou XW. Mixed Transition-Metal Oxides: Design, Synthesis, and Energy-Related Applications. *Angew Chem Int Ed* 2014; 53: 1488–1504.
- [19] Pereira C, Pereira AM, Fernandes C, Rocha M, Mendes R, Fernández-García MP, Guedes A, Tavares PB, Grenèche J-M, Araújo JP, Freire C. Superparamagnetic MFe₂O₄ (M = Fe, Co, Mn) Nanoparticles: Tuning the Particle Size and Magnetic Properties through a Novel One-Step Coprecipitation Route. *Chem Mater* 2012; 24: 1496–1504.
- [20] Fernandes C, Pereira C, Fernández-García MP, Pereira AM, Guedes A, Fernández-Pacheco R, Ibarra A, Ibarra MR, Araújo JP, Freire C. Tailored design of CoxMn1-xFe₂O₄ nanoferrites: a new route for dual control of size and magnetic properties. *J. Mater Chem C* 2014; 2: 5818–5828.
- [21] Fernandes DM, Costa M, Pereira C, Bachiller-Baeza B, Rodríguez-Ramos I, Guerrero-Ruiz A, Freire C. Novel electrochemical sensor based on N-doped carbon nanotubes and Fe₃O₄ nanoparticles: Simultaneous voltammetric determination of ascorbic acid, dopamine and uric acid. *J Colloid Interface Sci* 2014; 432: 207–213.
- [22] Faba L, Criado YA, Gallegos-Suárez E, Pérez-Cadenas M, Díaz E, Rodríguez-Ramos I, Guerrero-Ruiz A, Ordóñez S. *Appl Catal A* 2013; 458: 155–161.
- [23] Lipert K, Ritschel M, Leonhardt A, Krupskaya Y, Büchner B, Klingeler Rüdiger. Magnetic properties of carbon nanotubes with and without catalyst. *J Phys Conf. Ser* 2010; 200: 072061.

Biogas valorisation through catalytic decomposition to produce synthesis gas and carbon nanofibres

S. de Llobet Cucalón Presented in 2015 *Instituto de Carboquímica (CSIC), 50018 Zaragoza, Spain.*

Supervisors: I. Suelves Laiglesia (*Instituto de Carboquímica, Zaragoza*) and R. Moliner Álvarez (*Instituto de Carboquímica, Zaragoza*).

OBJECTIVES AND NOVELTY

Traditionally, biogas has been considered a non-value by-product which was generally burned in flares. Most recently, different alternatives for biogas utilization have been proposed such as heat, electricity or bio-methane production. However, from an economical point of view, the aforementioned applications depend on government feed in tariff and therefore renewable energy producers face an unstable scenario. For that reason, the production of new products from biogas is not only interesting but necessary to diminish the profitability barriers.

In that context, the simultaneous production of syngas and carbon nanofilaments is proposed (Figure 1). On the one hand, syngas constitutes the base of the C1 chemistry and depending on its $H_2:CO$ ratio it can be used to produce methanol, dimethyl ether, liquid hydrocarbons or H_2 . On the other hand, carbon nanofilaments are high added value material due to their unique properties (thermal and electricity conductivity and textural properties) that make them a promising material as catalyst support, synthetic graphite or graphene precursor or additive in polymer composites. This process, in which syngas and carbon nanofilaments are simultaneously produced from biogas, has been studied for the first time during the course of this thesis and it has been named "Catalytic Decomposition of Biogas (CDB)". Thus, the purpose of the thesis work was to study the technical viability of the biogas valorisation through catalytic decomposition to obtain syngas and high added value carbon nanofilaments.

RESULTS

First of all, and due to the research group background, the CDB was compared with the catalytic decomposition of CH_4 (CDM). The presence of CO_2 in the biogas changes the balance of carbon on the surface of the catalyst particles as compared to the CDM. Its presence results in a decrease of surface carbon concentration due to the formation of CO (Figure 1) and as a result, catalyst stability is significantly increased.

Regarding the study of the CDB, different massive catalysts, with an active phase/Al molar ratio of 67:33 (X: Ni, Co or Fe), were synthesized using the fusion method and evaluated according to their activity, stability and amount and quality of the carbonaceous material produced.

The effect of the operating conditions (temperature, space velocity and $CH_4:CO_2$ ratio) was studied using a Ni-based catalyst. Increasing the value of any of the operating variables provokes an increase of the catalytic activity. At the same time, surface carbon concentration raises up and it is transformed into encapsulating carbon that reduces catalyst stability. It was found that there is a compromise between catalytic activity and stability that maximizes the production of carbon which is, indeed, the main objective. However, with increasing reaction time, the catalyst stability turns into the most decisive factor.

In order to avoid or reduce the use of nickel, two different approaches were considered: the use of alternative active phases (Fe and Co) and the synthesis of bimetallic Ni-Co catalysts. The Fe-based catalyst is not a suitable catalyst for the CDB since high temperatures ($900\text{ }^\circ\text{C}$) are required to achieve similar catalytic activities than those obtained with the Ni catalyst. Besides, both quantity and quality of the carbonaceous material produced are low. The performance of the Co catalyst is closer to that of the Ni based catalyst. Nevertheless, at low temperatures ($600\text{--}700\text{ }^\circ\text{C}$), it is considerably deactivated during the first hour of reaction and as a result, the amount of carbon produced is much lower. Therefore, this catalyst is also not a good alternative to the Ni-based catalyst. Finally, results obtained with an equimolar Ni-Co based catalyst improved those obtained with the Ni-based catalyst. By reducing its nickel content a 50%, similar activity and a greater stability were obtained, allowing the production of greater amounts of carbon nanofilaments with similar characteristics.

Carbon type and carbon nanofilaments structure depend on the operating conditions, being the temperature the most determining variable. An increase of its value considerably reduces the proportion of

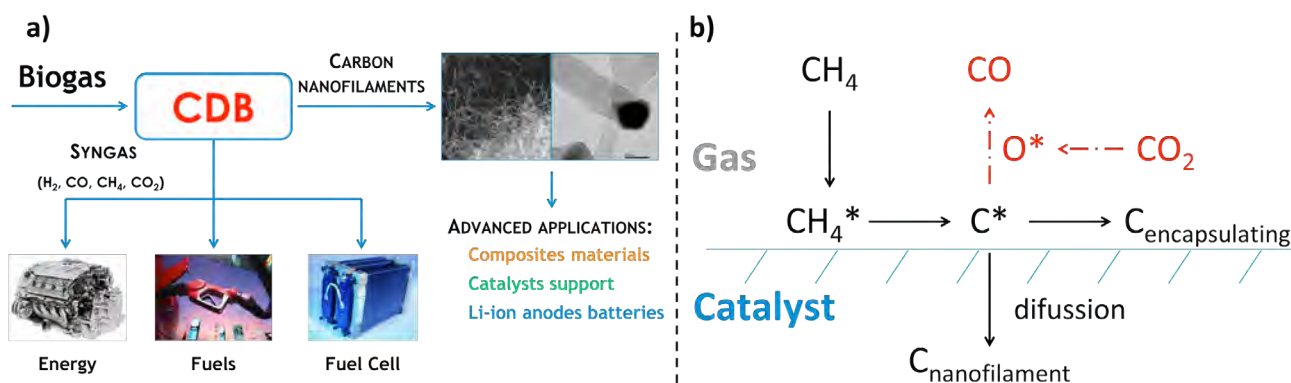


Figure 1. (a) CDB scheme process and (b) simplified mechanism of surface carbon formation/transformation in a Ni catalyst during the CDM and CDB (red steps only take place during the CDB).

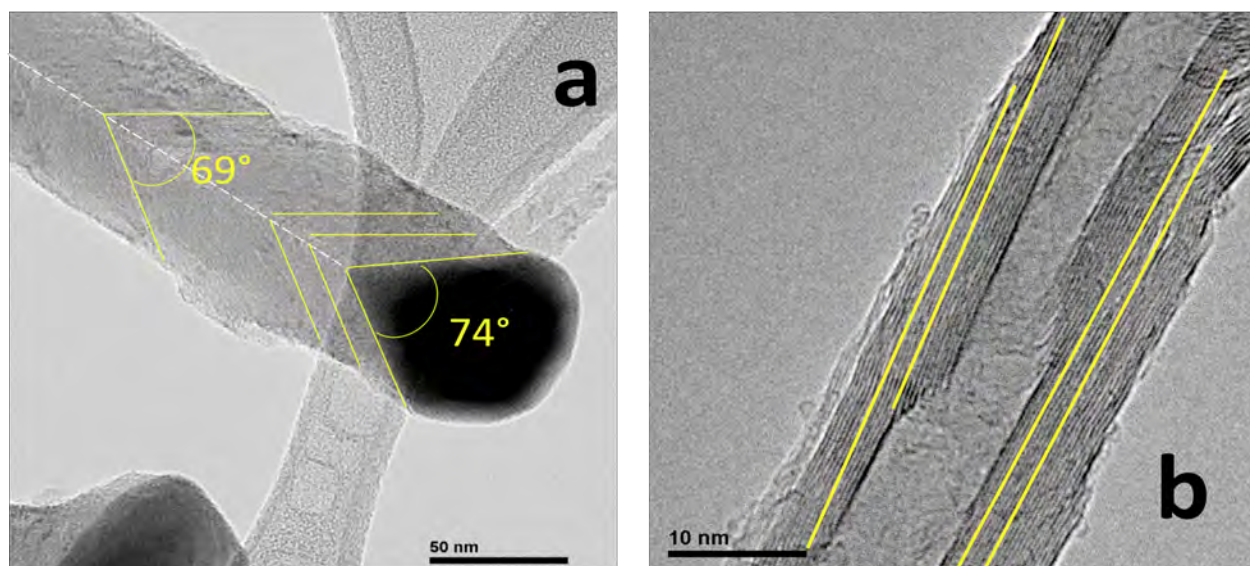


Figure 2. (a) Fishbone and (b) parallel carbon nanofibres produced in the CDB.

carbon nanofilaments as compared to encapsulating carbon. Therefore, working at 800 and 900 °C is inadvisable. Depending on the operating conditions, the catalyst particles deformation/elongation varies, so that the orientation of the graphene layers. By increasing the value of the operating conditions, carbon nanofilaments evolve from a fishbone type to a parallel type structure (Figure 2).

Since biogas contains minor compounds that can hamper its use, the effect of NH_3 and siloxanes was studied. Concentrations below 500 ppmv of NH_3 have no effect on the activity or stability of the catalysts. In contrast, the presence of siloxanes causes progressive deactivation of the catalysts, probably due to the formation of SiO_2 . Their negative effect could be minimized by reducing temperature and space velocity and the catalytic activity of the catalysts can be maintained for at least 180 minutes even though the concentration used, 50 ppmv ($287 \text{ mg}_{\text{Si}} \cdot \text{m}^{-3}$), is much higher than that of a real biogas ($10\text{-}20 \text{ mg}_{\text{Si}} \cdot \text{m}^{-3}$).

Finally, the scaling-up of the process using a rotary reactor and a fluidized bed reactor was considered. Results show that from the technical point of view the scale-up of the process is feasible. Catalysts activity and stability were similar to those observed in the fixed bed reactor and carbon nanofilaments properties remain invariable. Besides, the preliminary economic study suggested that the use of biogas in the CDB could be a very interesting alternative to energy production through its direct combustion. Incomes from syngas combustion for electricity production are reduced about a 30 % as compared to direct biogas combustion. However, benefits from the simultaneous production of a carbonaceous material with high added value could be two orders of magnitude higher than earnings from energy production.

CONCLUSIONS

Massive Ni and Ni-Co based catalysts present the best activity and stability and allow to produce great amounts of carbon materials composed principally of carbon nanofibres. Carbon type and carbon nanofilaments structure greatly depend on the active phase and the operating conditions, being the temperature the most determining variable. Thus, the

most suitable range to operate is 600-700 °C. Results related to the effect of minor compounds imply that cleaning stages associated with NH_3 and siloxanes could be probably eliminated if the CDB is scaled-up, thereby reducing process costs. From research conducted in this thesis work, it can be concluded that the CDB for the simultaneous production of syngas and carbon nanofibres is a feasible alternative, both technically and economically, to the production of energy from biogas combustion.

RELATED PUBLICATIONS

- [1] Pinilla J.L., de Llobet S., Suelves I., Utrilla R., Lázaro M.J., Moliner R. Catalytic decomposition of methane and methane/ CO_2 mixtures to produce synthesis gas and nanostructured carbonaceous materials. *Fuel* 2011; 90, 2245-2253.
- [2] de Llobet S., Pinilla J.L., Lázaro M.J., Moliner R., Suelves I. Catalytic decomposition of biogas to produce H_2 -rich fuel gas and carbon nanofibers. Parametric study and characterization. *Int. J. Hydr. Energy* 2012; 37, 7067-7076.
- [3] de Llobet S., Pinilla J.L., Lázaro M.J., Moliner R., Suelves I. CH_4 and CO_2 partial pressures influence and deactivation study on the Catalytic Decomposition of Biogas over a Ni catalyst. *Fuel* 2013; 111, 778-783.
- [4] De Llobet S., Purón H., Pinilla J.L., Moliner R., Millán M., Suelves I., Tailored synthesis of organised mesoporous aluminas prepared by non-ionic surfactant templating using a Box-Wilson CCF design. *Micro. Meso. Mat.* 2013; 179, 69-77.
- [5] de Llobet S., Pinilla J.L., Moliner R., Suelves I., Arroyo J., Moreno F., Muñoz M., Monné C., Cameán I., Ramos A., Cuesta N., García A.B. Catalytic decomposition of biogas to produce hydrogen rich fuels for SI engines and valuable nanocarbons. *Int. J. Hydro. Energy* 2013; 38, 15084-15091.
- [6] de Llobet S., Pinilla J.L., Moliner R., Suelves I. Relationship between carbon morphology and catalyst deactivation in the catalytic decomposition of biogas using Ni, Co and Fe based catalysts. *Fuel* 2015; 139, 71-78.
- [7] de Llobet S., Pinilla J.L., Moliner R., Suelves I. Effect of the synthesis conditions of Ni/ Al_2O_3 catalysts on the biogas decomposition to produce H_2 -rich gas and carbon nanofibers. *Appl. Catal. B: Environ.* 2015; 165, 457-465.

Full Thesis can be downloaded from
<https://zaguan.unizar.es/record/47426>

Socios protectores del Grupo Español del carbón
